FIR FILTER DESIGN BY CONVEX OPTIMIZATION USING RANK REFINEMENT

A THESIS SUBMITTED TO

THE GRADUATE SCHOOL OF ENGINEERING AND SCIENCE

OF BILKENT UNIVERSITY

IN PARTIAL FULFILLMENT OF THE REQUIREMENTS FOR

THE DEGREE OF

MASTER OF SCIENCE

IN

ELECTRICAL AND ELECTRONICS ENGINEERING

By

Mehmet Dedeoğlu

December, 2014

FIR FILTER DESIGN BY CONVEX OPTIMIZATION USING RANK REFINEMENT
By Mehmet Dedeoğlu
December, 2014

We certify that we have read this thesis and that in our opinion it is fully adequate, in scope and in quality, as a thesis for the degree of Master of Science.

Prof. Dr. Orhan Arıkan (Advisor)

Prof. Dr. A. Enis Çetin

Prof. Dr. Mustafa Ç. Pınar

Approved for the Graduate School of Engineering and Science:

Prof. Dr. Levent Onural
Director of the Graduate School

ABSTRACT

FIR FILTER DESIGN BY CONVEX OPTIMIZATION USING RANK REFINEMENT

Mehmet Dedeoğlu
M.S. in Electrical and Electronics Engineering
Supervisor: Prof. Dr. Orhan Arıkan
December, 2014

Finite impulse response filters have been one of the primary topics of digital signal processing since their inception. Consequently, diverse class of design techniques including Chebyshev approximation, Fast Fourier Transform and optimization based methods had been proposed in the literature. With developments in computational tools, new design technique tools and formulations on filters including interior-point solvers and semidefinite programming (SDP), emerged. Since FIR filter design problem can be modelled as a quadratically constrained quadratic program, filter design problem can be solved via interior-point based convex optimization methods such as semidefinite programming. Unfortunately, SDP formulation of problem is nonconvex due to positive lower limit constraint in the passband. To overcome that problem, nonconvex problem can be cast into a convex SDP using semidefinite relaxation, which can be solved in polynomial time. Since relaxed formulation does not guarantee rank-1 solution matrix, recently proposed directed iterative rank refinement (DIRR) algorithm is used to impose a convex rank-1 constraint. Due to utilization of semidefinite relaxation and DIRR, addition of various constraints, such as phase and group delay masks, in convex manner is made possible. For feasibility type optimization formulations of filter design problem, a convergence rate improved version of DIRR is developed. Proposed techniques are applied on filter design problems with different set of constraints including phase and group delay constraints. Explicit simulations demostrate that the proposed technique is capable of solving nonlinear phase, phase constrained, and group delay constrained filter design problems.

Keywords: Convex optimization, FIR filter design, semidefinite programming, semidefinite relaxation, iterative rank refinement, spectral mask.

ÖZET

KERTE ARITIMI İLE DIŞBÜKEY ENİYİLEME TABANLI FIR SÜZGEÇ TASARIMI

Mehmet Dedeoğlu
Elektrik ve Elektronik Mühendisliği, Yüksek Lisans
Tez Yöneticisi: Prof. Dr. Orhan Arıkan
Aralık, 2014

FIR süzgeçler sayısal sinyal işlemenin hemen her alanında kullanıldıklarından, literatürde, Chebyshev yaklaşımı, Hızlı Fourier Dönüşümü ve eniyileme tabanlı algoritmalar gibi birçok süzgeç tasarım tekniği önerilmiştir. Hesaplama teknolojilerinin gelişmesiyle birlikte, iç-nokta çözücüler, yarıkesin programlama (SDP) gibi yeni süzgeç tasarım araçları ve formülasyonları ortaya çıkmıştır. FIR süzgeç tasarım problemi bir karesel kısıtlamalı karesel program olarak formüle edilebildiğinden, SDP gibi dışbükey eniyileme teknikleri ve iç-nokta çözücüler ile verimli bir şekilde çözülebilmektedir. Ancak, problemin SDP formülasyonu, geçirgen banda konulan pozitif alt maske kısıtı sebebiyle dışbükey olmamaktadır. Bu nedenle, dışbükey olmayan SDP, yarıkesin rahatlatma ile, polinom zamanda çözülebilen dışbükey bir SDP haline getirilmektedir. Ancak rahatlatılmış formülasyon çözüm matrisinin kerte-1 olmasını garantilemediğinden, çözüm matrisini kerte-1 olmaya zorlayan bir kısıt koymak için yönlü döngüsel kerte arıtımı (DIRR) algoritması kullanılmştır. Yarıkesin rahatlatma ve DIRR tekniklerinin birleşik kullanılması, faz ve grup gecikmesi maskeleri gibi çeşitli kısıtlamaların süzgeç tasarım problemine dışbükey olarak eklenmesine olanak tanımıştır. Süzgeç tasarımının olurluk eniyileme problemi modellemesinin çözümünde kullanılmak üzere, yakınsama hızı arttırılmış bir DIRR algoritması geliştirilmiştir. Önerilen teknikler, faz ve grup gecikmesi kısıtlamalarını içeren, farklı kısıt kümelerinden oluşan FIR süzgeç tasarım problemleri üzerine uygulanmıştır. Benzetimler sonucunda, önerilen tekniğin doğrusal olmayan fazlı, faz kısıtlamalı ve grup gecikmesi kısıtlamalı FIR süzgeç tasarımı problemlerini çözmede başarılı olduğu gözlemlenmiştir.

Anahtar sözcükler: Dışbükey eniyileme, FIR süzgeç tasarımı, yarıkesin programlama, yarıkesin rahatlatma, döngüsel kerte arıtımı, spektral maske.

Acknowledgement

I would like to thank my supervisor Prof. Dr. Orhan Arıkan and express my gratitude for his valuable guidance, suggestions and encouragement throughout this work. He is a dignified, kind and considerate academician who is always thoughtful to his students. I would like to extend my special thanks to Prof. Dr. A. Enis Çetin and Prof. Dr. Mustafa Ç. Pınar for agreeing to join my thesis committee with their valuable comments and suggestions on the thesis.

I also would like state my special thanks to Dr. Yaşar Kemal Alp, as he provided me with many valuable insights and guidance. He was always helpful whenever it was required.

I also appreciate the value of the financial support from the Scientific and Technical Research Council of Turkey (TUBITAK).

I would like to express my thanks to all of my friends, who above all else encouraged me throughout this thesis.

Finally, my deepest gratitude goes to my parents for their sincere love, patience and continuous support in every step of my life.

Contents

List of Figures

List of Tables

Chapter 1

Introduction to Finite Impulse Response Filter Design

Since its inception, digital finite impulse response (FIR) filters have been one of the prominent building blocks in digital signal processing (DSP) because of their benefits on hardware implementation in terms of cost, efficiency and design flexibility [1–3]. Accordingly, a diverse class of FIR filter design techniques including windowing, Fast Fourier Transform (FFT), Chebyshev approximation, least squares error, and convex optimization based techniques have been proposed in the literature [4–16]. Among prominent techniques, optimization based FIR filter design methods significantly flourished compared to others with the progression in computing resources in last 2 decades [1, 17]. Development of efficient convex optimization solvers, i.e., interior-point solvers, and introduction of flexible convex formulations such as Semidefinite Programming (SDP) and Second-Order Cone Programming (SOCP) triggered new possibilities in FIR filter design via convex optimization [18–29].

The primary concern in FIR filter design is to find the minimum length finite filter coefficients for a given set of specifications. However, several other properties of FIR filters such as minimum phase, linear phase, maximally flat passband, and equiripple frequency response are as important as primary concern in certain applications. Minimum phase FIR filters are desired in data communication systems, where the minimum delay is essential [10]. Maximally flatness of passband response, is desired in radar applications, where periodic amplitude modulations would be produced in case there exist ripples in the passband [8]. Though these ripples are usually undesired in many applications, in applications requiring low complexity with less precision, ripples can be acceptable up to a specific limit. In those cases, equiripple filters provide the worst acceptable performance with minimal coefficient length [6, 7]. However, by all means, the linearity of phase is the mostly desired property in many filtering applications since linear phase systems provide constant group delay, which in return prevents any phase distortion caused by the filtering [6, 7, 10, 30]. A related property, group delay of an FIR filter is important in real time applications such as speech coding, digital modem synchronization [31] since the group delay of a linear phase FIR filter increases with the number of filter coefficients [32]. In addition, linear phase filters with sharp transition regions that are usually used in narrow frequency band selection applications can have unacceptably high group delays. Thus, there have been a growing interest in finding filter coefficients with low group delays [33].

Since, in real time applications low group delay is required, group delay constraints are more desired compared to phase constraints in these applications.

Windowing based FIR filter design techniques make use of frequency response of an ideal filter [34]. The design procedure starts with the selection of a desired frequency response, which is typically realizable by infinite length filter coefficients. Since in reality, only finite length coefficients can be used, a finite subset of infinite number of coefficients is selected using a window function in time domain. Hence, resulting frequency response becomes an approximation of desired frequency response. Though windowing based filter design techniques are fast, they do not satisfy any optimality criteria and filter coefficients satisfying the predefined specifications are found in an *ad-hoc* manner.

Other than windowing, there exist different tools as Chebyshev approximation, FFT, least squares error design, and convex optimization, which can be combined to obtain filter design techniques with improved robustness and efficiency.

Unified linear phase FIR filter design, i.e., Parks-McClellan technique, relies on Chebyshev approximation and is one of the milestone techniques in terms of its efficiency and robustness [7]. In Parks-McClellan technique, well-known Chebychev approximation and Remez exchange algorithm are combined to propose a unified equiripple linear phase FIR filter design procedure [9,11,13,14]. However, due to underlying Remez exchange algorithm, Parks-McClellan technique can not achieve the optimal filter response even though it can obtain the best equiripple approximation to the desired response [7].

In [4], METEOR, a technique based on limit approach is proposed. FIR filter design problem for a given set of mask constraints is formulated as a linearly constrained linear program and solved using simplex algorithm. Hence, METEOR is capable of finding locally optimum solutions for any given set of constraints. Around the time METEOR was developed, it was considered a versatile technique as it is capable of designing linear phase, minimum phase, and flat passband filters. On the other hand, METEOR is not capable of designing nonlinear phase filters and is not able to obtain globally optimal solutions.

In [5, 8], Chebyshev approximation is used to model FIR filter design problem and solved using a multiple exchange algorithm, which is derived directly from Kuhn-Tucker conditions. In this formulation, objective is chosen to be the minimization of least-squares approximation error for given set of linear constraints. Hence, the technique is named as peak-constrained least-squares (PCLS) appoach. Similar to Remez exchange algorithm, PCLS lacks the optimality. However, efficiency of PCLS outperformed the Parks-McClellan technique since Remez exchange algorithm is replaced with a multiple exchange algorithm. Even though, PCLS is capable of implementing phase and group delay constraints, for the convergence of PCLS, appropriate choice of its parameters is essential.

In [6], based on projection on convex sets (POCS) [35], an efficient FFT based equiripple FIR filter design technique is proposed. In the proposed approach, iterations are performed between time and frequency domains using efficient FFT algorithm. Since Fourier transform preserves convexity, algorithm is guarnteed to converge to a design that satisfies predefined constraints if a solution exists.

Proposed technique is capable of designing equiripple filters with a similar performance to Parks-McClellan algorithm.

As an outcome of the developments in computing resources, new convex optimization solvers [27, 29, 36, 37] are introduced that are capable of solving more general convex optimization problems in a more efficient way. As a result, a rich class of FIR filter design formulations, which can be solved in a more efficient and reliable manner, emerged. Some notable formulations that make use of convex solvers include linear programming (LP) [38], quadratically constrained quadratic programming (QCQP) [39–41], second-order cone programming (SOCP) [20, 42], and semidefinite programming (SDP) [19, 43, 44] problems. Among these, QCQP formulation of FIR filter design is capable of finding filter coefficients with spectral mask constraints in frequency domain [18, 45]. However, QCQP is not capable of implementing nonconvex constraints of the form $\mathbf{x}^T\mathbf{A}\mathbf{x} \geq b$, where $\mathbf{A}$ is a positive semidefinite (PSD) matrix and $b \geq 0$. Hence, QCQP formulation does not guarantee a lower bound for the filter gain in the passband. In applications such as ultra-wideband (UWB) pulse design, where the passband energy with a maximum passband gain constraint is desired to be maximized, QCQP formulation produce optimal solutions for a given spectral mask [42, 46].

In [19, 38], it is shown that nonconvex QCQP formulation of filter design problem can be cast as an LP using autocorrelation function. In this technique, autocorrelation coefficients are found by solving an LP problem and then filter coefficients are decomposed by applying spectral factorization on autocorrelation vector. One advantage of this technique is that obtained filters do not have to be linear phase contrary to classical LP formulations of FIR filter design problem. However, due to spectral factorization, types of constraints that can be enforced in this formulation is limited.

In [47], a linear matrix inequality (LMI) based SDP formulation of QCQP problems including FIR filter design is suggested. Since the proposed approach uses LMI instead of frequency sampling, obtained filter coefficients are guaranteed to satisfy the constraints. Solution of the obtained SDP problem using interior-point solvers is quite fast and efficient. In addition, it is possible to implement spectral mask constraints, which are used in many applications in addition to filter design problem. However, the proposed technique is not capable of implementing some useful constraints in filter design such as group delay and phase response constraints. Hence, proposed technique is useful on nonlinear phase FIR filter design applications. In [33], an SDP based model, which can implement group delay constraints, is proposed. Unlike the proposed approach in [47], in the proposed approach, frequency sampling is used. To impose group delay constraints, problem is formulated as a QCQP with an additional group delay constraint in the form of $\mathbf{h}^T\mathbf{P}\mathbf{h} \leq p$, where $\mathbf{P}$ and p are matrix, which maps filter coefficients to group delay samples, and group delay upper limit constant, respectively. However, $\mathbf{P}$ is not guaranteed to be a positive semidefinite matrix, which renders the design formulation as a nonconvex optimization problem. Hence, authors propose a PSD approximation of $\mathbf{P}$ matrix, so that the design problem becomes a convex optimization problem. Because of this approximation, obtained filter coefficients do not always satisfy the predefined group delay constraints.

In [44], by using convex relaxation techniques, a convex SDP formulation of nonconvex QCQP problems is proposed. To enforce solution matrix to be rank-1, iterative solution of a relaxed SDP with convex rank cost is considered. Proposed technique is capable of solving nonconvex QCQP problems in a few iterations. Advantage of this technique over the previously proposed convex optimization based techniques is that proposed iterative formulation enables the inclusion of a large set of constraints in SDP formulation, which were not possible in the LP and the QCQP formulations. However, authors do not investigate any FIR filter design applications of the proposed technique in [44]. Additionally, suggested method may fail to provide rank-1 solutions and may get stuck at a local optima for tightly constrained FIR filter designs.

In this thesis, a more general version of SDP based FIR filter design technique, which has been reported in [48], is proposed and analyzed. Suggested technique makes use of frequency sampling and semidefinite relaxation (SDR) besides SDP formulation of filter design problem. Problem is first modelled as a quadratically constrained quadratic programming (QCQP) problem for a given set of spectral mask constraints on magnitude, phase and group delay. QCQP model of filter design problem is not convex due to positive lower mask constraint in frequency domain. Hence, model is equivalently cast as an SDP with additional rank-1 constraint. Then, this model is relaxed to a convex SDP using SDR, whose argument is now an $L \times L$ dimensional matrix $\mathbf{H}$. Since relaxed SDP does not guarantee that obtained solution for $\mathbf{H}$ will be rank-1, a constraint or a cost function, which will enforce $\mathbf{H}$ to be rank-1, is required. For this purpose, the use of directed iterative rank refinement (DIRR) [43,48], which is similar to convex iterations algorithm [44], is proposed. In the propsoed setting, a cost function is incorporated to the convex SDP problem, which tries to minimize the negative inner product of argument matrix with selected singular vector that is determined in the previous iteration. In addition, upper energy constraints for the inner product of argument matrix with each singular vector other than the selected singular vector of the solution matrix can also be introduced in those problems with tight constraints. By performing this operation, the rank of the solution matrix is reduced at each iteration converging to a practically rank-1 matrix. To specify the end of the procedure, a stopping criterion on the ratio of the chosen singular value of the solution matrix $\mathbf{H}$ to the total energy of $\mathbf{H}$ is used. Once the stopping criterion is satisfied, solution matrix $\mathbf{H}$ is decomposed to FIR filter coefficients simply via rank-1 approximation of $\mathbf{H}$ and singular value decomposition (SVD). The propsoed technique is capable of designing filters under phase and group delay constraints. Different formulations of FIR filter design problem are demonstrated to show that proposed technique can perform controlled tradeoff between robustness, efficiency and convergence rate.

Motivated by the goal of achieving a rank-1 solution matrix $\mathbf{H}$, the goal is to find an $\mathbf{H}$ with most energy concentrated along one of the chosen singular vector of $\mathbf{H}$. This corresponds to finding an orthogonal set of vectors in L dimensional space with most energy concentrated along one of the vectors. Since feasible set may contain more than one locally optimal solutions depending on the tightness of constraints, convergence of the algorithm is adaptive on the constraints. In order to improve the convergence of DIRR, convex rank constraints can be removed in loose problems. In this case, only the maximization of energy along one direction is applied. Because of the fact that convex optimization problem is solved iteratively, complexity of the technique is higher than autocorrelation based techniques. However, the addition of large class of constraints is made possible at a reasonable cost of complexity for offline systems.

In *Chapter 2*, classical convex optimization based FIR filter design problem will be investigated in detail. Some milestone techniques including QCQP and autocorrelation based LP formulations will be derived. As it will be discussed, autocorrelation based LP technique provides optimal solution for nonlinear phase filter design problems. However, due to spectral factorization applied in the last step of the technique, this method is not capable of designing filters with phase and group delay constraints. These constraints are important in many applications since high value of group delay or high nonlinearity in phase cause distortions in signal. For that reason, SDP and SDR formulations, which enable the addition of phase and group delay constraints, are demonstrated.

In *Chapter 3*, FIR filter design using DIRR is proposed and explained in detail. In DIRR method, a convex SDP objective searching for rank-1 solutions is added to the relaxed SDP formulation. Proposed convex SDP problem is solved iteratively. At each iteration, knowledge from the previous iteration is used via $\mathbf{H}$, i.e., $\mathbf{H}$ matrix found in the previous iteration is input to the current iteration. After a number of iterations solution matrix $\mathbf{H}$ converges to a rank-1 matrix that can be decomposed to a filter coefficient vector $\mathbf{h}$ using simple signal processing tools such as singular value decomposition (SVD). Secondly, DIRR with rank constraints is proposed. In this technique, convex SDP formulations of rank constraints are attached to DIRR. Hence, by adjusting thresholds on the rank constraints, rank-1 solutions can be obtained in tight constrained filter design problems. DIRR and its variant formulations are demonstrated on non-linear phase FIR filter design problems.

In *Chapter 4*, semidefinite expressions for phase and group delay constraints are derived. By adding these newly derived semidefinite constraints to original semidefinite non-linear phase FIR filter design formulation, we are able to solve phase and/or group delay constrained FIR filter design problems. Simple numerical examples are demonstrated using proposed DIRR technique for both phase and group delay constrained FIR filter design problems.

Throughout this thesis, bold small, and bold capital letters will represent vectors, and matrices respectively. $(.)^H$ and $(.)^T$ are hermitian and transpose operations, respectively. $\hat{(.)}$ is used to show real representation of a complex variable, vector , or matrix. $Re(.)$ and $Im(.)$ operations take real and imaginary parts of their argument, respectively. Lastly, $\trianglerighteq$ is used to denote either $\leq$ or $\geq$ symbols. Other than these, special characters used in the formulas will be mentioned in the text.

Finally, remarks and conclusions are provided in *Chapter 5*.

Chapter 2

Convex Optimization Based FIR Filter Design with Spectral Mask Constraints

Convex optimization based FIR filter design has been intensively investigated in the literature. Hence, there exists many approaches such as least squared error minimization and mask constrained optimization techniques for FIR filter design [4–14, 16, 49]. In the past, due to their convex structure and low complexity, least squared error minimization based techniques were prefered [7–9, 11, 13, 50–52]. In least squares approach, the aim is to find filter coefficients that minimizes the total squared error from a desired filter response, i.e., an ideal filter response with infinite coefficient length. For that reason, the cost function of this optimization problem is occupied by squared error term and hence the addition of a desired objective to optimization problem is not trivial.

With the developments in computing resources and efficient interior-point solvers, mask constrained FIR filter design gained interest since it aims to solve a more general FIR filter design problem [4, 19, 19, 20, 38–44]. In mask constrained optimization approach, desired properties of FIR filter are specified by user defined mask constraints which constitute the feasible set of the problem. Hence, objective of the optimization problem is not occupied and can be used to implement any optimality criterion. Since the feasible set defined by the constraints is typically very large, mask constrained optimization problem possesses more complexity compared to least squared error approach, but can be solved efficiently by interior-point solvers such as YALMIP, SeDuMi and SDPT3 [27, 29, 36, 37].

In this chapter, various well-known formulations for convex optimization based FIR filter design with spectral mask constraints will be demonstrated and numerical examples will be provided. Finally, an introduction to the proposed FIR filter design formulation will be made.

2.1 Quadratically Constrained Quadratic Programming Formulation

An FIR filter of length L is typically characterized by either its impulse response $h_n, 0 \leq n \leq L-1$ or its frequency response as:

$$H(\omega) = \sum_{n=0}^{L-1} h_n e^{-j\omega n},\ \forall \omega \in [-\pi, \pi], \tag{2.1}$$

where ω is the normalized frequency. In optimization based FIR filter design, filter coefficients are typically obtained by imposing desired constraints on the magnitude response of the filter as in the following feasibility problem:

$$\begin{aligned} &\text{find } h_n \in \mathbb{R},\ 0 \leq n \leq L-1, && (2.2a)\\ &\text{subject to } |H(\omega)|^2 \leq M_u(\omega),\ \forall \omega \in [0, \pi], && (2.2b)\\ &\qquad |H(\omega)|^2 \geq M_l(\omega),\ \forall \omega \in [0, \omega_p], && (2.2c) \end{aligned}$$

where $M_u(\omega)$ and $M_l(\omega)$ are the upper and lower magnitude response masks shown in Fig. 2.1. The passband and stopband of the filter are defined as $[0, \omega_p]$ and $[\omega_s, \pi]$, respectively. Since the magnitude response of an FIR filter with real coefficients is an even function, design constraints can be imposed on the

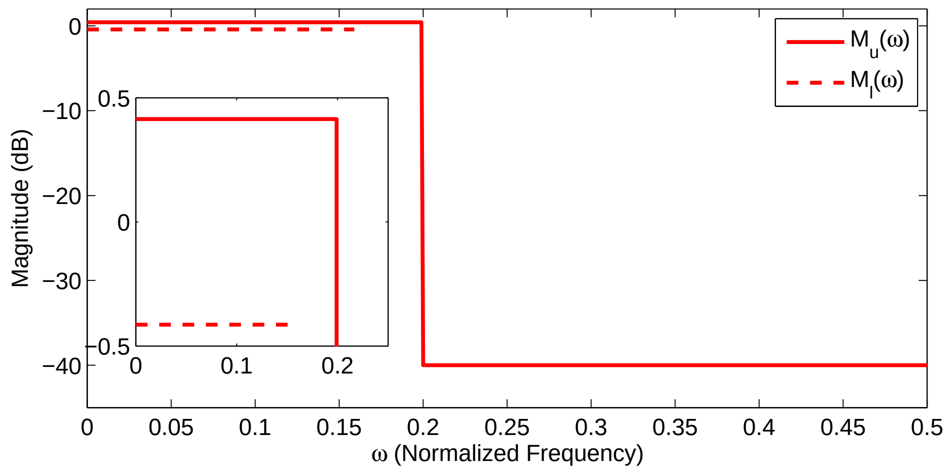

Figure 2.1: A typical set of mask constraints on the magnitude response of an FIR filter. $M_u(\omega)$ and $M_l(\omega) = 1/1.1$ are the upper and lower mask constraints on the magnitude response with transition band $\omega_p = 0.16 \leq \omega \leq 0.20 = \omega_s$, respectively. $M_u(\omega) = 1.1$ in the pass band and $M_u(\omega) = 0.0001$ in the stop band.

nonnegative part of the spectrum. Then, (2.2) can be written in vector form as:

$$\text{find } \mathbf{h} \in \mathbb{R}^L, \tag{2.3a}$$

$$\text{subject to } \mathbf{h}^T\mathbf{A}(\omega)\mathbf{h} \leq M_u(\omega),\ \forall\omega \in [0,\pi], \tag{2.3b}$$

$$\mathbf{h}^T\mathbf{A}(\omega)\mathbf{h} \geq M_l(\omega),\ \forall\omega \in [0,\omega_p]. \tag{2.3c}$$

Here, $\mathbf{h} = [h_0, h_1, ..., h_{L-1}]^T$ and $\mathbf{A}(\omega)$ is given as:

$$\mathbf{A}(\omega) = \mathbf{v}(\omega)\mathbf{v}^H(\omega), \tag{2.4a}$$

$$\mathbf{v}(\omega)=[1, e^{j\omega}, ..., e^{j\omega(L-1)}]^T. \tag{2.4b}$$

In (2.4b), $\mathbf{v}(\omega)$ denotes the Fourier Transform coefficients for a specific ω. Since the frequency variable ω is defined in a continium, this feasibility problem has uncountably many constraints that are semi-infinite. Semi-infinite constraints can be written in linear matrix inequality (LMI) form and (2.4) can be cast as an SDP [46, 47]. However, LMI formulation does not allow non-convex mask constraints such as phase and group delay mask constraints. Hence, frequency sampling approach, in which such constraints can be handled, will be adopted.

In practice, by using a dense enough frequency domain sampling, a quadratic feasibility problem with finite number of constraints can be obtained as:

$$\text{find } \mathbf{h} \in \mathbb{R}^L, \tag{2.5a}$$

$$\text{subject to } \mathbf{h}^T\mathbf{A}_k\mathbf{h} \leq a_k,\ 0 \leq k \leq K_u, \tag{2.5b}$$

$$\mathbf{h}^T\mathbf{A}_k\mathbf{h} \geq b_k,\ 0 \leq k \leq K_l, \tag{2.5c}$$

where $\mathbf{A}_k$=$\mathbf{v}(\omega_k)\mathbf{v}^H(\omega_k)$, a_k=$M_u(\omega_k)$ and b_k=$M_l(\omega_k)$. If the frequency sampling is uniform with a spacing of π/K, the resulting number of upper and lower frequency mask constraints are $K_u = K$ and $K_l = \lceil Kw_p/\pi \rceil$. Here, $\lceil . \rceil$ indicates the operator which returns the smallest integer that is greater than its argument. A rule of thumb for selecting K is K≈$15L$ [7]. However, as investigated in [53–55], judiciously chosen set of non-uniform frequency samples provides acceptable designs requiring fewer number of constraints.

In addition to the spectral mask constraints, stop band energy can also be incorporated to the cost function as:

$$\min_{\mathbf{h}\in\mathbb{R}^L} \mathbf{h}^T\mathbf{A}_s\mathbf{h}, \tag{2.6a}$$

$$\text{subject to } \mathbf{h}^T\mathbf{A}_k\mathbf{h} \leq a_k,\ 0 \leq k \leq K_u, \tag{2.6b}$$

$$\mathbf{h}^T\mathbf{A}_k\mathbf{h} \geq b_k,\ 0 \leq k \leq K_l. \tag{2.6c}$$

Here $\mathbf{A}_s$ is defined as:

$$\mathbf{A}_s = \int_{\omega_s}^{\pi} W(\omega)\mathbf{A}(\omega)d\omega, \tag{2.7}$$

where $W(\omega) \geq 0$ is a weight function providing further flexibility and control on the design. The optimization problem in (2.6) has quadratic cost function and quadratic constraint functions, hence it is a QCQP [56].

In general, filter coefficients obtained as the solution to (2.6) has non-linear phase response characteristic. Linear phase response filter coefficients can also be obtained from (2.6) by imposing additional constraints on the symmetry of the filter coefficients. For instance, for designing a real type-1 FIR filter, the following constraints should be incorporated to (2.6) [7]:

$$h_n = h_{L-1-n},\ 0 \leq n \leq (L-1)/2. \tag{2.8}$$

These constraints can be equivalently expressed as:

$$\mathbf{h} = \mathbf{\Pi}\boldsymbol{\theta}, \tag{2.9}$$

where, $\boldsymbol{\theta}$ is the vector of reduced filter coefficients, $\mathbf{\Pi} = [\mathbf{I}, \hat{\mathbf{I}}]^T$, $\mathbf{I}$ is an identity matrix of size $(L+1)/2 \times (L+1)/2$ and $\hat{\mathbf{I}}$ is the flipping matrix of size $(L-1)/2 \times (L+1)/2$ composed of zeros except for entries of $\left(i, \frac{L+1}{2} - i\right)$, $1 \leq i \leq \frac{L-1}{2}$ that are equal to 1. Hence the optimization problem in (2.6) takes the following form for designing type-1 FIR filters of odd length L:

$$\min_{\boldsymbol{\theta} \in \mathbb{R}^{(L+1)/2}} \ \boldsymbol{\theta}^T \mathbf{\Pi}^T \mathbf{A}_s \mathbf{\Pi} \boldsymbol{\theta}, \tag{2.10a}$$

$$\text{subject to } \boldsymbol{\theta}^T \mathbf{\Pi}^T \mathbf{A}_k \mathbf{\Pi} \boldsymbol{\theta} \leq a_k, \ 0 \leq k \leq K_u, \tag{2.10b}$$

$$\boldsymbol{\theta}^T \mathbf{\Pi}^T \mathbf{A}_k \mathbf{\Pi} \boldsymbol{\theta} \geq b_k, \ 0 \leq k \leq K_l. \tag{2.10c}$$

Since quadratic lower mask constraints are non-convex, the constructed QCQPs are non-convex optimization problems. Therefore, efficient convex solvers cannot be used directly to obtain their solutions. In the next section, convexifying these QCQPs by using linear programming (LP) will be presented [19, 38].

2.2 Linear Programming Formulation

Even though QCQPs given in (2.6) and (2.10) are NP-hard, these QCQPs can be rewritten in LP form by assuming that FIR filter coefficients are symmetric, i.e., frequency response of desired filter is real valued with zero phase [4, 7, 8, 19]. However, zero-phase response condition is too tight for many filtering applications. Hence, a convex filter design formulation that is not conditioned on phase is desired since non-linear phase formulations provide a larger feasible set for minimum length FIR filter design. A more general non-linear phase FIR filter design formulation is presented in [38], in which non-convex QCQP (2.6) is cast as an LP problem using autocorrelation vector.

Let $\mathbf{r}$ denote $2L-1$ length autocorrelation vector corresponding to filter coefficient vector $\mathbf{h}$ of length L. Then, for the spectral mask constraints given in

Fig. 2.1, problem (2.6) can be rewritten as [38]:

$$\min_{\mathbf{r}\in\mathbb{R}^{2L-1}} \quad \sum_{k=K_s+1}^{K_u} \mathbf{r}^T\mathbf{v}(\omega_k), \tag{2.11a}$$

$$\text{subject to} \quad \mathbf{r}^T\mathbf{v}(\omega_k) \leq a_k,\ 0 \leq k \leq K_u, \tag{2.11b}$$

$$\mathbf{r}^T\mathbf{v}(\omega_k) \geq b_k,\ 0 \leq k \leq K_l, \tag{2.11c}$$

$$\mathbf{r}^T\mathbf{v}(\omega_k) \geq 0,\ K_l + 1 \leq k \leq K_u, \tag{2.11d}$$

$$\mathbf{r} \text{ is symmetric}, \tag{2.11e}$$

where $K_s = \lceil K\omega_s/\pi \rceil$. (2.11) is an LP with an affine objective and linear constraints. Hence, on contrary to (2.6), (2.11) is convex and can be solved in polynomial time to obtain optimal autocorrelation vector $\mathbf{r}^\star$ using efficient interior-point solvers. (2.11d) and (2.11e) are attached to (2.11) in order to guarantee that $\mathbf{r}$ possesses the characteristics of an autocorrelation vector as frequency response of any autocorrelation vector is non-negative. Since autocorrelation sequence is obtained by the following convolution operation $\mathbf{r} = \mathbf{h}*\mathbf{h}$, where $*$ denotes convolution, to obtain optimal filter coefficients $\mathbf{h}^\star$, spectral factorization is applied on $\mathbf{r}^\star$. Hence, obtained $\mathbf{h}^\star$ is not unique, but satisfy the spectral mask constraints.

Note that $\mathbf{r}^T\mathbf{v}(\omega_k)$ in (2.11) is the frequency response of $\mathbf{r}$, which corresponds to the magnitude response of desired filter coefficients $\mathbf{h}$. Hence, even though $\mathbf{r}$ is restricted to possess zero-phase response, $\mathbf{h}$ is not restricted in terms of phase response and hence, obtained coefficients possess non-linear phase. However, since the decomposition of $\mathbf{r}^\star$ is not unique, depending on the spectral factorization algorithm used, $\mathbf{h}^\star$, which has minimum phase response, can also be obtained. *Algorithm 1* that is implementing (2.11) and *Algorithm 3*, which is a spectral factorization algorithm that provides $\mathbf{h}^\star$ with minimum phase response, are given in *Appendix A.1*. Next, a numerical example for designing non-linear phase FIR filters using LP formulation is demonstrated. Throughout the thesis, we use SDPT3 interior-point solver [28, 29] to solve constructed convex optimization problems.

Design 2.1 *Given the lower and upper magnitude response mask constraints,* $M_l(\omega)$ *and* $M_u(\omega)$ *shown in* Figure 2.1*, design a non-linear phase FIR filter of length* $L = 38$ *with minimum stop band energy by using* (2.11).

n	$h_n^\star$	n	$h_n^\star$	n	$h_n^\star$	n	$h_n^\star$
1	0.0075	11	-0.0850	21	0.0029	31	0.0164
2	0.0382	12	0.0230	22	-0.0347	32	0.0141
3	0.1055	13	0.0917	23	-0.0340	33	-0.0020
4	0.2011	14	0.0734	24	-0.0018	34	-0.0173
5	0.2840	15	-0.0027	25	0.0265	35	-0.0212
6	0.2981	16	-0.0630	26	0.0252	36	-0.0148
7	0.2123	17	-0.0581	27	0.0005	37	-0.0060
8	0.0559	18	-0.0026	28	-0.0204	38	-0.0009
9	-0.0892	19	0.0459	29	-0.0184		
10	-0.1423	20	0.0448	30	0.0008		

Table 2.1: Non-linear phase FIR filter coefficients for *Design 2.1* that are given in 4 significant digits.

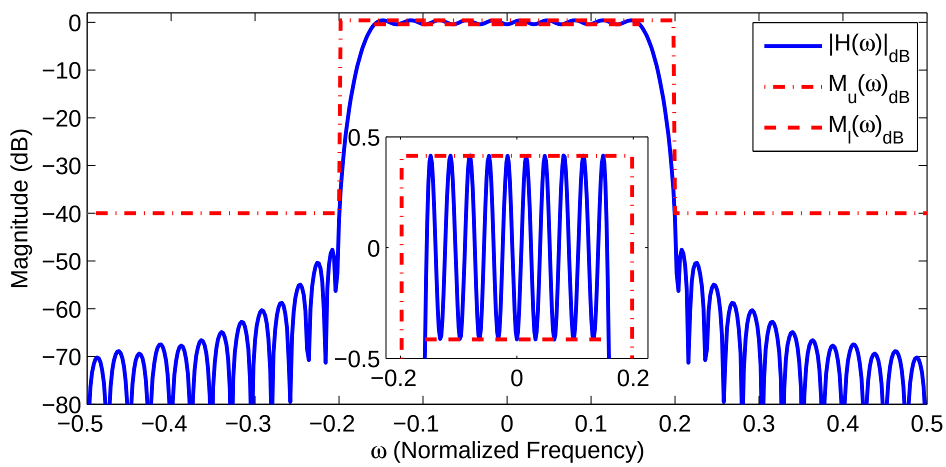

Figure 2.2: Magnitude response of $L = 38$ length FIR filter coefficients found using autorrelation based LP model. Magnitude response satisfies the constraints of *Design 2.1*. Stop band energy is $-60dB$.

For this design, the LP optimization problem in (2.11) is solved using *Algorithm 1* for $L = 38$. *Algorithm 3* is used as spectral factorization algorithm to obtain filter coefficients $\mathbf{h}^\star$ from autocorrelation coefficients $\mathbf{r}^\star$. Hence, $\mathbf{h}^\star$ possesses a minimum phase response and satisfy the magnitude response constraints. $\mathbf{h}^\star$, its magnitude response and phase response are given in *Table 2.1*, *Figure 2.2* and *Figure 2.3*, respectively. Achieved stop band energy in *Figure 2.2* is found to be −60dB. Note that since there is no phase constraints, the LP based design provides the global optimal in this set of constraints.

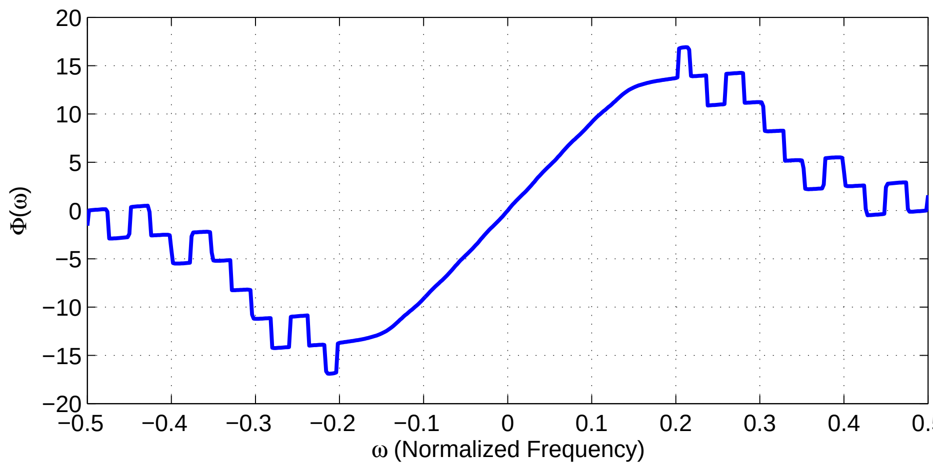

Figure 2.3: Phase response of $L = 38$ length FIR filter coefficients that is obtained using autocorrelation based LP model given in (2.11). Obtained phase is minimum but still non-linear.

Total stop band energy minimization goal of the LP given in (2.11) can be changed to peak stop band ripple minimization to obtain classical low-pass FIR filter design problem [38] by replacing affine term $\sum_{k=K_s+1}^{K_u} \mathbf{r}^T\mathbf{v}(\omega_k)$ with a variable δ^2 and by constraining energy corresponding to each frequency in the stop band by δ^2. Obtained LP with peak stop band ripple minimization can be written as:

$$\min_{\mathbf{r}\in\mathbb{R}^{2L-1},\delta^2\in\mathbb{R}} \quad \delta^2, \tag{2.12a}$$

$$\text{subject to} \quad \mathbf{r}^T\mathbf{v}(\omega_k) \leq a_k,\ 0 \leq k \leq K_s, \tag{2.12b}$$

$$\mathbf{r}^T\mathbf{v}(\omega_k) \leq \delta^2,\ K_s + 1 \leq k \leq K_u, \tag{2.12c}$$

$$\mathbf{r}^T\mathbf{v}(\omega_k) \geq b_k,\ 0 \leq k \leq K_l, \tag{2.12d}$$

$$\mathbf{r}^T\mathbf{v}(\omega_k) \geq 0,\ K_l + 1 \leq k \leq K_u, \tag{2.12e}$$

$$\mathbf{r} \text{ is symmetric.} \tag{2.12f}$$

Since the objective and newly introduced constraints are convex, LP given in (2.12) still produces globally optimal solutions. (2.12) can be solved using *Algorithm 1*. Next, a peak stop band ripple minimization type non-linear phase FIR filter design example is demonstrated.

n	$h_n^\star$	n	$h_n^\star$	n	$h_n^\star$	n	$h_n^\star$
1	0.0188	11	-0.0215	21	-0.0216	31	0.0172
2	0.0707	12	0.0712	22	-0.0395	32	0.0051
3	0.1594	13	0.0896	23	-0.0180	33	-0.0135
4	0.2558	14	0.0310	24	0.0168	34	-0.0231
5	0.3050	15	-0.0433	25	0.0302	35	-0.0192
6	0.2603	16	-0.0677	26	0.0132	36	-0.0085
7	0.1254	17	-0.0288	27	-0.0133	37	-0.0002
8	-0.0349	18	0.0294	28	-0.0229	38	0.0029
9	-0.1319	19	0.0517	29	-0.0093		
10	-0.1175	20	0.0235	30	0.0109		

Table 2.2: Non-linear phase FIR filter coefficients for *Design 2.2* that are given in 4 significant digits.

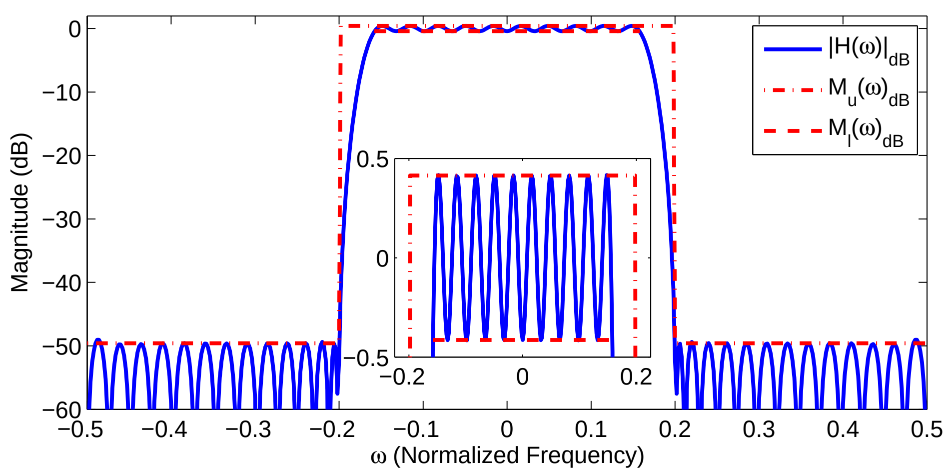

Figure 2.4: Magnitude response of $L = 38$ length FIR filter coefficients found by solving the problem given in *Design 2.2* using autorrelation based LP model. Total stop band energy is $-53dB$ and minimum peak stop band ripple is $\delta = -50dB$.

Design 2.2 *Given the lower and upper magnitude response mask constraints,* $M_l(\omega)$ *and* $M_u(\omega), 0 \leq \omega \leq \omega_s$ *shown in* Figure 2.1*, design a filter of length* $L = 38$ *with the minimum peak stop band ripple using* (2.12)*.*

For this design, the LP optimization problem in (2.12) is solved using *Algorithm 1* for $L = 38$. *Algorithm 3* is used as spectral factorization algorithm to obtain $\mathbf{h}^\star$ from $\mathbf{r}^\star$. Hence, $\mathbf{h}^\star$ possesses a minimum phase response and satisfy the

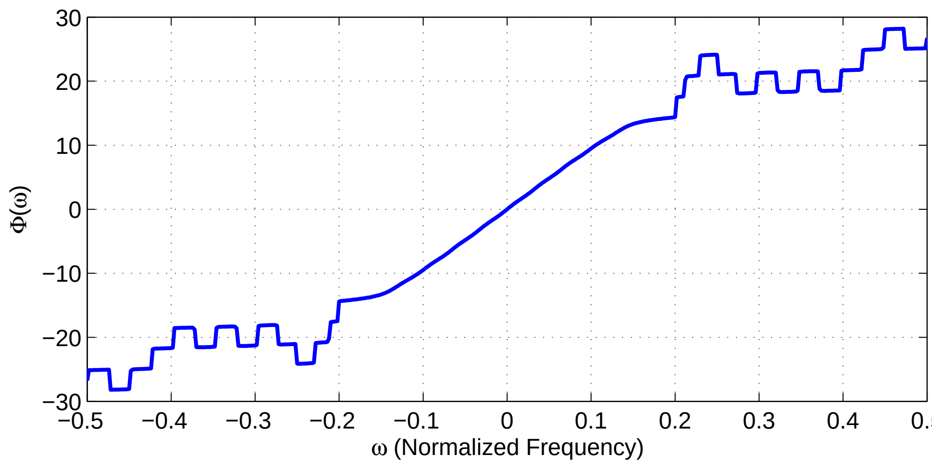

Figure 2.5: Phase response of $L = 38$ length FIR filter coefficients that is obtained using autocorrelation based LP model given in (2.12). Obtained phase is minimum but still non-linear.

magnitude response constraints. $\mathbf{h}^{\star}$, its magnitude response and phase response are given in *Table 2.2*, *Figure 2.4* and *Figure 2.5*, respectively. Achieved stop band energy and peak stop band ripple level in *Figure 2.4* are found to be -53dB and -50dB, respectively. Note that since there is no phase constraints, the LP based design provides the global optimal value in this set of constraints.

LP based model given in (2.11), can be rewritten for linear phase FIR filter design by enforcing symmetry condition on $\mathbf{h}$ rather than $\mathbf{r}$ [19]. If minimum stop band energy is desired, then linear objective of (2.11) is replaced with a quadratic objective since stop band energy of $\mathbf{h}$ is a quadratic function of $\mathbf{h}$. Hence, linear phase FIR filter design formulation can be written as:

$$\min_{\mathbf{h}\in\mathbb{R}^L} \quad \sum_{k=K_s+1}^{K_u} (\mathbf{h}^T\mathbf{v}(\omega_k))^2, \tag{2.13a}$$

$$\text{subject to} \quad \mathbf{h}^T\mathbf{v}(\omega_k) \leq a_k, \;\; 0 \leq k \leq K_u, \tag{2.13b}$$

$$\mathbf{h}^T\mathbf{v}(\omega_k) \geq b_k, \;\; 0 \leq k \leq K_u, \tag{2.13c}$$

$$\mathbf{h} \text{ is symmetric.} \tag{2.13d}$$

Note that constraints $\mathbf{h}^T\mathbf{v}(\omega_k) \geq 0,\;\; K_l + 1 \leq k \leq K_u$ are not included in (2.13) since $\mathbf{h}$ is not an autocorrelation vector. Because of (2.13d), phase response of any

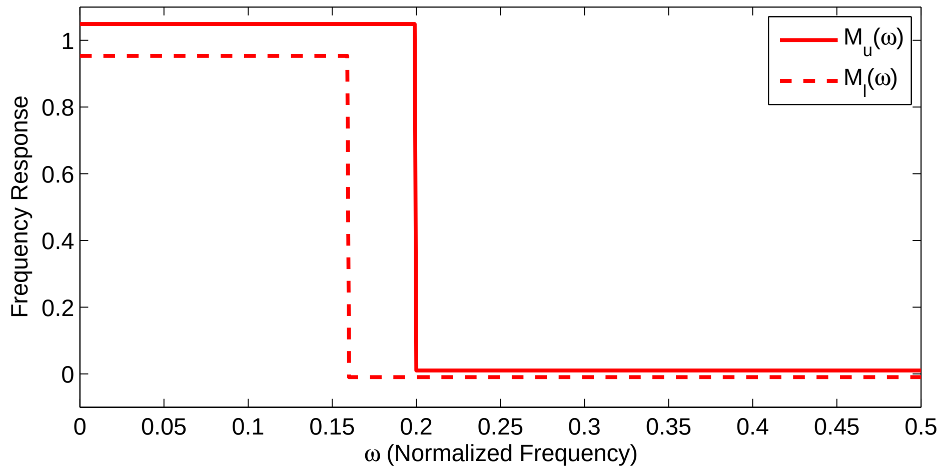

Figure 2.6: A typical set of mask constraints on the frequency response of an FIR filter. $M_u(\omega)$ and $M_l(\omega)$ are the upper and lower mask constraints on the frequency response with transition band $\omega_p = 0.16 \leq \omega \leq 0.20 = \omega_s$, respectively. $M_u(\omega) = \sqrt{1.1}$, $M_l(\omega) = \sqrt{1/1.1}$ in the pass band and $M_u(\omega) = 0.01$, $M_l(\omega) = -0.01$ in the stop band. Note that this frequency response masks correspond to magnitude response masks given in 2.1.

feasible solution to (2.13) is guaranteed to be linear. Hence, only linear phase FIR filters can be designed in this model. In addition, since objective and constraints are linear functions of $\mathbf{h}$, spectral mask constraints cannot be implemented in (2.13). *Algorithm 2* that is implementing (2.13), is given in the *Appendix A.1*. Next, a numerical example for designing linear phase FIR filters by using LP formulation is demonstrated.

Design 2.3 *Given the lower and upper frequency response mask constraints, $M_l(\omega)$ and $M_u(\omega)$ shown in* Figure 2.6*, design a linear phase filter of minimum length with the minimum stop band energy using* (2.13)*.*

For this design, the LP optimization problem given in (2.13) is solved using *Algorithm 2*. Since *Design 2.3* is a quasiconvex problem due to minimum length objective, (2.13) is solved for $30 \leq L \leq 40$ and minimum length solution is obtained at $L^{\star} = 39$. $\mathbf{h}^{\star}$, its magnitude and phase responses are given in *Table 2.3*, *Figure 2.7* and *Figure 2.8*, respectively. Achieved stop band energy in *Figure*

n	$h_n^\star$	n	$h_n^\star$	n	$h_n^\star$	n	$h_n^\star$
1	0.0042	11	-0.0141	21	0.2839	31	-0.0092
2	0.0010	12	0.0192	22	0.1269	32	0.0113
3	-0.0085	13	0.0402	23	-0.0176	33	0.0152
4	-0.0165	14	0.0162	24	-0.0734	34	0.0019
5	-0.0131	15	-0.0416	25	-0.0416	35	-0.0131
6	0.0019	16	-0.0734	26	0.0162	36	-0.0165
7	0.0152	17	-0.0176	27	0.0402	37	-0.0085
8	0.0113	18	0.1269	28	0.0192	38	0.0010
9	-0.0092	19	0.2839	29	-0.0141	39	0.0042
10	-0.0251	20	0.3518	30	-0.0251		

Table 2.3: Linear phase FIR filter coefficients for *Design 2.3* that are given in 4 significant digits.

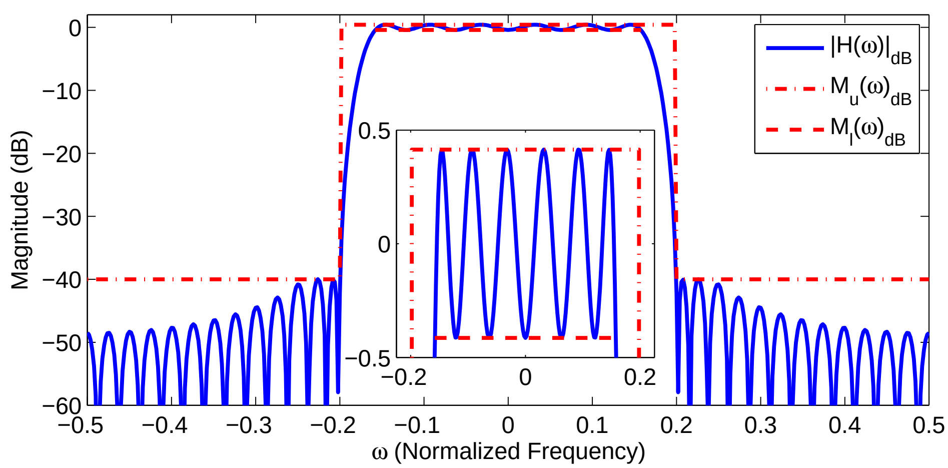

Figure 2.7: Magnitude response of $L^\star = 39$ length FIR filter coefficients found by solving the problem given in *Design 2.3* using (2.13). Total stop band energy is $-47dB$.

2.7 is found to be -47dB. Note that since $\mathbf{h}^\star$ is constrained to be symmetric, obtained solution has linear phase as shown in *Figure 2.8*. In addition, since (2.13) is a convex LP formulation, obtained filter coefficient vector $\mathbf{h}$ is guaranteed to have magnitude response with minimum total stop band energy.

Similar to non-linear phase FIR filter design, peak stop band ripple minimization can also be incorporated in linear phase FIR filter design in a similar formulation to (2.12). To obtain LP formulation of minimum peak stop band

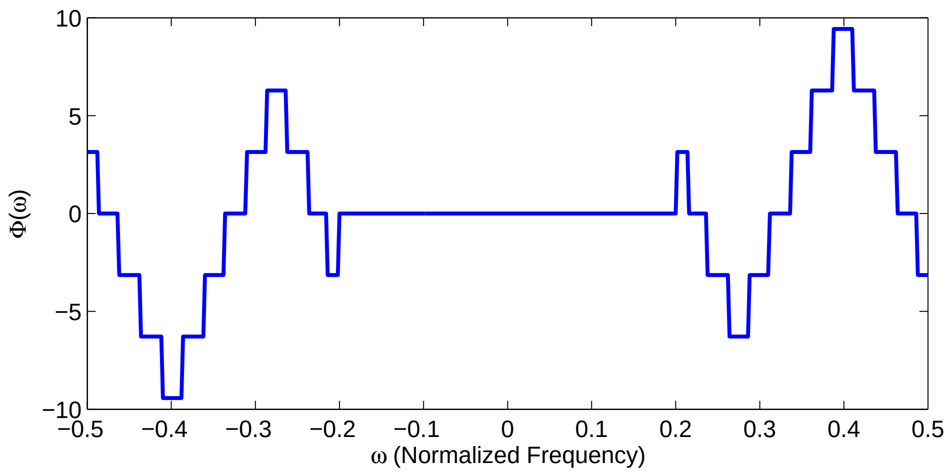

Figure 2.8: Phase response of $L^\star = 39$ length FIR filter coefficients that is obtained using LP model given in (2.13). Obtained $\mathbf{h}^\star$ provides linear phase response.

ripple linear phase FIR filter design, quadratic term $\sum_{k=K_s+1}^{K_u}(\mathbf{h}^T\mathbf{v}(\omega_k))^2$ is replaced with δ and frequency response of $\mathbf{h}$ is constrained with upper and lower bounds by δ for $K_s+1 \leq k \leq K_u$ and $-\delta$ for $K_l+1 \leq k \leq K_u$ in the stop band, respectively. Then, obtained peak stop band ripple minimization formulation can be written as:

$$\min_{\mathbf{h}\in\mathbb{R}^L,\delta\in\mathbb{R}} \quad \delta, \tag{2.14a}$$

$$\text{subject to} \quad \mathbf{h}^T\mathbf{v}(\omega_k) \leq a_k,\ 0 \leq k \leq K_s, \tag{2.14b}$$

$$\mathbf{h}^T\mathbf{v}(\omega_k) \leq \delta,\ K_s+1 \leq k \leq K_u, \tag{2.14c}$$

$$\mathbf{h}^T\mathbf{v}(\omega_k) \geq b_k,\ 0 \leq k \leq K_l, \tag{2.14d}$$

$$\mathbf{h}^T\mathbf{v}(\omega_k) \geq -\delta,\ K_l+1 \leq k \leq K_u, \tag{2.14e}$$

$$\mathbf{h} \text{ is symmetric.} \tag{2.14f}$$

(2.14) can be solved by using *Algorithm 2*. Since (2.14) is a convex LP formulation, obtained filter coefficients $\mathbf{h}^\star$ are globally optimal and hence, provide the minimum peak stop band ripple among linear phase filters for the given set of magnitude constraints. Next, a peak stop band ripple minimization type linear phase FIR filter design example is demonstrated.

n	$h_n^\star$	n	$h_n^\star$	n	$h_n^\star$	n	$h_n^\star$
1	0.0062	11	-0.0139	21	0.2837	31	-0.0098
2	0.0006	12	0.0196	22	0.1272	32	0.0109
3	-0.0086	13	0.0402	23	-0.0172	33	0.0150
4	-0.0165	14	0.0158	24	-0.0733	34	0.0018
5	-0.0132	15	-0.0420	25	-0.0420	35	-0.0132
6	0.0018	16	-0.0733	26	0.0158	36	-0.0165
7	0.0150	17	-0.0172	27	0.0402	37	-0.0086
8	0.0109	18	0.1272	28	0.0196	38	0.0006
9	-0.0098	19	0.2837	29	-0.0139	39	0.0062
10	-0.0254	20	0.3513	30	-0.0254		

Table 2.4: Linear phase FIR filter coefficients for *Design 2.4* are given in 4 significant digits.

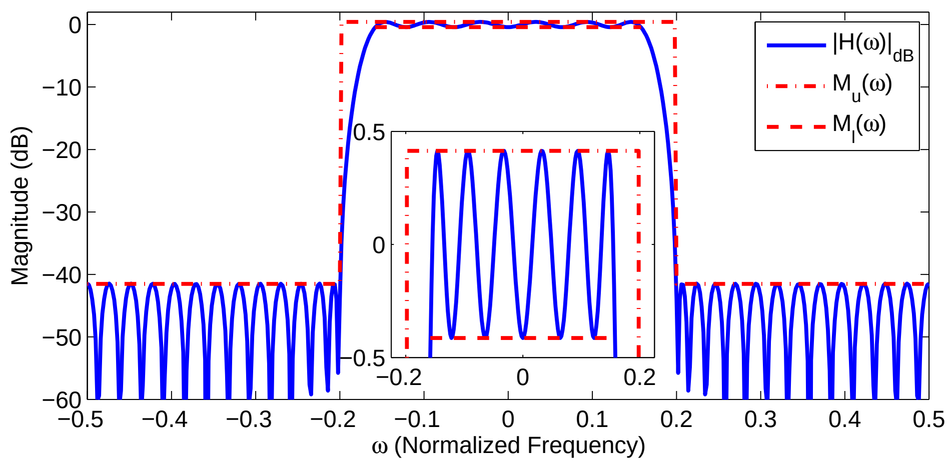

Figure 2.9: Magnitude response of $L^\star = 39$ length FIR filter coefficients found by solving the problem given in *Design 2.4* using LP model. Total stop band energy is $-45dB$ and peak stop band ripple is $-42dB$.

Design 2.4 *Given the lower and upper frequency response mask constraints,* $M_l(\omega)$, $0 \leq \omega \leq \omega_l$ *and* $M_u(\omega)$, $0 \leq \omega \leq \omega_s$ *shown in* Figure 2.6, *design a linear phase FIR filter with minimum peak stop band ripple for* $L = 39$ *by using* (2.14).

For this design, the LP optimization problem in (2.14) is solved for $L = 39$ using *Algorithm 2*. $\mathbf{h}^\star$, its magnitude response and phase response are given in *Table 2.4*, *Figure 2.9* and *Figure 2.10*, respectively. Achieved stop band energy and peak stop band ripple level in *Figure 2.10* are found to be -45dB and -42dB,

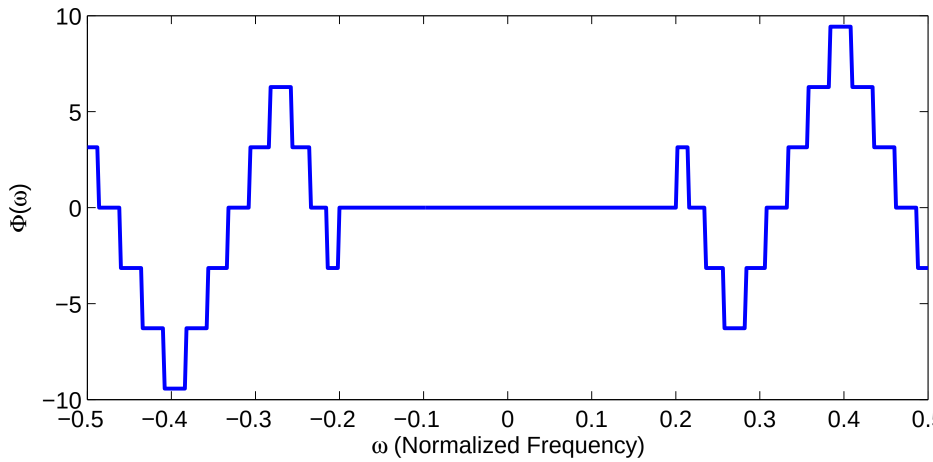

Figure 2.10: Phase response of $L^{\star} = 39$ length FIR filter coefficients that is obtained using LP model given in (2.14). Obtained $\mathbf{h}^{\star}$ provides linear phase response.

respectively. Note that obtained slution is globally optimal among linear phase solution set.

In this section, convex LP formulations of non-linear and linear phase FIR filter design are demonstrated. Design examples for minimal stop band energy and minimum peak stop band ripple formulations are shown. Even though constructed LPs are capable of designing optimal linear and non-linear phase filters, in some design problems, symmetry constraint in linear phase formulation can be too tight to satisfy or non-linear phase design may not satisfy desired phase constraints. Hence, in these applications one may desire to introduce phase or group delay mask constraints on a portion of frequency response, i.e., on pass band. However, since phase and group delay mask constraints cannot be formulated as a linear function of autocorrelation function, they cannot be introduced in LP formulations. Hence, it is not possible to design filters, which has phase response in between linear and non-linear phase. On contrast to LP and QCQP, phase and group delay mask constraints can be introduced in SDP, in which optimization is conducted over matrix variables. Hence, in the following sections, SDP is introduced and a convex SDP model, which can implement constraints on magnitude, phase and group delay, is obtained by applying semidefinite relaxation (SDR) on (2.6).

2.3 Semidefinite Programming Formulation

Since semidefinite programming is based on matrix variables, a larger set of constraints including phase and group delay mask constraints can be implemented in a convex and flexible manner in contrast to QCQP and LP formulations. In this section, SDP and Semidefinite Relaxation (SDR) for non-convex QCQP problems will be introduced. Then, SDP formulation of FIR filter design will be derived from non-convex QCQP given in (2.6) using SDR. Since SDR of (2.6) is equivalent to the second dual of (2.6), obtained formulation is guaranteed to be convex.

2.3.1 Semidefinite Programming

In semidefinite programming, the goal is to minimize a linear function subject to a positive semidefinite (PSD) matrix constraint. Other constraint types as linear and quadratic constraints can be implemented in SDP using matrix variables. Hence, SDP combines several standard problems such as linear and quadratic programming problems and is widely used in engineering and combinatorial optimization [57]. Below, *Definition 2.1* introduces the general form of an SDP problem.

Definition 2.1 (Semidefinite Programming) *[57] Consider the problem of minimizing a linear function of a variable* $\mathbf{x} \in \mathbb{R}^L$ *subject to a matrix inequality:*

$$\min_{\mathbf{x}\in\mathbb{R}^L} \mathbf{c}^T\mathbf{x}, \tag{2.15a}$$

$$\text{subject to } \mathbf{F}(\mathbf{x}) \succeq 0, \tag{2.15b}$$

where

$$\mathbf{F}(\mathbf{x}) \triangleq \mathbf{F}_0 + \sum_{i=1}^{L} \mathbf{x}_i \mathbf{F}_i. \tag{2.16}$$

In (2.15) *and* (2.16), $\mathbf{c} \in \mathbb{R}^L$, $\mathbf{F}(\mathbf{x})$ *is* $\mathbf{x}$ *dependent PSD matrix and* $\mathbf{F}_i \in \mathbb{R}^{m\times m}$ *in general for* $i = 1, .., L$ *are all real symmetric matrices. Sign* $\succeq$ *in* (2.15) *means that* $\mathbf{F}(\mathbf{x})$ *is PSD, i.e.,* $\mathbf{z}^T\mathbf{F}(\mathbf{x})\mathbf{z} \geq 0$ *for all* $\mathbf{z} \in \mathbb{R}^m$*. Since both objective and constraint in* (2.15) *are convex, this model is convex and called semidefinite programming problem.*

Non-convex QCQP of (2.6) can be written in the form of (2.15) using the following equalities:

$$\mathbf{h}^T\mathbf{A}_s\mathbf{h} = \mathrm{Tr}(\mathbf{h}^T\mathbf{A}_s\mathbf{h}) = \mathrm{Tr}(\mathbf{A}_s\mathbf{h}\mathbf{h}^T) = \mathrm{Tr}(\mathbf{A}_s\mathbf{H}), \tag{2.17a}$$

$$\mathbf{h}^T\mathbf{A}_k\mathbf{h} = \mathrm{Tr}(\mathbf{h}^T\mathbf{A}_k\mathbf{h}) = \mathrm{Tr}(\mathbf{A}_k\mathbf{h}\mathbf{h}^T) = \mathrm{Tr}(\mathbf{A}_k\mathbf{H}), \tag{2.17b}$$

where $\mathbf{h}\mathbf{h}^T = \mathbf{H}$ and $\mathbf{H} \succeq 0$, i.e., positive semidefinite. In addition, $\mathbf{H}$ is rank-1 since it is outer product of $\mathbf{h}$. Then, (2.6) can be rewritten as follows:

$$\min_{\mathbf{H}\in\mathbb{R}^{L\times L}} \quad \mathrm{Tr}(\mathbf{A}_s\mathbf{H}), \tag{2.18a}$$

$$\text{subject to} \quad \mathrm{Tr}(\mathbf{A}_k\mathbf{H}) \le a_k,\ 0 \le k \le K_u, \tag{2.18b}$$

$$\mathrm{Tr}(\mathbf{A}_k\mathbf{H}) \ge b_k,\ 0 \le k \le K_l, \tag{2.18c}$$

$$\mathbf{H} \succeq 0, \tag{2.18d}$$

$$\mathrm{rank}(\mathbf{H}) = 1. \tag{2.18e}$$

In (2.18), objective is an affine function of $\mathbf{H}$ and hence is in the form of (2.15a). Similarly, constraints (2.18b) and (2.18c) are affine and hence convex. In addition, (2.18d) is directly equivalent to (2.15b). This can easily be observed by putting $\mathbf{h}$ instead of $\mathbf{x}$ and writing the equality $\mathbf{F}(\mathbf{h}) = \mathbf{h}\mathbf{h}^T = \mathbf{H}$, i.e., $\mathbf{F}_1 = [\mathbf{h}, \mathbf{0}, .., \mathbf{0}]^T, \mathbf{F}_2 = [\mathbf{0}, \mathbf{h}, \mathbf{0}, .., \mathbf{0}]^T, ..., \mathbf{F}_L = [\mathbf{0}, \mathbf{0}, \mathbf{0}, .., \mathbf{h}]^T$. However, (2.18e) is not in the form of (2.15) and indeed is non-convex since rank-1 constraint can be written as $\mathbf{H} = \mathbf{h}\mathbf{h}^T$ and outer product $\mathbf{h}\mathbf{h}^T$ contains cross terms $h_j h_k$, which are non-convex multiplications of two variables. Hence, even though non-convex (2.6c) became convex in (2.18c) by using (2.17b), because of non-convex rank-1 constraint (2.18e), (2.18) is still non-convex. In order to obtain a convex SDP model, rank-1 constraint can be omitted and (2.18) can be rewritten as follows:

$$\min_{\mathbf{H}\in\mathbb{R}^{L\times L}} \quad \mathrm{Tr}(\mathbf{A}_s\mathbf{H}), \tag{2.19a}$$

$$\text{subject to} \quad \mathrm{Tr}(\mathbf{A}_k\mathbf{H}) \le a_k,\ 0 \le k \le K_u, \tag{2.19b}$$

$$\mathrm{Tr}(\mathbf{A}_k\mathbf{H}) \ge b_k,\ 0 \le k \le K_l, \tag{2.19c}$$

$$\mathbf{H} \succeq 0. \tag{2.19d}$$

(2.19) is an SDP formulation since it is completely in the form of (2.15). The procedure that is applied above to obtain convex SDP (2.19) from non-convex

QCQP (2.6) is named lifting. As it will be shown in the next section, applying lifting on (2.6) and finding the second dual of (2.6) are equivalent. Since second dual of a minimization problem is guaranteed to be convex, NP-hard QCQPs can be cast as SDP problems using lifting.

2.3.2 Semidefinite Relaxation for NP-Hard QCQP Problems

In this section, semidefinite relaxation (SDR) will be derived and applied on non-convex (2.6) to obtain a convex SDP formulation. Obtained SDP will turn out to be equivalent to (2.19). In order to derive SDR, first underlying theory of duality will be reviewed.

2.3.2.1 Duality

Before giving the definition of *Duality*, we first introduce *Lagrangian* of an optimization problem since *Duality* is defined over *Lagrangian*. In order to obtain the definition of *Lagrangian*, the following general optimization problem, not necessarily convex, is defined [24]:

$$\min_{\mathbf{x}\in\mathbb{R}^L} \quad f_0(\mathbf{x}), \tag{2.20a}$$

$$\text{subject to} \quad f_i(\mathbf{x}) \leq 0,\ 1 \leq i \leq m, \tag{2.20b}$$

$$h_i(\mathbf{x}) = 0,\ 1 \leq i \leq p, \tag{2.20c}$$

where the domain of (2.20) $\mathbb{D}$ is defined as $\mathbb{D} = \bigcap_{i=0}^{m} \mathbf{dom}(f_i(\mathbf{x})) \cap \bigcap_{i=0}^{p} \mathbf{dom}(h_i(\mathbf{x}))$ and $\mathbb{D}$ is non-empty.

Definition 2.2 (Lagrangian): *[24] For standard optimization problem given in* (2.20), Lagrangian $\mathcal{L} : \mathbb{R}^L \times \mathbb{R}^m \times \mathbb{R}^p \rightarrow \mathbb{R}$ *is written as follows:*

$$\mathcal{L}(\mathbf{x}, \boldsymbol{\lambda}, \boldsymbol{\nu}) = f_0(\mathbf{x}) + \sum_{i=1}^{m} \lambda_i f_i(\mathbf{x}) + \sum_{i=1}^{p} \nu_i h_i(\mathbf{x}), \tag{2.21}$$

where $\mathbf{dom}(\mathcal{L}) = \mathbb{D} \times \mathbb{R}^m \times \mathbb{R}^p$. *Coefficients* λ_i *and* ν_i *are referred as* Lagrange multipliers *associated with* i^{th} *inequality and equality constraints, respectively.* $\boldsymbol{\lambda}$ *and* $\boldsymbol{\nu}$ *are called the* dual variables *[24].*

Definition 2.3 (Dual function): *[24] Infimum of* Lagrangian $\mathcal{L}$ *given in* (2.21) *is defined as the* dual function *of* (2.20) *and written as:*

$$g(\boldsymbol{\lambda}, \boldsymbol{\nu}) = \inf_{\mathbf{x} \in \mathbb{D}} \mathcal{L}(\mathbf{x}, \boldsymbol{\lambda}, \boldsymbol{\nu}) = \inf_{\mathbf{x} \in \mathbb{D}} \left(f_0(\mathbf{x}) + \sum_{i=1}^{m} \lambda_i f_i(\mathbf{x}) + \sum_{i=1}^{p} \nu_i h_i(\mathbf{x}) \right), \tag{2.22}$$

where $g(\boldsymbol{\lambda}, \boldsymbol{\nu})$ *denotes the* dual function *and* $\inf(.)$ *represents* infimum *operation.*

Proposition 2.1 *[24] For the minimization problem given in* (2.20), dual function $g(\boldsymbol{\lambda}, \boldsymbol{\nu})$ *is always concave since* $g(\boldsymbol{\lambda}, \boldsymbol{\nu})$ *is the infimum of a family of affine functions of* $\boldsymbol{\lambda}$ *and* $\boldsymbol{\nu}$. *Similarly, for a maximization problem,* $g(\boldsymbol{\lambda}, \boldsymbol{\nu})$ *is always convex.*

Proposition 2.2 (Lower bound): *[24] Let* $p^\star$ *denote the optimal value of* primal *optimization problem, i.e. minimum value for* (2.20). *Then, for any* $\boldsymbol{\lambda} \succeq 0$*, i.e.,* $\lambda_i \geq 0, \forall i = 1, .., m$ *(all* Lagrange multipliers *for each inequality constraint) and any* $\boldsymbol{\nu}$ *(all* Lagrange multipliers *for each equality constraint), following inequality is true:*

$$g(\boldsymbol{\lambda}, \boldsymbol{\nu}) \leq p^\star. \tag{2.23}$$

Proof and details of *Property 2.2* can be found in [24] in section 5.1.3.

Definition 2.4 (Lagrange dual problem): *[24] By using* Definition 2.3, Property 2.1 *and* Property 2.2, Lagrange dual problem *is written as follows:*

$$\max_{\boldsymbol{\lambda} \in \mathbb{R}^m, \boldsymbol{\nu} \in \mathbb{R}^p} \quad g(\boldsymbol{\lambda}, \boldsymbol{\nu}) \tag{2.24a}$$

$$\text{subject to} \quad \boldsymbol{\lambda} \succeq 0, \tag{2.24b}$$

where the goal of (2.24) *is to obtain the best lower bound to* primal problem (2.20). *In* (2.24), $(\boldsymbol{\lambda}, \boldsymbol{\nu})$ *is called* dual feasible *if* $\boldsymbol{\lambda} \succeq 0$ *and* $g(\boldsymbol{\lambda}, \boldsymbol{\nu}) \geq -\infty$. $(\boldsymbol{\lambda}^\star, \boldsymbol{\nu}^\star)$ *is referred as* dual optimal *if they are optimal variable values for* (2.24).

There exist additional important properties, definitions, and theorems for *Duality* such as weak duality, strong duality, and Slater's conditions. However, further discussion will be referred to literature [24, 44, 58] since definitions and properties defined in this section are enough to derive SDR for QCQP problems. Further discussion regarding *Duality* can be found in [24], in chapter 5.

2.3.2.2 Semidefinite Relaxation

In this section, a convexified formulation for the QCQP problem given in (2.6) will be derived. First, *Lagrangian dual* (D) of *primal* (P), i.e., (2.6), will be obtained. Then, second dual (DD) of (P) will be obtained by finding the dual of (D). *Property 2.1* guarantees that (DD) is a convex function for (P) since (P) is a minimization problem. It will be shown that (DD) is equivalent to the SDP given in (2.19) that is obtained by lifting. Finally, the definition of SDR will be given for QCQP problems of type (2.6).

Proposition 2.3 (Existence of global solution): *[24] Reconsider the problem* (2.6)*:*

$$
\text{(P)} \qquad \begin{aligned}
\min_{\mathbf{h}\in\mathbb{R}^L} \quad & \mathbf{h}^T\mathbf{A}_s\mathbf{h}, && \text{(2.6a)}\\
\text{subject to} \quad & \mathbf{h}^T\mathbf{A}_k\mathbf{h} \le a_k,\ 0 \le k \le K_u, && \text{(2.6b)}\\
& \mathbf{h}^T\mathbf{A}_k\mathbf{h} \ge b_k,\ 0 \le k \le K_l. && \text{(2.6c)}
\end{aligned}
$$

Note that $\mathbf{A}_k \succeq 0$ *and hence,* $0 \le \mathbf{h}^T\mathbf{A}_k\mathbf{h} \le a_k,\ 0 \le k \le K_u$*. For that reason,* (2.6) *is bounded below and above. Since spectral mask constraints of form Figure 2.1 and Figure 2.6 are considered in FIR filter design,* $a_k \ge b_k, 0 \le k \le K_u$*. Hence, feasible set of* (2.6) *is non-empty for large enough* L*. In addition, the feasible set, which is defined by the constraints of* (2.6)*, is closed and* (2.6a), (2.6b) *and* (2.6c) *are continuous functions of* $\mathbf{h}$*. Hence, feasible set of* (2.6) *is compact and hence,* (2.6) *possesses a global minimum as stated by Weierstrass extreme value theorem.*

Since (2.6) is bounded, *Lagrangian dual* can be obtained through *Lagrangian* of (P), which can be written as:

$$\mathcal{L}(\mathbf{h}, \boldsymbol{\lambda}) = \mathbf{h}^T \mathbf{A}_s \mathbf{h} + \sum_{k=0}^{K_u} \lambda_k (\mathbf{h}^T \mathbf{A}_k \mathbf{h} - a_k) + \sum_{k=0}^{K_l} \lambda_{K+k} (b_k - \mathbf{h}^T \mathbf{A}_k \mathbf{h}), \tag{2.25}$$

where $K = K_u + 1$ and $\boldsymbol{\lambda} \succeq 0$ is chosen to meet the requirements given in *Property 2.2*. Lagrangian dual can be found by taking infimum over $\mathbf{h}$ of the Lagrangian that is given in (2.25), as follows:

$$\begin{aligned} g(\boldsymbol{\lambda}) &= \inf_{\mathbf{h} \in \mathbb{R}^L} \mathcal{L}(\mathbf{h}, \boldsymbol{\lambda}) \\ &= \inf_{\mathbf{h} \in \mathbb{R}^L} \left(\mathbf{h}^T \mathbf{A}_s \mathbf{h} + \sum_{k=0}^{K_u} \lambda_k (\mathbf{h}^T \mathbf{A}_k \mathbf{h} - a_k) + \sum_{k=0}^{K_l} \lambda_{K+k} (b_k - \mathbf{h}^T \mathbf{A}_k \mathbf{h}) \right), \end{aligned} \tag{2.26}$$

where K_l is smaller than K_u. Note that the result of (2.26) will be a concave function as stated in *Property 2.1* since primal is a minimization problem. By making some algebraic manipulations and vectorizing $\boldsymbol{\lambda}$, (2.26) can be written in a more compact form as follows:

$$\begin{aligned} g(\boldsymbol{\lambda}) &= \inf_{\mathbf{h} \in \mathbb{R}^L} \left(\mathbf{h}^T \mathbf{A}_s \mathbf{h} + \sum_{k=0}^{K_u} \lambda_k \mathbf{h}^T \mathbf{A}_k \mathbf{h} - \sum_{k=0}^{K_l} \lambda_{K+k} \mathbf{h}^T \mathbf{A}_k \mathbf{h} - \sum_{k=0}^{K_u} \lambda_k a_k + \sum_{k=0}^{K_l} \lambda_{K+k} b_k \right) \\ &= \inf_{\mathbf{h} \in \mathbb{R}^L} \left(\mathbf{h}^T \mathbf{A}_s \mathbf{h} + \sum_{k=0}^{K_u} \mathbf{h}^T (\lambda_k \mathbf{A}_k) \mathbf{h} - \sum_{k=0}^{K_l} \mathbf{h}^T (\lambda_{K+k} \mathbf{A}_k) \mathbf{h} - \sum_{k=0}^{K_u} \lambda_k a_k + \sum_{k=0}^{K_l} \lambda_{K+k} b_k \right) \\ &= \inf_{\mathbf{h} \in \mathbb{R}^L} \left(\mathbf{h}^T \left(\mathbf{A}_s + \sum_{k=0}^{K_u} \lambda_k \mathbf{A}_k - \sum_{k=0}^{K_l} \lambda_{K+k} \mathbf{A}_k \right) \mathbf{h} - \sum_{k=0}^{K_u} \lambda_k a_k + \sum_{k=0}^{K_l} \lambda_{K+k} b_k \right) \\ &= \inf_{\mathbf{h} \in \mathbb{R}^L} \left(\mathbf{h}^T \mathbf{C}(\boldsymbol{\lambda}) \mathbf{h} - \boldsymbol{\lambda}^T \mathbf{c} \right), \end{aligned} \tag{2.27}$$

where the following equalities are used:

$$\mathbf{C}(\boldsymbol{\lambda}) = \mathbf{A}_s + \sum_{k=0}^{K_u} \lambda_k \mathbf{A}_k - \sum_{k=0}^{K_l} \lambda_{K+k} \mathbf{A}_k, \tag{2.28a}$$

$$\boldsymbol{\lambda}^T \mathbf{c} = \sum_{k=0}^{K_u} \lambda_k a_k + \sum_{k=0}^{K_l} \lambda_{K+k} b_k. \tag{2.28b}$$

In (2.28), $\boldsymbol{\lambda}$ and $\mathbf{c}$ are given as column vectors, $\boldsymbol{\lambda} = [\lambda_0, ..., \lambda_{K+K_l}]^T$ and $\mathbf{c} = [a_0, ..., a_{K-1}, -b_0, ..., -b_{K_l}]^T$, respectively. By evaluating the expression in (2.27),

$g(\boldsymbol{\lambda})$ is obtained in piecewise function form as:

$$g(\boldsymbol{\lambda}) = \begin{cases} -\boldsymbol{\lambda}^T \mathbf{c}, & \text{if } \mathbf{C}(\boldsymbol{\lambda}) \succeq 0, \quad (2.29a) \\ -\infty, & \text{otherwise.} \quad (2.29b) \end{cases}$$

In (2.29), $\boldsymbol{\lambda} \succeq 0$ because of *Property 2.2*. By using (2.29), $\boldsymbol{\lambda} \succeq 0$ and *Definition 2.4*, (D) can be written as:

$$\text{(D)} \quad \begin{aligned} &\max_{\boldsymbol{\lambda} \in \mathbb{R}^{K+K_l+1}} && -\boldsymbol{\lambda}^T \mathbf{c} && (2.30a) \\ &\text{subject to} && \boldsymbol{\lambda} \succeq 0, && (2.30b) \\ & && \mathbf{C}(\boldsymbol{\lambda}) \succeq 0. && (2.30c) \end{aligned}$$

In accordance with *Property 2.1*, (2.30) is a concave optimization problem. However, it can be transformed to a convex problem by changing the sign of objective function and replacing max with min as follows:

$$\text{(D)} \quad \begin{aligned} &\min_{\boldsymbol{\lambda} \in \mathbb{R}^{K+K_l+1}} && \boldsymbol{\lambda}^T \mathbf{c} && (2.31a) \\ &\text{subject to} && \boldsymbol{\lambda} \succeq 0, && (2.31b) \\ & && \mathbf{C}(\boldsymbol{\lambda}) \succeq 0. && (2.31c) \end{aligned}$$

Note that obtained *dual* (2.31) is a convex SDP formulation of form (2.15) with linear objective, affine constraints (2.31b) and semidefinite constraint (2.31c).

Next, second dual (DD) of (P) will be obtained by deriving the *Lagrangian dual* of (D). Since (D) given in (2.30) is concave, (DD) will be convex as stated in *Property 1*. At the end, it will be shown that obtained convex optimization problem is a convex relaxation to (P). To obtain (DD), first *Lagrangian* of (2.30) is written as:

$$\mathcal{L}_D(\boldsymbol{\lambda}, \mathbf{H}) = -\boldsymbol{\lambda}^T \mathbf{c} + \langle \mathbf{C}(\boldsymbol{\lambda}), \mathbf{H} \rangle , \tag{2.32}$$

where subscript $(.)_D$ denotes dual and $\langle ., . \rangle$ refers to inner product. To proceed further, following properties of inner product will be given and proven.

Proposition 2.4 *For any three matrix* $\mathbf{X}, \mathbf{Y}, \mathbf{Z} \in \mathbb{R}^{m \times n}$ *and scalar* ζ*, the following equalities exist:*

$$\langle \mathbf{X}, \mathbf{Y} \rangle = \mathrm{Tr}(\mathbf{X}^T \mathbf{Y}) = \mathrm{Tr}(\mathbf{Y}^T \mathbf{X}) = \langle \mathbf{Y}, \mathbf{X} \rangle , \tag{2.33a}$$

$$\langle \zeta \mathbf{X} + \mathbf{Z}, \mathbf{Y} \rangle = \zeta \langle \mathbf{X}, \mathbf{Y} \rangle + \langle \mathbf{Z}, \mathbf{Y} \rangle . \tag{2.33b}$$

Proof 2.1 (2.33a):

$$\langle \mathbf{X}, \mathbf{Y} \rangle = \langle \mathbf{Y}, \mathbf{X} \rangle = \sum_{i=1}^{m} \sum_{j=1}^{n} \mathbf{X}_{ij} \mathbf{Y}_{ij}$$

$$= \sum_{j=1}^{n} \sum_{i=1}^{m} (\mathbf{X}^T)_{ji} \mathbf{Y}_{ij} = \sum_{j=1}^{n} (\mathbf{X}^T \mathbf{Y})_{jj} = \mathrm{Tr}(\mathbf{X}^T \mathbf{Y}), \tag{2.34a}$$

or

$$= \sum_{j=1}^{n} \sum_{i=1}^{m} (\mathbf{Y}^T)_{ji} \mathbf{X}_{ij} = \sum_{j=1}^{n} (\mathbf{Y}^T \mathbf{X})_{jj} = \mathrm{Tr}(\mathbf{Y}^T \mathbf{X}), \tag{2.34b}$$

where subscripts $(.)_{ij}$ *refer to the value at* i^{th} *column and* j^{th} *row of their matrix argument.*

Proof 2.2 (2.33b):

$$\langle \zeta \mathbf{X} + \mathbf{Z}, \mathbf{Y} \rangle = \mathrm{Tr}(\mathbf{Y}^T (\zeta \mathbf{X} + \mathbf{Z})) = \mathrm{Tr}(\zeta \mathbf{Y}^T \mathbf{X} + \mathbf{Y}^T \mathbf{Z})$$

$$= \zeta \mathrm{Tr}(\mathbf{Y}^T \mathbf{X}) + \mathrm{Tr}(\mathbf{Y}^T \mathbf{Z}) = \zeta \langle \mathbf{X}, \mathbf{Y} \rangle + \langle \mathbf{Z}, \mathbf{Y} \rangle, \tag{2.35}$$

where in (2.35) *linearity of trace operation and* (2.33a) *are used.*

Using $\mathcal{L}_D(\boldsymbol{\lambda}, \mathbf{H})$ and *Property 2.4*, *dual function* $f(\mathbf{H})$ can be obtained as:

$$\begin{aligned} f(\mathbf{H}) &= \sup_{\boldsymbol{\lambda} \succeq 0} \left(-\boldsymbol{\lambda}^T \mathbf{c} + \langle \mathbf{C}(\boldsymbol{\lambda}), \mathbf{H} \rangle \right) \\ &= \sup_{\boldsymbol{\lambda} \succeq 0} \left(-\boldsymbol{\lambda}^T \mathbf{c} + \left\langle \mathbf{A}_s + \sum_{k=0}^{K_u} \lambda_k \mathbf{A}_k - \sum_{k=0}^{K_l} \lambda_{K+k} \mathbf{A}_k, \mathbf{H} \right\rangle \right) \\ &= \sup_{\boldsymbol{\lambda} \succeq 0} \left(-\boldsymbol{\lambda}^T \mathbf{c} + \langle \mathbf{A}_s, \mathbf{H} \rangle + \left\langle \sum_{k=0}^{K_u} \lambda_k \mathbf{A}_k, \mathbf{H} \right\rangle - \left\langle \sum_{k=0}^{K_l} \lambda_{K+k} \mathbf{A}_k, \mathbf{H} \right\rangle \right) \\ &= \sup_{\boldsymbol{\lambda} \succeq 0} \left(-\boldsymbol{\lambda}^T \mathbf{c} + \langle \mathbf{A}_s, \mathbf{H} \rangle + \sum_{k=0}^{K_u} \lambda_k \langle \mathbf{A}_k, \mathbf{H} \rangle - \sum_{k=0}^{K_l} \lambda_{K+k} \langle \mathbf{A}_k, \mathbf{H} \rangle \right) \\ &= \sup_{\boldsymbol{\lambda} \succeq 0} \left(-\boldsymbol{\lambda}^T \mathbf{c} + \langle \mathbf{A}_s, \mathbf{H} \rangle + \boldsymbol{\lambda}^T \boldsymbol{\eta} \right) \\ &= \sup_{\boldsymbol{\lambda} \succeq 0} \left(\boldsymbol{\lambda}^T (\boldsymbol{\eta} - \mathbf{c}) + \langle \mathbf{A}_s, \mathbf{H} \rangle \right), \end{aligned} \tag{2.36}$$

where sup(.) denotes the supremum operation and $\boldsymbol{\lambda}^T \boldsymbol{\eta}$, $\boldsymbol{\eta}$ are given as:

$$\boldsymbol{\lambda}^T \boldsymbol{\eta} = \sum_{k=0}^{K_u} \lambda_k \langle \mathbf{A}_k, \mathbf{H} \rangle - \sum_{k=0}^{K_l} \lambda_{K+k} \langle \mathbf{A}_k, \mathbf{H} \rangle, \tag{2.37a}$$

$$\boldsymbol{\eta} = [\langle \mathbf{A}_0, \mathbf{H} \rangle, \langle \mathbf{A}_1, \mathbf{H} \rangle, ..., \langle \mathbf{A}_{K_u}, \mathbf{H} \rangle, -\langle \mathbf{A}_0, \mathbf{H} \rangle, ..., -\langle \mathbf{A}_{K_l}, \mathbf{H} \rangle]^T. \tag{2.37b}$$

By evaluating the expression in (2.36), *Lagrangian dual* $f(\mathbf{H})$ is obtained as:

$$g(\boldsymbol{\lambda}) = \begin{cases} \langle \mathbf{A}_s, \mathbf{H} \rangle, & \text{if } \boldsymbol{\eta} \preceq \mathbf{c}, \quad (2.38a) \\ \infty, & \text{otherwise.} \quad (2.38b) \end{cases}$$

In (2.38), $\mathbf{H} \succeq 0$ because of *Property 2.2*. By using (2.38), $\mathbf{H} \succeq 0$ and *Definition 2.4*, *Lagrangian dual problem* (DD) is written as:

$$\text{(DD)} \qquad \begin{aligned} \min_{\mathbf{H} \in \mathbb{R}^{L \times L}} \ & \langle \mathbf{A}_s, \mathbf{H} \rangle && (2.39a) \\ \text{subject to} \ & \mathbf{H} \succeq 0, && (2.39b) \\ & \boldsymbol{\eta} \preceq \mathbf{c}. && (2.39c) \end{aligned}$$

Note that (2.39) is the second dual of primal non-convex problem (P) and it is a convex SDP problem. Hence, (DD) is indeed a convex relaxation to (P). Obtained convex SDP can be rewritten in a more suitable form for FIR filter design problems by expanding $\boldsymbol{\eta}$ and $\mathbf{c}$ in (2.39) as:

$$\text{(DD)} \qquad \begin{aligned} \min_{\mathbf{H} \in \mathbb{R}^{L \times L}} \ & \langle \mathbf{A}_s, \mathbf{H} \rangle && (2.40a) \\ \text{subject to} \ & \mathbf{H} \succeq 0, && (2.40b) \\ & \langle \mathbf{A}_k, \mathbf{H} \rangle \leq a_k, \ 0 \leq k \leq K_u, && (2.40c) \\ & \langle \mathbf{A}_k, \mathbf{H} \rangle \geq b_k, \ 0 \leq k \leq K_l. && (2.40d) \end{aligned}$$

Then, by using *Property 2.4* and noting that $\mathbf{A}_k = \mathbf{A}_k^T$, $0 \leq k \leq K_u$, and $\mathbf{A}_s = \mathbf{A}_s^T$, (2.40) can be written as:

$$\text{(DD)} \qquad \begin{aligned} \min_{\mathbf{H} \in \mathbb{R}^{L \times L}} \ & \mathrm{Tr}(\mathbf{A}_s \mathbf{H}) && (2.41a) \\ \text{subject to} \ & \mathrm{Tr}(\mathbf{A}_k \mathbf{H}) \leq a_k, \ 0 \leq k \leq K_u, && (2.41b) \\ & \mathrm{Tr}(\mathbf{A}_k \mathbf{H}) \geq b_k, \ 0 \leq k \leq K_l, && (2.41c) \\ & \mathbf{H} \succeq 0. && (2.41d) \end{aligned}$$

Note that (2.41) is in the form of an SDP that is defined in (2.15) and is indeed equivalent to (2.18), which is obtained by applying lifting on (2.6). Both (2.18) and (2.41) are called semidefinite relaxation (SDR) of non-convex QCQP given in (2.6). Since (2.18), equivalently (2.41), is convex, globally optimal solution of (2.18) can be obtained in an efficient manner by using interior-point solvers. Finally, the general definition of semidefinite relaxation is given below.

Definition 2.5 (Semidefinite Relaxation): *[59] Let* $\mathbf{M}$ *and* $\mathbf{N}_i$ *be all real symmetric matrices and* d_i *be real* $\forall i$. *Then, define the QCQP problem:*

$$\min_{\mathbf{x}\in\mathbb{R}^L} \ \mathbf{x}^T\mathbf{M}\mathbf{x} \tag{2.42a}$$

$$\text{subject to } \mathbf{x}^T\mathbf{N}_i\mathbf{x} \trianglerighteq_i d_i, \ \forall i, \tag{2.42b}$$

where optimization is conducted over $\mathbf{x}$ *and* $\trianglerighteq_i$ *can be replaced by* $\leq$, $\geq$, *or* $=$, *for any* i. *Then, semidefinite relaxation for* (2.42) *is given by the following convex SDP problem:*

$$\min_{\mathbf{X}\in\mathbb{R}^{L\times L}} \ \mathrm{Tr}(\mathbf{M}\mathbf{X}) \tag{2.43a}$$

$$\text{subject to } \mathrm{Tr}(\mathbf{N}_i\mathbf{X}) \trianglerighteq_i d_i, \ \forall i, \tag{2.43b}$$

$$\mathbf{X} \succeq 0. \tag{2.43c}$$

SDR is indeed a tight relaxation in certain cases, i.e., solving relaxed problem is equivalent to solving original QCQP problem. Hence, SDR is quite handful for QCQP formulations. Details on the tightness of SDR can be found in [59], whereas the derivation of *Definition 2.5* is already given above.

Even though (2.41), SDR of (2.6), is convex, optimization in (2.41) is conducted over non-negative symmetric matrices rather than vectors. Since $\mathbf{H}$ is symmetric, by increasing the number of variables from L to $L(L+1)/2$, quadratic cost function and quadratic constraints of (2.6) are handled as linear cost and linear constraints in (2.41). Hence, obtained solution $\mathbf{H}^\star$ is optimal, but must be decomposed to FIR filter coefficient vector. $\mathbf{H}^\star$ can be factored as $\mathbf{H}^\star = \mathbf{h}^\star\mathbf{h}^{\star T}$, where $\mathbf{h}^\star$ is an optimal solution to (2.6), if $\mathbf{H}^\star$ is rank-1. However, since (2.41) does not restrict feasible set to rank-1 matrices and since interior-point optimization solvers tend to find the solution with maximal rank among all the solutions [59], $\mathbf{H}^\star$ can possess higher rank. Then, $\tilde{\mathbf{h}}^*$, the estimate of $\mathbf{h}^\star$, can be obtained as:

$$\tilde{\mathbf{h}}^\star = \sqrt{\sigma_1^\star}\mathbf{u}_1^\star, \tag{2.44}$$

where $\sigma_1^\star$ is the largest singular value of $\mathbf{H}^\star$ and $\mathbf{u}_1^\star$ is the corresponding singular vector. However, $\mathbf{H}^*$ can deviate from a rank-1 matrix significantly. Hence, the response of the resulting filter coefficients in (2.41) typically violates the constraints. This phenomenon is demonstrated on a non-linear phase FIR filter design example in *Design 2.5*.

n	$h_n^\star$	n	$h_n^\star$	n	$h_n^\star$	n	$h_n^\star$
1	-0.0033	11	-0.0190	21	0.0377	31	-0.0300
2	-0.0166	12	-0.0406	22	0.0177	32	0.0197
3	-0.0425	13	-0.0222	23	-0.0205	33	0.0678
4	-0.0723	14	0.0172	24	-0.0383	34	0.0864
5	-0.0864	15	0.0383	25	-0.0171	35	0.0724
6	-0.0677	16	0.0206	26	0.0222	36	0.0425
7	-0.0197	17	-0.0177	27	0.0406	37	0.0166
8	0.0300	18	-0.0376	28	0.0190	38	0.0033
9	0.0479	19	-0.0190	29	-0.0236		
10	0.0236	20	0.0190	30	-0.0479		

Table 2.5: Non-linear phase FIR filter coefficients for *Design 2.5* are given in 4 significant digits.

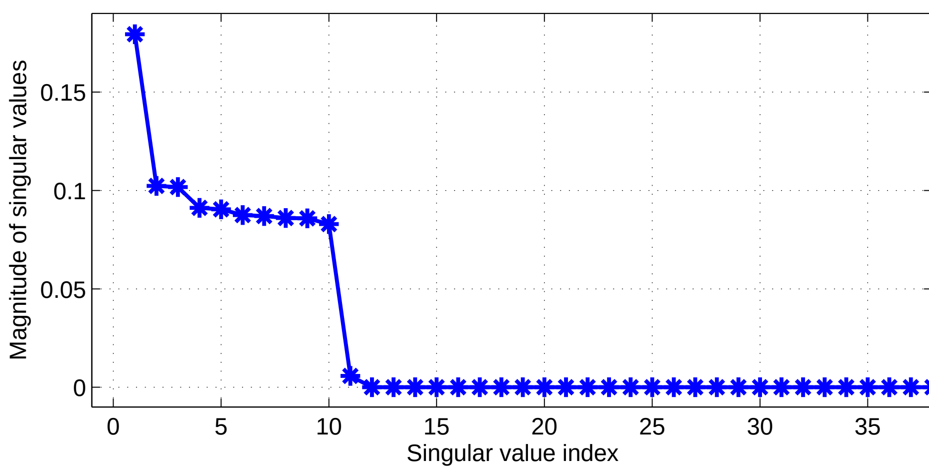

Figure 2.11: Singular values of $\mathbf{H}^\star$ for $L = 38$ that is obtained by solving (2.41). First singular value, $\sigma_1^\star$, is 18% of the sum of all singular values, $\sum_{i=1}^{L} \sigma_i^\star$.

Design 2.5 *Given the lower and upper magnitude response mask constraints,* $M_l(\omega)$ *and* $M_u(\omega)$ *shown in* Figure 2.1, *design a non-linear phase filter of length* $L = 38$ *with minimum stop band energy by using* (2.41).

For this design, the SDP optimization problem in (2.41) is solved using *Algorithm 4*, which is given in *Section A.2*, for $L = 38$. (2.44) is used to obtain the estimate filter coefficients $\tilde{\mathbf{h}}^\star$ from solution matrix $\mathbf{H}^\star$. Since obtained $\mathbf{H}^\star$ is not

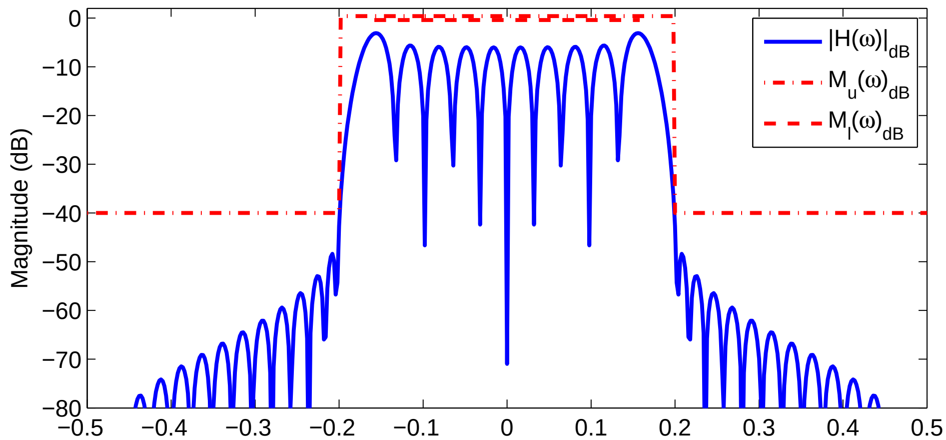

Figure 2.12: Magnitude response of $L = 38$ length FIR filter coefficients that are estimated from $\mathbf{H}^{\star}$. Magnitude response does not satisfy the constraints of *Design 2.5* since $\mathbf{H}^{\star}$ is not rank-1.

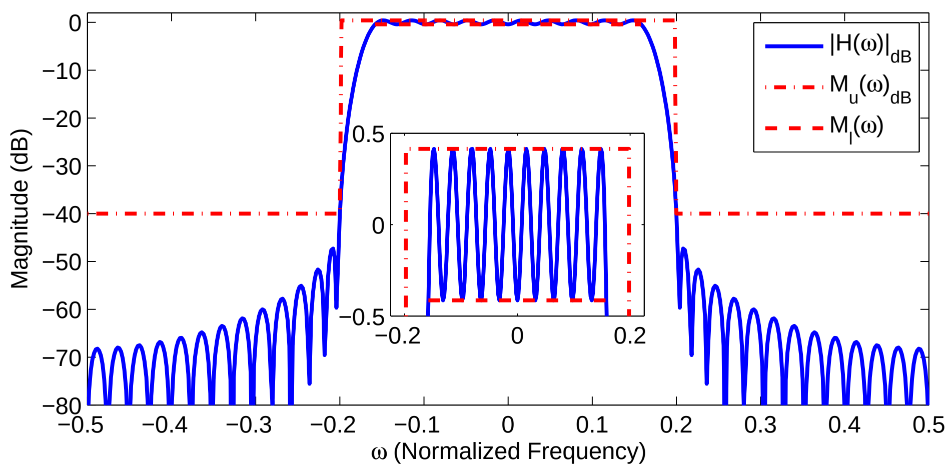

Figure 2.13: Magnitude response corresponding to $\mathbf{H}^{\star}$ for $L = 38$ that is obtained by solving (2.41). Magnitude response satisfies the constraints of *Design 2.5*. Stop band energy is around $-60dB$.

rank-1 (*Figure 2.11*) in this design, $\tilde{\mathbf{h}}^{\star}$ does not satisfy the magnitude response constraints. $\tilde{\mathbf{h}}^{\star}$ and its magnitude response are given in *Table 2.5* and *Figure 2.12*, respectively. The magnitude response that is obtained by using $\mathbf{H}^\star$ is also plotted in *Figure 2.13* to demonstrate the difference between obtained solution and its rank-1 estimation. Magnitude response of $\mathbf{H}^\star$ satisfy the magnitude constraints and achieved stop band energy in *Figure 2.13* is found to be -60dB. Since no spectral factorization is applied nor on $\mathbf{H}^\star$ nor on $\tilde{\mathbf{h}}^\star$, obtained phase is not minimum, but non-linear. Note that since (2.41) is convex, found $\mathbf{H}^\star$ provides optimal solution and obtained stop band energy is indeed equivalent to stop band energy achieved in *Design 2.1* by the LP based non-linear phase FIR filter design formulation.

Even though there exist low rank matrix factorization techniques for SDPs [15, 60–62], these techniques cannot be used to obtain a rank-1 solution matrix for SDPs with many affine constraints as in (2.41). Also, randomization based approaches [63] have significant challenges in problems with large number of affine constraints. To overcome this difficulty, in *Chapter 3*, a novel iterative algorithm will be introduced to obtain practically rank-1 solution matrix that satisfies the design constraints.

Chapter 3

FIR Filter Design Using Semidefinite Programming with Rank Refinement

In [43,48], an iterative algorithm to reduce the rank of the solution matrix of SDP problems in the form of (2.41) is already proposed. In this chapter, a generalized and improved version of this iterative algorithm is proposed. To obtain rank-1 solution, new convex constraints, which enforce optimization problem to obtain reduced rank solutions, are attached to (2.41) or the objective of (2.41) is changed to a proposed SDP objective, which searches for reduced rank solutions. In the following sections, formulations for both cases and for their combinations will given.

3.1 Directed Iterative Rank Refinement

To obtain a rank-1 solution matrix, we propose a novel iterative algorithm, where at each iteration the cost function of constructed SDP is updated and new convex constraints are introduced. The proposed algorithm makes use of singular value decomposition (SVD) of the obtained matrix $\mathbf{H}^i$ at iteration i to formulate the

SDP to be solved in the next iteration. Let $\mathbf{H}^i$ be a feasible point of the following feasibility problem:

$$\text{find } \mathbf{H}^i \in \mathbb{R}^{L\times L} \tag{3.1a}$$

$$\text{subject to } \mathrm{Tr}(\mathbf{A}_k\mathbf{H}^i) \leq a_k,\ 0 \leq k \leq K_u, \tag{3.1b}$$

$$\mathrm{Tr}(\mathbf{A}_k\mathbf{H}^i) \geq b_k,\ 0 \leq k \leq K_l, \tag{3.1c}$$

$$\mathbf{H}^i \succeq 0. \tag{3.1d}$$

Since $\mathbf{H}^i$ is a positive semidefinite and symmetric matrix, its singular value decomposition is in the following form:

$$\mathbf{H}^i = \mathbf{U}^i\mathbf{\Sigma}^i\mathbf{U}^{iT} = \sum_{l=1}^{L} \sigma_l^i \mathbf{u}_l^i \mathbf{u}_l^{iT}. \tag{3.2}$$

Here, $\mathbf{U}^i = [\mathbf{u}_1^i, \mathbf{u}_2^i, ..., \mathbf{u}_L^i]$ where $\mathbf{u}_l^i, 1 \leq l \leq L$ are the singular vectors and $\mathbf{\Sigma}^i = \mathrm{diag}([\sigma_1^i, ..., \sigma_L^i])$, where $\sigma_1^i \geq ... \geq \sigma_L^i \geq 0$ are the ordered singular values of $\mathbf{H}^i$. Since the energy of $\mathbf{H}^i$ is upper bounded by the upper mask constraints $M_u(\omega)$, maximizing the energy of $\mathbf{H}^{i+1}$ along the ℓ^{th} singular vector $\mathbf{u}_\ell^i$ of $\mathbf{H}^i$ in the next iteration will be a bounded objective. Maximization of the energy of $\mathbf{H}^{i+1}$ along $\mathbf{u}_\ell^i$ can be added to (3.1) as a cost function in SDP form as:

$$\min_{\mathbf{H}^{i+1}\in\mathbb{R}^{L\times L}} \ -\mathrm{Tr}(\mathbf{u}_\ell^i \mathbf{u}_\ell^{iT} \mathbf{H}^{i+1}) \tag{3.3a}$$

$$\text{subject to } \mathrm{Tr}(\mathbf{A}_k\mathbf{H}^{i+1}) \leq a_k,\ 0 \leq k \leq K_u, \tag{3.3b}$$

$$\mathrm{Tr}(\mathbf{A}_k\mathbf{H}^{i+1}) \geq b_k\ 0 \leq k \leq K_l, \tag{3.3c}$$

$$\mathbf{H}^{i+1} \succeq 0. \tag{3.3d}$$

Since SVD has high complexity, power iterations based techniques can also be used to find $\mathbf{u}_\ell^i$ [64]. If $\ell = 1$, following facts can be proven for the iterations in (3.3).

Proposition 3.1 *The cost of constructed SDP that is given in* (3.3) *monotonically decreases at each iteration:*

$$J^{i+1}(\mathbf{H}^{i+1}) \leq J^i(\mathbf{H}^i), \tag{3.4}$$

where $J^i(\mathbf{H}^i) = -\mathrm{Tr}(\mathbf{u}_1^{i-1}(\mathbf{u}_1^{i-1})^T\mathbf{H}^i)$ *denotes the cost function of the optimization problem at iteration* i *of* (3.3) *and* $\mathbf{H}^i$ *is the corresponding optimal solution.*

Proof 3.1 *Since the feasible set of optimization problem remains the same for all iterations,*

$$J^{i+1}(\mathbf{H}^{i+1}) \leq J^{i+1}(\mathbf{H}^i) \tag{3.5}$$

always holds. As given in (3.2), $\mathbf{H}^i$ *has the following singular value decomposition:*

$$\mathbf{H}^i = \sum_{l=1}^{L} \sigma_l^i \mathbf{u}_l^i (\mathbf{u}_l^i)^T \tag{3.6}$$

with $\sigma_1^i \geq \sigma_2^i \geq .. \geq \sigma_L^i \geq 0$ *and* $\|\mathbf{u}_l^i\|_2 = 1, \ \forall l$. *Hence, right hand side (RHS) of* (3.5) *can be found as:*

$$\begin{aligned} J^{i+1}(\mathbf{H}^i) &= -\mathrm{Tr}(\mathbf{u}_1^i (\mathbf{u}_1^i)^T \mathbf{H}^i) \\ &= -(\mathbf{u}_1^i)^T \mathbf{H}^i \mathbf{u}_1^i \\ &= -\sigma_1^i. \end{aligned} \tag{3.7}$$

Similarly, the cost function that is evaluated at $\mathbf{H}^i$ *at iteration* i *can be written as:*

$$\begin{aligned} J^{i}(\mathbf{H}^i) &= -\mathrm{Tr}(\mathbf{u}_1^{i-1} (\mathbf{u}_1^{i-1})^T \mathbf{H}^i) \\ &= -(\mathbf{u}_1^{i-1})^T \mathbf{H}^i \mathbf{u}_1^{i-1} \\ &\geq \min_{\|\mathbf{u}_1^{i-1}\|_2 = 1} -(\mathbf{u}_1^{i-1})^T \mathbf{H}^i \mathbf{u}_1^{i-1} \\ &= -\sigma_1^i = J^{i+1}(\mathbf{H}^i), \end{aligned} \tag{3.8}$$

with equality iff $\mathbf{H}^i = \mathbf{H}^{i-1}$. *Hence,*

$$J^{i+1}(\mathbf{H}^i) \leq J^{i}(\mathbf{H}^i) \ . \tag{3.9}$$

Then, together with (3.5), (3.4) *follows.*

Next, we would like to show that the optimal solution is a fixed point of iterations in (3.3). We first define the non-convex optimization problem that possesses optimal solution to (3.3) and prove that the cost of (3.3) is lower bounded by the optimal cost of defined optimization problem.

Proposition 3.2 *The cost of* (3.3)*, which monotonically decreases at each iteration, is lower bounded by the optimal cost to the following non-convex optimization problem:*

$$\begin{aligned}
\min_{\mathbf{H}\in\mathbb{R}^{L\times L}} \quad & -\operatorname{Tr}(\mathbf{H}) && \text{(3.10a)}\\
\text{subject to} \quad & \operatorname{Tr}(\mathbf{A}_k\mathbf{H}) \le a_k,\ 0 \le k \le K_u, && \text{(3.10b)}\\
& \operatorname{Tr}(\mathbf{A}_k\mathbf{H}) \ge b_k\ 0 \le k \le K_l, && \text{(3.10c)}\\
& \mathbf{H} \succeq 0, && \text{(3.10d)}\\
& \operatorname{rank}(\mathbf{H}) = 1. && \text{(3.10e)}
\end{aligned}$$

Proof 3.2 *Consider the relaxed convex version of* (3.10)

$$\begin{aligned}
\min_{\mathbf{H}\in\mathbb{R}^{L\times L}} \quad & -\operatorname{Tr}(\mathbf{H}) && \text{(3.11a)}\\
\text{subject to} \quad & \operatorname{Tr}(\mathbf{A}_k\mathbf{H}) \le a_k,\ 0 \le k \le K_u, && \text{(3.11b)}\\
& \operatorname{Tr}(\mathbf{A}_k\mathbf{H}) \ge b_k\ 0 \le k \le K_l, && \text{(3.11c)}\\
& \mathbf{H} \succeq 0. && \text{(3.11d)}
\end{aligned}$$

Let $\bar{\mathbf{H}}^\star$ *be the optimal solution of* (3.11)*, which is not necessarily rank-1, with its corresponding cost* $-\operatorname{Tr}(\bar{\mathbf{H}}^\star) = -\sum_{i=1}^{L} \bar{\sigma}_i^\star$*. Note that* $-\operatorname{Tr}(\bar{\mathbf{H}}^\star) \le -\operatorname{Tr}(\mathbf{H}^i) \le -\sigma_1^i = J^{i+1}(\mathbf{H}^i) \le J^i(\mathbf{H}^i)$ *always holds because of* (3.8) *and the equivalence of the feasible sets of* (3.3) *and* (3.11)*. Then, because of the coexistence of high rank and rank-1 solutions, which is shown in section 4.1.1.3 of [44], there exists a rank-1 solution matrix with exactly the same cost* $-\operatorname{Tr}(\bar{\mathbf{H}}^\star) = -\operatorname{Tr}(\hat{\mathbf{H}}^\star)$*. Hence, the cost of* (3.3) *is lower bounded by the optimal cost of* (3.10)*:*

$$\operatorname{Tr}(\hat{\mathbf{H}}^\star) \le J^i(\mathbf{H}^i),\ \forall i. \tag{3.12}$$

Coexistence of high rank and rank-1 solutions can be visualized in the following way. Since $\bar{\mathbf{H}}^\star$ *is PSD and symmetric,* $\bar{\mathbf{H}}^\star$ *can uniquely be transformed to an autocorrelation sequence* $\bar{\mathbf{r}}^\star$ *as:*

$$\bar{\mathbf{r}}_k^\star = \sum_{k=-L+1}^{L-1} \operatorname{diag}(\bar{\mathbf{H}}^\star, k), \tag{3.13}$$

where diag$(\bar{\mathbf{H}}^\star, k)$ *operation gets the* k^{th} *off-diagonal vector of* $\bar{\mathbf{H}}^\star$*. Then, filter coefficients* $\bar{\mathbf{x}}^\star$ *can be obtained by decomposing* $\bar{\mathbf{r}}^\star$ *via spectral factorization. Hence, a rank-1 matrix with exactly the same cost value* $-\mathrm{Tr}(\bar{\mathbf{H}}^\star)$ *can be obtained as* $\bar{\mathbf{x}}^\star(\bar{\mathbf{x}}^\star)^T$*.*

Next, we prove that the optimal solution to (3.10) is a fixed point of iterations in (3.3).

Proposition 3.3 *The optimal solution to* (3.10)*,* $\hat{\mathbf{H}}^\star$*, that can be decomposed as:*

$$\hat{\mathbf{H}}^\star = \hat{\sigma}_1^\star (\hat{\mathbf{u}}_1^\star)^T \hat{\mathbf{u}}_1^\star, \tag{3.14}$$

with $\hat{\sigma}_1^\star > 0$ *and* $\|\hat{\mathbf{u}}_1^\star\|_2 = 1$*, is a fixed point of iterations in* (3.3)*.*

Proof 3.3 *Because of coexistence, if a high rank solution exists in the feasible set of* (3.11)*, then at least one rank-1 solution exists in the same feasible set. Since the feasible sets of* (3.11) *and* (3.3) *are the same,* $\hat{\mathbf{H}}^\star$*, which possesses the largest singular value* $\hat{\sigma}_1^\star$ *in the feasible set, is also a candidate solution for* (3.3)*. Hence,* $\hat{\mathbf{H}}^\star$*, optimal solution of* (3.10)*, can be obtained by the proposed directed iterative rank refinement (DIRR) formulation at iteration* i*. Then, optimization problem at* $(i+1)^{th}$ *iteration becomes:*

$$\min_{\mathbf{H}^{i+1} \in \mathbb{R}^{L \times L}} \; -\mathrm{Tr}(\hat{\mathbf{u}}_1^\star (\hat{\mathbf{u}}_1^\star)^T \mathbf{H}^{i+1}) \tag{3.15a}$$

$$\text{subject to } \mathrm{Tr}(\mathbf{A}_k \mathbf{H}^{i+1}) \le a_k, \; 0 \le k \le K_u, \tag{3.15b}$$

$$\mathrm{Tr}(\mathbf{A}_k \mathbf{H}^{i+1}) \ge b_k \; 0 \le k \le K_l, \tag{3.15c}$$

$$\mathbf{H}^{i+1} \succeq 0, \tag{3.15d}$$

where $\hat{\mathbf{H}}^\star = \hat{\sigma}_1^\star \hat{\mathbf{u}}_1^\star (\hat{\mathbf{u}}_1^\star)^T$ *as* $\hat{\mathbf{H}}^\star$ *is rank-1. Because of* (3.5)*,* (3.7) *and* (3.12)*, the cost function of* (3.15) *is lower and upper bounded as:*

$$-\hat{\sigma}_1^\star \le -\mathrm{Tr}(\hat{\mathbf{u}}_1^\star (\hat{\mathbf{u}}_1^\star)^T \mathbf{H}^{i+1}) \le J^{i+1}(\hat{\mathbf{H}}^\star) = -\hat{\sigma}_1^\star, \tag{3.16}$$

which is attained only for the choice of $\mathbf{H}^{i+1} = \hat{\mathbf{H}}^\star$*. Hence, if* $\hat{\mathbf{H}}^\star$ *is the optimal solution to* (3.10)*, then is the fixed point of the proposed iterations in* (3.3)*.*

n	$h_n^\star$	n	$h_n^\star$	n	$h_n^\star$	n	$h_n^\star$
1	-0.0389	11	-0.0587	21	0.0382	31	-0.0014
2	-0.1207	12	-0.0937	22	0.0141	32	0.0096
3	-0.2339	13	-0.0418	23	-0.0194	33	0.0090
4	-0.3200	14	0.0368	24	-0.0283	34	0.0003
5	-0.3130	15	0.0681	25	-0.0082	35	-0.0063
6	-0.1927	16	0.0317	26	0.0162	36	-0.0056
7	-0.0148	17	-0.0276	27	0.0203	37	-0.0005
8	0.1190	18	-0.0508	28	0.0040	38	0.0057
9	0.1352	19	-0.0221	29	-0.0129		
10	0.0468	20	0.0228	30	-0.0139		

Table 3.1: Non-linear phase FIR filter coefficients for *Design 3.1* are given in 4 significant digits.

As *Proposition 3.1* suggests, the cost of (3.3) gets smaller and the gap μ between $-(\mathbf{u}_1^{i-1})^T\mathbf{H}^i\mathbf{u}_1^{i-1}$ and min $-(\mathbf{u}_1^{i-1})^T\mathbf{H}^i\mathbf{u}_1^{i-1}$ is always greater than 0, that is $\mu = \sum_{k=1}^{L}(\sigma_1^i - \sigma_k^i)((\mathbf{u}_1^{i-1})^T\mathbf{u}_k^i)^2 > 0$ if $\langle \mathbf{u}_1^{i-1}, \mathbf{u}_k^i\rangle \neq 0,\ \forall k \in [1, L]$ for $\sigma_1^i > \sigma_k^i,\ \forall k \in [2, L]$. On the other hand, if the gap is $\mu = 0$, then singular vectors of solutions at current and previous iterations are the same and inner product $\langle \mathbf{u}_1^{i-1}, \mathbf{u}_k^i\rangle = 0,\ \forall k \in [2, L]$ for $\sigma_1^i > \sigma_k^i,\ \forall k \in [2, L]$. Hence, DIRR converged to a minima that is either a local minima or global minima $\hat{\mathbf{H}}^\star$. Convergence to a local minima can be identified by computing the following ratio:

$$R^i = \frac{\sigma_1^i}{\sum\limits_{l=1}^{L}\sigma_l^i} \geq \rho, \tag{3.17}$$

where ρ is predefined threshold and is typically chosen as $\rho = 1 - 10^{-4}$. If ρ is exceeded by R^i, then an almost rank-1 solution is obtained by DIRR and the iterations are terminated. On the other hand, if $R^i < \rho$, then ℓ is updated as $\ell = \ell + 1$ and DIRR iterations given in *Algorithm 5* are continued. Although all L directions can be searched for a solution in DIRR procedure, the convergence to a rank-1 solution is not guaranteed. In cases, at which a rank-1 solution could not be found, *ad-hoc* procedures such as constraining singular values σ_l corresponding to singular vectors $\mathbf{u}_l$ by a user defined upper limit τ or minimizing the negative energy in multiple directions simultaneously rather than minimizing the cost only along ℓ^{th} direction, can be applied at the expense of complexity. Next, a non-linear phase FIR filter design is demonstrated by using proposed DIRR technique.

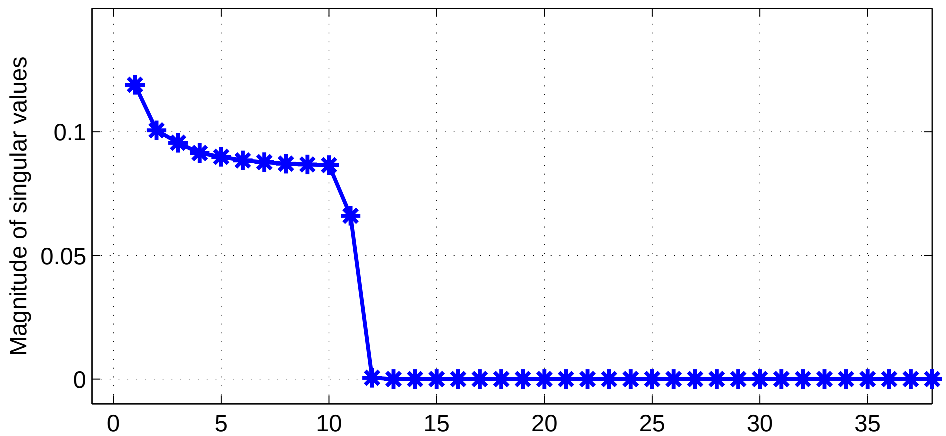

Figure 3.1: Singular values of $\mathbf{H}^i$ at $i = 1$ that is obtained by solving (3.3). Obtained singular value ratio is $R^i = 0.1190$. Since ratio is not high enough resulting filter coefficients will not satisfy the predefined mask constraints.

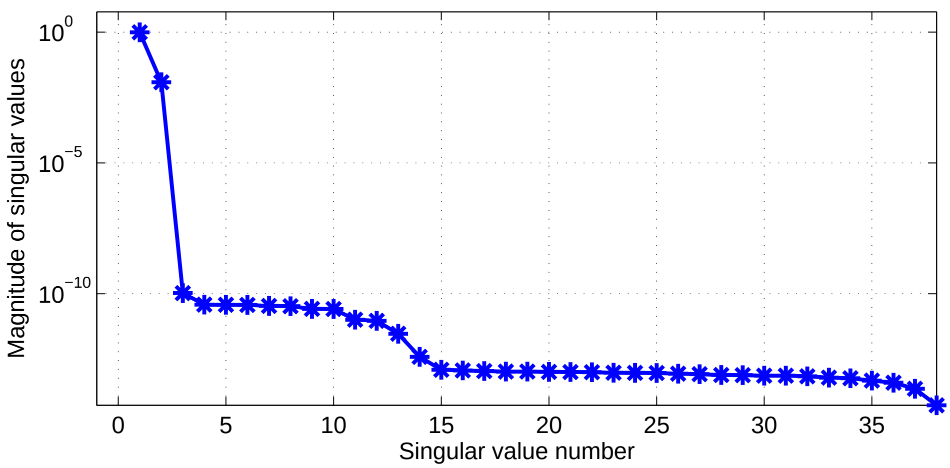

Figure 3.2: Singular values of $\mathbf{H}^i$ at $i = 2$ that is obtained by solving (3.3). Obtained singular value ratio is $R^i = 0.9878$. Since ratio is not high enough resulting filter coefficients will not satisfy the predefined mask constraints.

Design 3.1 *Given the lower and upper magnitude response mask constraints,* $M_l(\omega)$ *and* $M_u(\omega)$ *shown in* Figure 2.1, *design a non-linear phase filter of length* $L = 38$ *by using* (3.3).

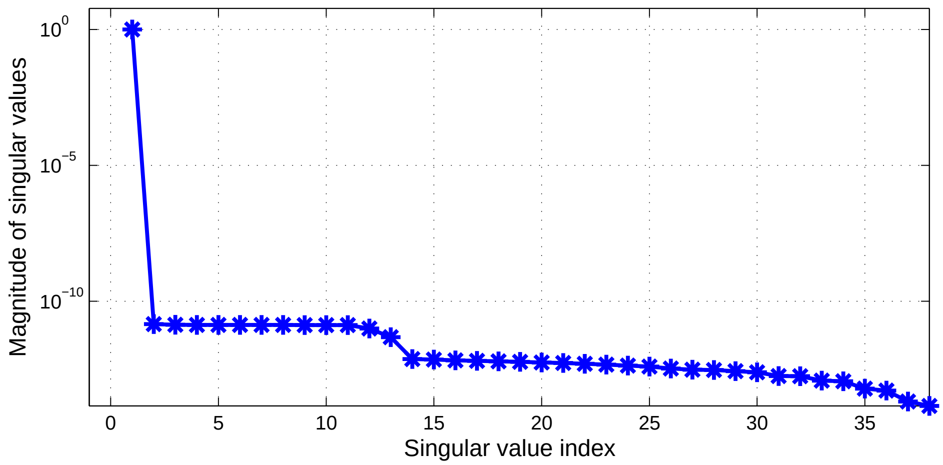

Figure 3.3: Singular values of $\mathbf{H}^i$ at $i = 3$ that is obtained by solving (3.3). Obtained singular value ratio is $R^i = 1$. Since $\mathbf{H}$ is almost rank-1, estimated filter coefficients $\mathbf{h}$ will satisfy the magnitude mask constraints.

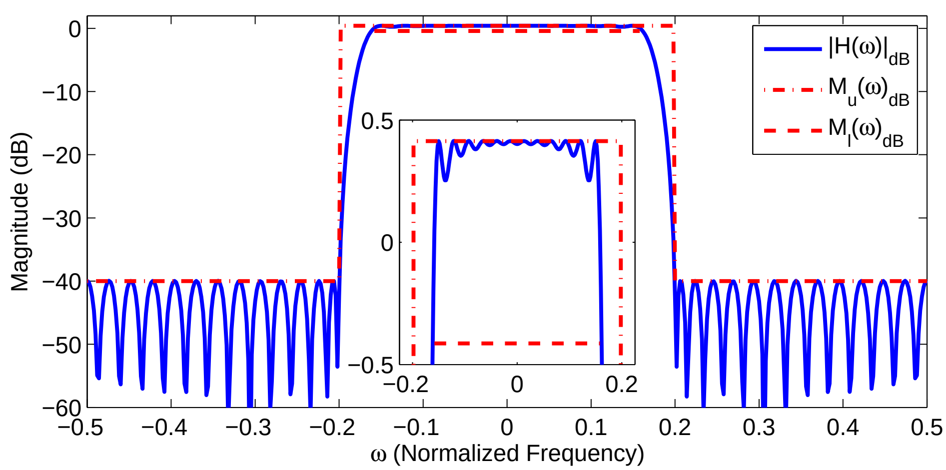

Figure 3.4: Magnitude response of $L = 38$ length non-linear phase FIR filter coefficients that are obtained by solving DIRR given in (3.3). Magnitude response of $\mathbf{h}$ satisfy the constraints of *Design 3.1* since $\mathbf{H}^i$ is almost rank-1. Obtained stop band energy is around $-43dB$.

For this design, constructed iterative convex optimization problem (3.3) is solved for $L = 38$ using *Algorithm 5* given in *Section A.3*. After $i = 3$ iterations on the direction of $\ell = 1$, $\mathbf{H}^i$ becomes almost rank-1 with $R^i = 1$ as shown in *Figures 3.1, 3.2* and *3.3*. Hence, obtained filter coefficients $\mathbf{h}$ via (2.44) satisfy the magnitude constraints and filter coefficients are given in *Table 3.1*. Obtained magnitude response is plotted in *Figure 3.4* and stop band energy in *Figure 3.4* is found to be around $-43dB$. Since *Design 3.1* is a feasibility problem, obtained stop band energy is not minimum value in the feasible set of *Design 3.1*. In the next section, implementation of cost functions in DIRR formulation will be demonstrated.

3.2 Incorporation of Cost Functions to Directed Iterative Rank Refinement

DIRR formulation given in (3.3) can be incorporated with properly chosen convex cost functions. Since minimum stop band energy can be obtained by an LP based technique presented in *Chapter 2*, we emphasize the choice of stop band energy based cost functions in this chapter.

To achieve a minimum stop band energy with a rank-1 solution matrix, at each iteration the following SDP is solved:

$$\min_{\mathbf{H}^{i+1} \in \mathbb{R}^{L \times L}} \ \mathrm{Tr}(((1-\xi)\mathbf{A}_s - \xi \mathbf{u}_\ell^i \mathbf{u}_\ell^{i^T})\mathbf{H}^{i+1}) \tag{3.18a}$$

$$\text{subject to } \mathrm{Tr}(\mathbf{A}_k \mathbf{H}^{i+1}) \le a_k,\ 0 \le k \le K_u, \tag{3.18b}$$

$$\mathrm{Tr}(\mathbf{A}_k \mathbf{H}^{i+1}) \ge b_k,\ 0 \le k \le K_l, \tag{3.18c}$$

$$\mathbf{H}^{i+1} \succeq 0, \tag{3.18d}$$

where $0 < \xi < 1$ is the parameter controlling the tradeoff between rank of the solution matrix and the stop band energy of the filter. In design examples ξ is chosen as a function of R^i for improved convergence. Since obtaining a rank-1 solution is the priority in the solution of (3.18), $\xi(R^i)$ is chosen to be a monotone decreasing function of R^i such as $\xi(R^i) = 1 - (R^i)^\alpha$, where α is a non-negative real number that is determined by the user. For $\alpha \gg 1$, DIRR for (3.18) tends

n	$h_n^\star$	n	$h_n^\star$	n	$h_n^\star$	n	$h_n^\star$
1	-0.0009	11	-0.0808	21	0.1195	31	0.1480
2	-0.0072	12	-0.0657	22	0.1373	32	0.2030
3	-0.0197	13	0.0115	23	0.0645	33	0.2267
4	-0.0308	14	0.0946	24	-0.0398	34	0.2043
5	-0.0268	15	0.1117	25	-0.1070	35	0.1463
6	-0.0002	16	0.0380	26	-0.1098	36	0.0803
7	0.0360	17	-0.0754	27	-0.0679	37	0.0311
8	0.0520	18	-0.1390	28	-0.0150	38	0.0067
9	0.0246	19	-0.0991	29	0.0345		
10	-0.0352	20	0.0160	30	0.0871		

Table 3.2: Non-linear phase FIR filter coefficients for *Design 3.2* are given in 4 significant digits.

to converge to a rank-1 solution faster. On the other hand, for $\alpha \ll 1$ DIRR for (3.18) tends to converge to a rank-1 solution slower with significantly suppressed stop band energy. Choosing appropriate values for α will be investigated as a design example is demonstrated next.

Design 3.2 *Given the lower and upper magnitude response mask constraints,* $M_l(\omega)$ *and* $M_u(\omega)$ *shown in* Figure 2.1, *design a filter of length* $L = 38$ *with minimum stop band energy by using* (3.18).

For this design, the optimization problem in (3.18) is solved using DIRR with $\ell = 1$ and $\xi = 1 - (R^i)^\alpha$ for $\alpha = 0.005$, where R^i is defined in (3.17). Exponent term on R^i can be made even smaller to increase the effect of stop band minimization term in the objective. However, for the current choice of ξ, proposed technique is able to converge in 3 iterations, with a stop band energy of $-60dB$. As it is shown in *Figure 3.5*, the choice of $\alpha = 0.005$ provides minimal stop band energy with minimum number of iterations. Note that *Design 3.1* corresponds to the $\alpha = \infty$ case in *Figure 3.5.* The singular values of the obtained solution matrix are shown in *Figure 3.6.* The ratio of first singular value to the sum of all singular values is found to be $R^i = 1$ at iteration $i = 3$. As observed, proposed iterations provided a rank-1 matrix. Obtained filter coefficients are given in *Table 3.2.* As shown in *Figure 3.7*, the designed filter satisfies the magnitude constraints.

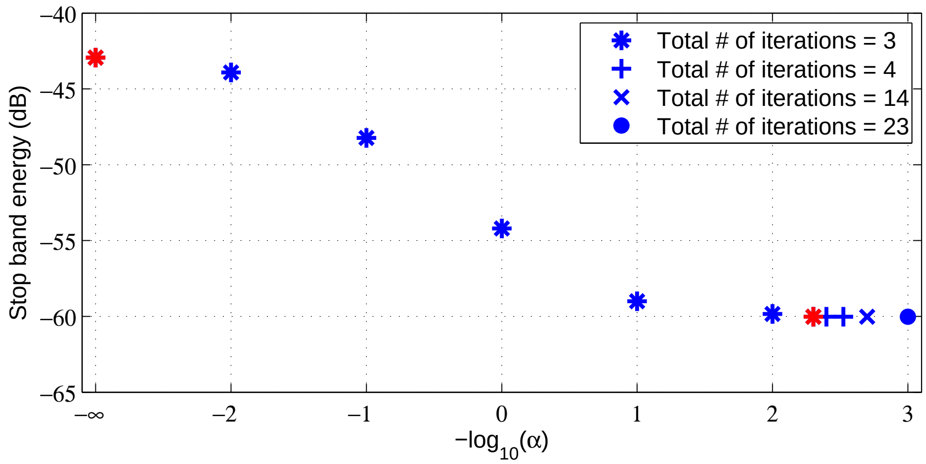

Figure 3.5: As a function of α, the required number of iterations and the corresponding stop band energy. The appropriate value of α that determines design parameter ξ in *Algorithm 5* can be determined via this tradeoff curve. Typically, the largest value of $-\log_{10}(\alpha)$ for the smallest total number of iterations provides the best design tradeoff.

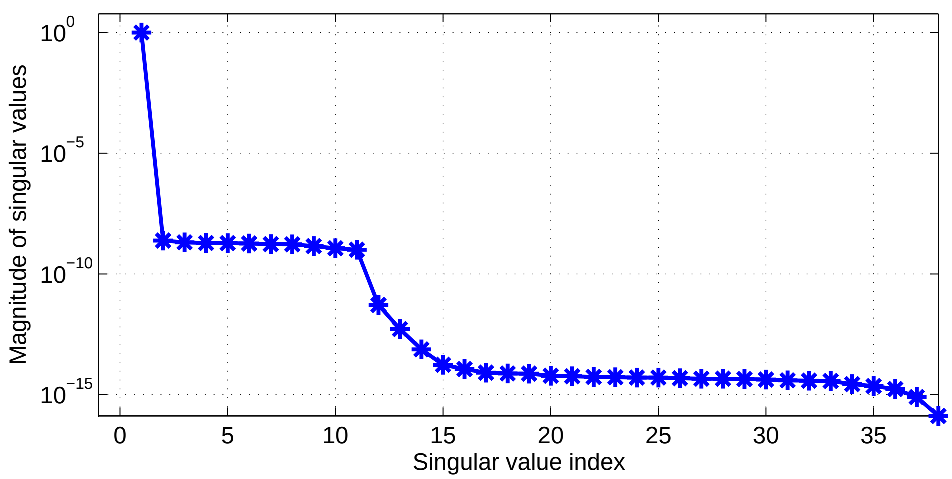

Figure 3.6: Singular values of $\mathbf{H}^i$ at $i = 3$ that is obtained by solving (3.18). Obtained singular value ratio is $R^i = 1$. Since $\mathbf{H}$ is almost rank-1, estimated filter coefficients $\mathbf{h}$ will satisfy the magnitude mask constraints.

Note that *Design 3.2* is equivalent to *Design 2.1*. Hence, we compare the performance of proposed technique with the well known autocorrelation based method, which is already presented in *Chapter 2* [19]. Since there is no phase

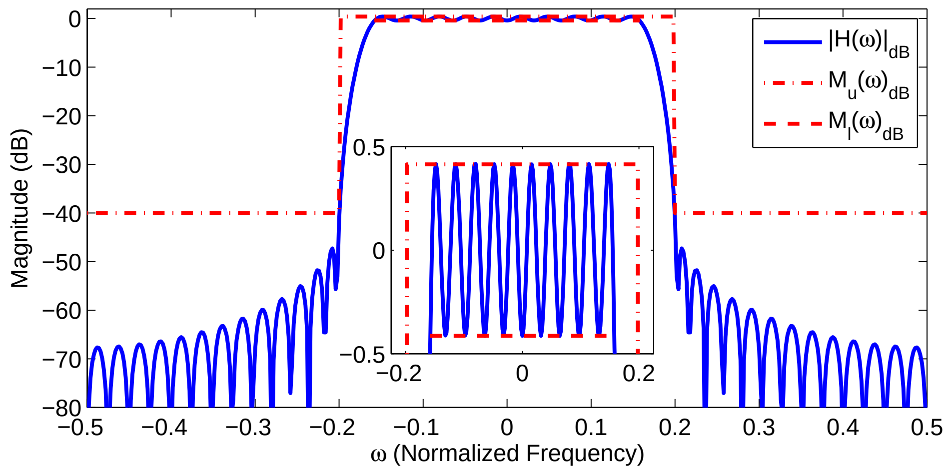

Figure 3.7: Magnitude response of $L = 38$ length non-linear phase FIR filter coefficients that are obtained by solving DIRR given in (3.18). Magnitude response of $\mathbf{h}$ satisfy the constraints of *Design 3.2* since $\mathbf{H}^i$ is almost rank-1. Obtained stop band energy is around $-60dB$.

constraints, the autocorrelation based design technique provides the global optimal for this design. The magnitude response of the resulting filter coefficients designed by this method is already given in *Figure 2.2* and the achieved stop band energy is -60dB. Note that, proposed algorithm provides very similar design performance with the optimal autocorrelation based design technique.

Total stop band energy minimization goal of the SDP given in (3.18) can be changed to peak stop band ripple minimization to obtain classical low-pass FIR filter design problem that is already presented in *Section 2.2* [38] by replacing semidefinite term $-\mathrm{Tr}(\mathbf{A}_s\mathbf{H}^{i+1})$ with a variable δ^2 and by constraining energy corresponding to each frequency in the stop band by δ^2. Obtained SDP is given as:

$$\min_{\mathbf{H}^{i+1}\in\mathbb{R}^{L\times L},\delta^2\in\mathbb{R}} (1-\xi)\delta^2 - \xi\mathrm{Tr}(\mathbf{u}_\ell^i\mathbf{u}_\ell^{i\,T}\mathbf{H}^{i+1}) \tag{3.19a}$$

$$\text{subject to } \mathrm{Tr}(\mathbf{A}_k\mathbf{H}^{i+1}) \le a_k,\ 0 \le k \le K_s, \tag{3.19b}$$

$$\mathrm{Tr}(\mathbf{A}_k\mathbf{H}^{i+1}) \le \delta^2,\ K_s < k \le K_u, \tag{3.19c}$$

$$\mathrm{Tr}(\mathbf{A}_k\mathbf{H}^{i+1}) \ge b_k\ 0 \le k \le K_l, \tag{3.19d}$$

$$\mathbf{H}^{i+1} \succeq 0. \tag{3.19e}$$

n	$h_n^\star$	n	$h_n^\star$	n	$h_n^\star$	n	$h_n^\star$
1	-0.0076	11	0.0056	21	-0.0599	31	0.2584
2	-0.0167	12	0.0268	22	-0.0523	32	0.3147
3	-0.0219	13	0.0221	23	0.0119	33	0.2684
4	-0.0154	14	-0.0082	24	0.0772	34	0.1642
5	0.0012	15	-0.0353	25	0.0779	35	0.0643
6	0.0156	16	-0.0285	26	0.0003	36	0.0059
7	0.0141	17	0.0111	27	-0.0966	37	-0.0109
8	-0.0033	18	0.0462	28	-0.1260	38	-0.0072
9	-0.0200	19	0.0377	29	-0.0439		
10	-0.0173	20	-0.0131	30	0.1136		

Table 3.3: Non-linear phase FIR filter coefficients for *Design 3.3* are given in 4 significant digits.

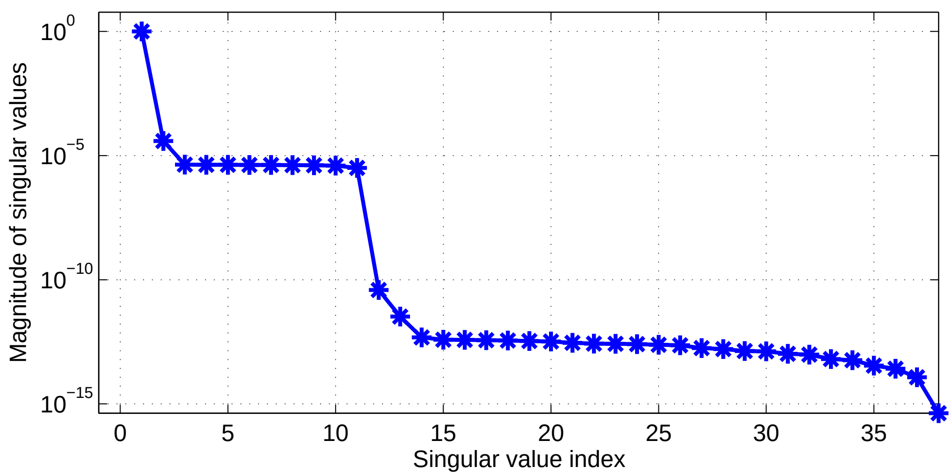

Figure 3.8: Singular values of $\mathbf{H}^i$ at iteration $i = 24$ that are obtained by solving the problem given in *Design 3.3* using DIRR.

Since the objective and newly introduced constraints are convex, (3.19) is still an iterative convex SDP problem. Hence, (3.19) can be solved by using DIRR by choosing (3.19) at steps 2 and 13 in *Algorithm 5*. Next, a design example is demonstrated.

Design 3.3 *Given the lower and upper magnitude response mask constraints,*

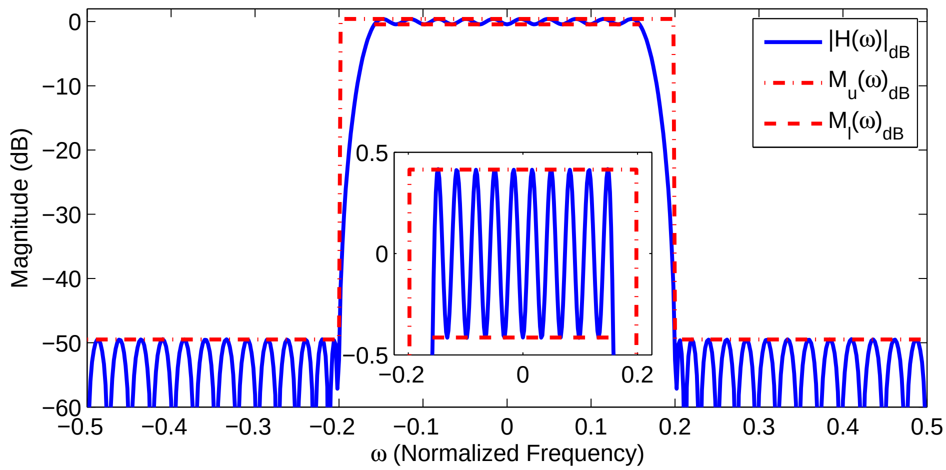

Figure 3.9: Magnitude response of $L = 38$ length FIR filter coefficients that are obtained by solving the problem given in *Design 3.3* using DIRR. Total stop band energy is $-53dB$ and minimum peak stop band ripple is $\delta = -50dB$.

$M_l(\omega)$ *and* $M_u(\omega), 0 \leq \omega \leq \omega_s$ *shown in* Figure 2.1, *design a filter of length* $L = 38$ *with the minimum peak stop band ripple by using* (3.19).

For this design, the optimization problem in (3.19) is solved using DIRR with $\ell = 1$ and $\xi = 1-(R^i)^\alpha$ for $\alpha = 0.00001$. Proposed technique was able to converge in 24 iterations, with a stop band energy of $-53dB$. The singular values of the obtained solution matrix are shown in *Figure 3.8*. The ratio of first singular value to the sum of all singular values is found to be $R^i = 0.99992$ at iteration $i = 24$, indicating that the obtained solution matrix is practically a rank-1 matrix. As shown in *Figure 3.9*, the designed filter satisfies the constraints and minimum peak stop band ripple $\delta^2 = -50dB$. Obtained filter coefficients are given in *Table 3.3*. Result is compared with the optimal solution that is obtained by solving *Design 2.2*, which is already presented in *Section 2.2* [38]. This optimal method achieved a stop band energy of $-53dB$ and minimum peak stop band ripple level is found to be $\delta^2 = -50dB$ in *Figure 2.4*. Note that, proposed algorithm again provides similar design performance with the optimal technique.

As stated earlier, even though proposed DIRR searches all directions ℓ, for

$\ell \in [1, L]$, it might converge to a local minima for tight constrained problems. Hence, next we demonstrate a more general formulation of DIRR, which introduces spectral constraints on singular values of $\mathbf{H}$. By upper bounding these rank constraints by thresholds κ, which are updated at each iteration in an *ad-hoc* manner, rank-1 solution matrices can still be obtained.

3.3 Directed Iterative Rank Refinement with Cost Functions and Rank Constraints

In (3.3), maximization of energy of $\mathbf{H}^{i+1}$ along $\mathbf{u}_\ell^i$ is implemented as a cost function in SDP form. In a similar manner, the energies of $\mathbf{H}^{i+1}$ along all other directions can be upper bounded by user defined κ by attaching constraints to (3.18) in the form of (3.3a) as:

$$\min_{\mathbf{H}^{i+1} \in \mathbb{R}^{L \times L}} \ \mathrm{Tr}(((1-\xi)\mathbf{A}_s - \xi \mathbf{u}_\ell^i {\mathbf{u}_\ell^i}^T)\mathbf{H}^{i+1}) \tag{3.20a}$$

$$\text{subject to } \mathrm{Tr}(\mathbf{A}_k \mathbf{H}^{i+1}) \leq a_k,\ 0 \leq k \leq K_u, \tag{3.20b}$$

$$\mathrm{Tr}(\mathbf{A}_k \mathbf{H}^{i+1}) \geq b_k,\ 0 \leq k \leq K_l, \tag{3.20c}$$

$$\mathrm{Tr}(\mathbf{u}_\eta^i {\mathbf{u}_\eta^i}^T \mathbf{H}^{i+1}) \leq \kappa^i,\ \forall \eta \in [1, L] \setminus \ell, \tag{3.20d}$$

$$\mathbf{H}^{i+1} \succeq 0, \tag{3.20e}$$

where κ are user defined thresholds on the energies of $\mathbf{H}^{i+1}$. Note that (3.20) is a generalized version of (3.3) and (3.18) so that (3.20) becomes (3.18) if (3.20d) is removed and becomes (3.3) if (3.20d) and term $(1-\xi)\mathbf{A}_s$ in (3.20a) are removed. Iterative algorithm proposed in [48] can also be obtained from (3.20) by removing term $\xi \mathbf{u}_\ell^i {\mathbf{u}_\ell^i}^T$ in (3.20a).

An algorithm implementing (3.20) is given in *Algorithm 6* under *Section A.4*. Since user defined threshold κ is updated at each iteration, the convergence of DIRR now also depends on the choice of κ. A suggested procedure for updating κ is also mentioned in *Algorithm 6*. According to *Algorithm 6*, κ is updated as $\kappa^{i+1} = \kappa^i/2$ if a feasible solution to (3.20) is obtained at iteration i. If (3.20) is not feasible for the current choice of κ^i, κ is updated as $\kappa^{i+1} = (\kappa^{i^\star} + \kappa^i)/2$, where $i^\star$ is the last iteration at which (3.20) is feasible. Design examples using (3.20) will be given in *Chapter 4* after phase and group delay constrainted DIRR, which are tight constrained FIR filter design formulations, are introduced. In the next chapter, implementation of phase and group delay constraints in SDP form and phase and group delay constrained FIR filter design formulations using DIRR will be presented.

Chapter 4

FIR Filter Design Under Phase and Group Delay Constraints

As demonstrated in *Chapter 2*, LP formulations of non-linear and linear phase filters are not capable of implementing phase and group delay constraints. Hence, SDP formulation, which is defined over matrix variables, was introduced in *Section 2.3*. In this chapter, we demonstrate the foretold advantages of SDP over LP for the design of FIR filters by deriving SDP formulations for phase and group delay constraints. Then, phase and group delay constrained FIR filter design problems are constructed and solved by using proposed DIRR technique. We demonstrate that SDP provides a more flexible way of designing FIR filters compared to LP.

4.1 Phase Constrained FIR Filter Design By Directed Iterative Rank Refinement

Linear phase filters are commonly used in practice since they provide constant group delay. However, linear phase response requires filter coefficients to have a certain symmetry, resulting in reduced degrees of freedom in the design and

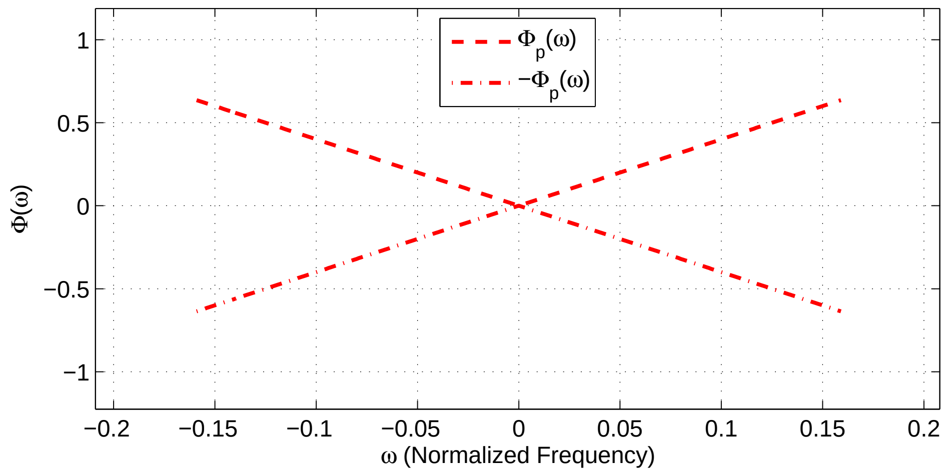

Figure 4.1: Typical zero-phase mask constraints that are used in phase constrained FIR filter design. Upper and lower phase mask constraints are given as $\Phi_p(\omega) = -\Phi_p(\omega) = 4|\omega| + 4 \times 10^{-5}$ for $|\omega| < 0.16$.

requiring longer filters to satisfy the magnitude constraints. Hence, there is a tradeoff between magnitude response and phase response linearity of the filter. To operate at a desired point in this tradeoff, additional constraints on the phase response can be introduced to the constructed optimization problem. An exchange based method is proposed in [8] for handling such constraints. However, since the constructed problem is non-convex, substantial effort is required for the converge of the algorithm. A least squares and SDP based approach is proposed in [65], where a desired filter response is used as a template. Unlike these approaches, we use spectral mask constraints on the phase response of the filter that can be imposed in proposed iterative convex form. As a result, FIR filters satisfying the design constraints with fewer coefficients can be designed.

Consider the following constraints on the phase response $\Phi(\omega) = \measuredangle H(\omega)$ of the filter:

$$|\Phi(\omega_k)| \leq \Phi_p(\omega_k),\ 1 \leq k \leq K_p, \tag{4.1}$$

where $\omega_k \in [0, \pi/2]\ \forall k$. (4.1) can be written in cartesian coordinates as

$$-\Phi_p(\omega_k) \leq \tan^{-1}\left(\frac{Im(H(\omega_k))}{Re(H(\omega_k))}\right) \leq \Phi_p(\omega_k). \tag{4.2}$$

Since $\tan(\omega)$ is a a monotonically increasing function and continuous in the interval $\omega \in [0, \pi/2]$, (4.2) can be equivalently written as:

$$-\tan(\Phi_p(\omega_k)) \leq \frac{Im(H(\omega_k))}{Re(H(\omega_k))} \leq \tan(\Phi_p(\omega)). \tag{4.3}$$

Then, it follows that

$$0 \leq \left| \frac{Im(H(\omega_k))}{Re(H(\omega_k))} \right|^2 \leq \tan^2(\Phi_p(\omega_k)), \tag{4.4}$$

which can be equivalently written as:

$$|Im(H(\omega_k))|^2 - |Re(H(\omega_k))|^2 \beta(\omega_k) \leq 0, \tag{4.5}$$

where $\beta(\omega_k) = \tan^2(\Phi_c(\omega_k))$. For simplification, the following vectors are defined:

$$\mathbf{s}(\omega_k) = [1, -\sin(\omega_k), ..., -\sin((L-1)\omega_k)]^T, \tag{4.6a}$$

$$\mathbf{c}(\omega_k) = [1, \cos(\omega_k), ..., \cos((L-1)\omega_k)]^T. \tag{4.6b}$$

Also define $\mathbf{S}(\omega_k) = \mathbf{s}(\omega_k)\mathbf{s}(\omega_k)^T$, $\mathbf{C}(\omega_k) = \mathbf{c}(\omega_k)\mathbf{c}(\omega_k)^T$, and express the constraints on the phase in (4.5) as:

$$\mathrm{Tr}(\mathbf{P}_k\mathbf{H}) \leq 0, \ 1 \leq k \leq K_p, \tag{4.7}$$

where $\mathbf{P}_k = \mathbf{S}(\omega_k) - \beta^2(\omega_k)\mathbf{C}(\omega_k)$, and $\mathbf{H} = \mathbf{h}\mathbf{h}^T$. The convex SDP, which includes constraints on both magnitude and phase response of the filter can be expressed as:

$$\min_{\mathbf{H} \in \mathbb{R}^{L \times L}} \ \mathrm{Tr}(\mathbf{A}_s\mathbf{H}) \tag{4.8a}$$

$$\text{subject to } \mathrm{Tr}(\mathbf{A}_k\mathbf{H}) \leq a_k, \ 0 \leq k \leq K_u, \tag{4.8b}$$

$$\mathrm{Tr}(\mathbf{A}_k\mathbf{H}) \geq b_k, \ 0 \leq k \leq K_l, \tag{4.8c}$$

$$\mathrm{Tr}(\mathbf{P}_k\mathbf{H}) \leq 0, \ 1 \leq k \leq K_p, \tag{4.8d}$$

$$\mathbf{H} \succeq 0. \tag{4.8e}$$

Finally, (4.8) can be rewritten in the form of (3.18) and (3.20) in order to obtain an iterative formulation so that DIRR algorithm provide a solution that satisfies

n	$h_n^\star$	n	$h_n^\star$	n	$h_n^\star$	n	$h_n^\star$
1	-0.0114	11	-0.0032	21	-0.0124	31	0.0167
2	-0.0269	12	0.0011	22	-0.0989	32	0.0392
3	-0.0338	13	-0.0133	23	-0.0733	33	0.0334
4	-0.0203	14	-0.0244	24	0.0118	34	0.0157
5	0.0100	15	0.0133	25	0.0711	35	0.0028
6	0.0368	16	0.1214	26	0.0581		
7	0.0396	17	0.2599	27	-0.0057		
8	0.0181	18	0.3425	28	-0.0613		
9	-0.0067	19	0.3028	29	-0.0675		
10	-0.0132	20	0.1544	30	-0.0293		

Table 4.1: Phase constrained FIR filter coefficients for *Design 4.1* are given in 4 significant digits.

both magnitude and phase constraints:

$$\min_{\mathbf{H}^{i+1}\in\mathbb{R}^{L\times L}} \ \mathrm{Tr}(((1-\xi)\mathbf{A}_s - \xi\mathbf{u}_\ell^i{\mathbf{u}_\ell^i}^T)\mathbf{H}^{i+1}) \tag{4.9a}$$

$$\text{subject to } \mathrm{Tr}(\mathbf{A}_k\mathbf{H}^{i+1}) \leq a_k,\ 0 \leq k \leq K_u, \tag{4.9b}$$

$$\mathrm{Tr}(\mathbf{A}_k\mathbf{H}^{i+1}) \geq b_k,\ 0 \leq k \leq K_l, \tag{4.9c}$$

$$\mathrm{Tr}(\mathbf{P}_k\mathbf{H}^{i+1}) \leq 0,\ 1 \leq k \leq K_p, \tag{4.9d}$$

$$\mathbf{H}^{i+1} \succeq 0. \tag{4.9e}$$

$$\min_{\mathbf{H}^{i+1}\in\mathbb{R}^{L\times L}} \ \mathrm{Tr}(((1-\xi)\mathbf{A}_s - \xi\mathbf{u}_\ell^i{\mathbf{u}_\ell^i}^T)\mathbf{H}^{i+1}) \tag{4.10a}$$

$$\text{subject to } \mathrm{Tr}(\mathbf{A}_k\mathbf{H}^{i+1}) \leq a_k,\ 0 \leq k \leq K_u, \tag{4.10b}$$

$$\mathrm{Tr}(\mathbf{A}_k\mathbf{H}^{i+1}) \geq b_k,\ 0 \leq k \leq K_l, \tag{4.10c}$$

$$\mathrm{Tr}(\mathbf{u}_\eta^i{\mathbf{u}_\eta^i}^T\mathbf{H}^{i+1}) \leq \kappa^i,\ \forall\eta \in [1, L] \setminus \ell, \tag{4.10d}$$

$$\mathrm{Tr}(\mathbf{P}_k\mathbf{H}^{i+1}) \leq 0,\ 1 \leq k \leq K_p, \tag{4.10e}$$

$$\mathbf{H}^{i+1} \succeq 0. \tag{4.10f}$$

Next, a phase constrained FIR filter design example by using (4.9) is demonstrated.

Design 4.1 *Given the magnitude and phase response constraints, $M_l(\omega)$, $M_u(\omega)$ shown in* Figure 2.1 *and $\Phi_p(\omega)$ shown in* Figure 4.1*, respectively, design the lowest order filter with minimum stop band energy.*

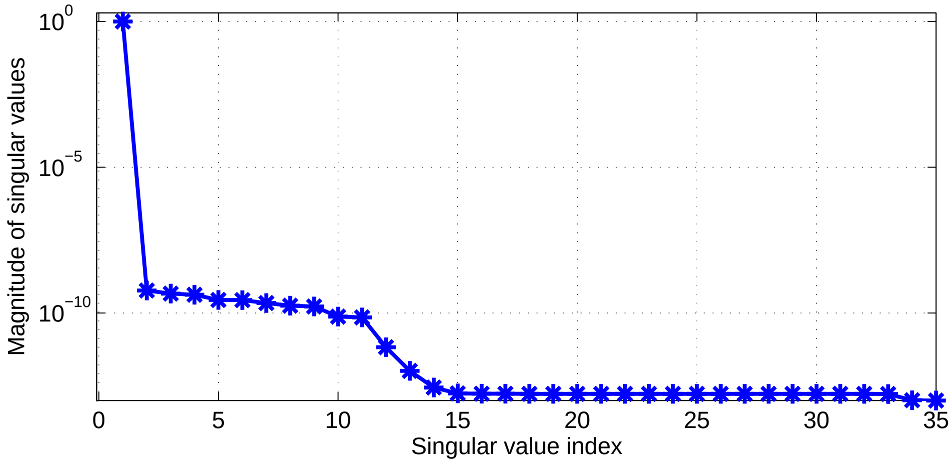

Figure 4.2: Singular values of $\mathbf{H}^i$ at iteration $i = 5$ that are obtained by solving *Design 4.1* using DIRR.

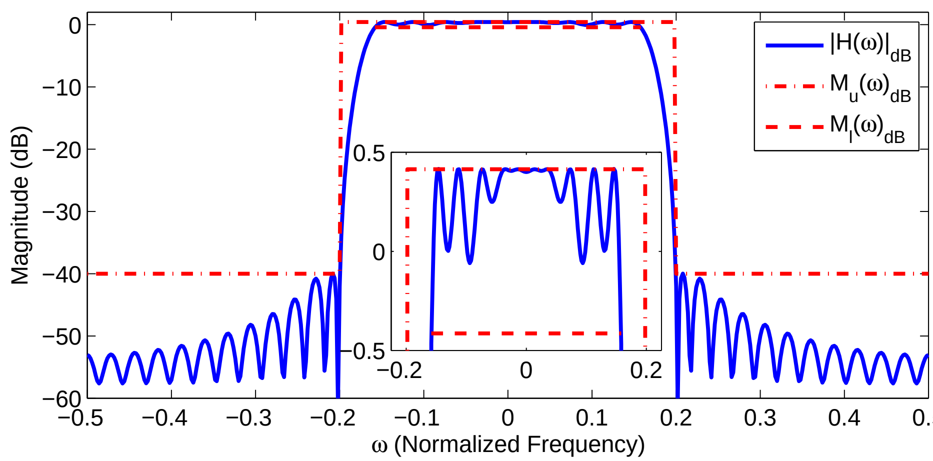

Figure 4.3: Magnitude response of $L^* = 35$ length FIR filter coefficients that are obtained by solving problem given in *Design 4.1* using DIRR. Magnitude response satisfies the constraints of *Design 4.1*. Stop band energy level is $-49dB$.

Phase and group delay constraints normally cannot be implemented in techniques using convex optimization with stop band energy minimization type of objectives as in the optimal autocorrelation based technique that is demonstrated in *Chapter 2*. Even though minimax type of optimization formulations can implement such constraints, they do not provide freedom to user to choose stop band

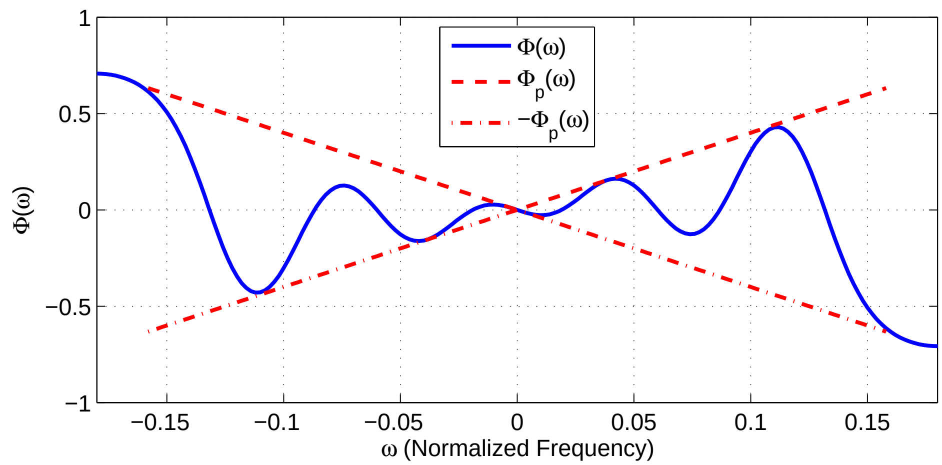

Figure 4.4: Phase response of $L^* = 35$ length FIR filter coefficients that are obtained by solving problem given in *Design 4.1* using DIRR.

energy minimization as an objective. However, since proposed iterative technique is capable of convexifying the non-convex constraints to SDP form, phase and group delay constraints and minimization type of objectives can be handled.

Finding the lowest order FIR filter satisfying the given constraints is a quasiconvex problem. This problem can be handled by solving (4.9), whose goal is finding $\mathbf{H}^\star$ with the least stop band energy possible. For this problem, DIRR given in *Algorithm 5* is utilized with parameters $\lambda = 1 - (R^i)^\alpha$ for $\alpha = 1$. The solution is obtained on the direction of 2^{nd} singular vector of $\mathbf{H}^1$ at 5^{th} iteration with $R^i = 1$. Filter coefficients and the singular values of the obtained solution matrix are shown in *Table 4.1* and *Figure 4.2*, respectively. Resulting filter order is found to be $L^\star = 35$. As shown in *Figure 4.3* and *Figure 4.4*, all the constraints on the magnitude and phase response of the filter are satisfied. Achieved stop band energy is $-49dB$. Optimal LP based linear phase filter design formulation proposed in [19] and shown in *Chapter 2* was not able to find filter coefficients with $L^\star = 35$ for the same magnitude constraint set of *Design 4.1* since linear phase constraint is tight. Note that LP based design technique could provide a design that satisfies the constraints for a filter of length $L^* = 39$. Next, SDP formulation for group delay constrained FIR filter design by using DIRR is formulated.

4.2 Group Delay Constrained FIR Filter Design By Directed Iterative Rank Refinement

The proposed technique can be used to obtain filter designs under directly imposed group delay constraints as well. An alternative technique, where least squares error from a desired group delay response is constrained with LMI constraints using SDP framework, is presented in [33]. However, the LMI matrix, which characterizes the group delay constraints, may not be PSD in that formulation and hence, a PSD approximation must be applied on that LMI matrix so that the constructed problem is convex. Hence, constructed optimization problem is indeed an approximation to the original group delay constrained problem. Here, we use group delay mask constraints for exact representation in the optimization. At each desired frequency, we restrict the group delay of the filter to be in a desired interval. In addition, since DIRR can handle non-convex constraints induced by indefinite constraint matrices, non-convex group delay constraints can be imposed as well. Consider the following constraints on the group delay (*Figure 4.5*) of the filter:

$$G_l(\omega_k) \leq G(\omega_k) \leq G_u(\omega_k),\ 0 \leq k \leq K_g, \tag{4.11}$$

where $G_l(\omega_k)$ and $G_u(\omega_k)$ are the lower and upper group delay constraints, and the group delay $G(\omega_k)$ is:

$$G(\omega_k) = -\frac{\partial \Phi(\omega_k)}{\partial \omega_k}. \tag{4.12}$$

By using the following identity for $\tan^{-1}(.)$

$$\frac{\partial \tan^{-1} f(\omega_k)}{\partial \omega_k} = \frac{1}{1+f^2(\omega_k)} \frac{\partial f(\omega_k)}{\partial \omega_k}, \tag{4.13}$$

the group delay can be written as:

$$G(\omega_k) = -\frac{1}{1+\frac{Im^2(H(\omega_k))}{Re^2(H(\omega_k))}} \frac{\partial \left(\frac{Im(H(\omega_k))}{Re(H(\omega_k))}\right)}{\partial \omega_k}. \tag{4.14}$$

Now, by using (4.6a) and (4.6b) we obtain:

$$G(\omega_k) = -\frac{1}{1+\frac{|\mathbf{s}(\omega_k)^T\mathbf{h}|^2}{|\mathbf{c}(\omega_k)^T\mathbf{h}|^2}} \frac{\partial \left(\frac{\mathbf{s}(\omega_k)^T\mathbf{h}}{\mathbf{c}(\omega_k)^T\mathbf{h}}\right)}{\partial \omega_k}. \tag{4.15}$$

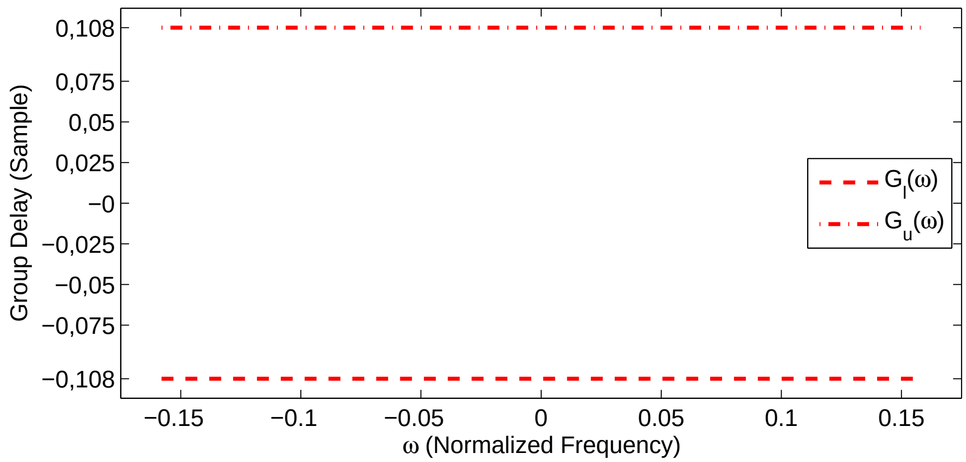

Figure 4.5: Typical group delay mask constraints that are used in group delay constrained FIR filter design. Upper and lower group delay mask constraints are given as $G_l(\omega) = -G_u(\omega) = 0.108$ for $|\omega| < 0.16$.

By using closed form expressions of the involved derivatives, we obtain:

$$\begin{aligned} G(\omega_k) &= \frac{(\mathbf{s}(\omega_k)^T\mathbf{h})^T\tilde{\mathbf{c}}(\omega_k)^T\mathbf{h} - (\mathbf{c}(\omega_k)^T\mathbf{h})^T\tilde{\mathbf{s}}(\omega_k)^T\mathbf{h}}{\mathbf{h}^T\mathbf{A}(\omega_k)\mathbf{h}} \\ &= \frac{\mathbf{h}^T(\mathbf{s}_k\tilde{\mathbf{c}}_k^T - \mathbf{c}_k\tilde{\mathbf{s}}_k^T)\mathbf{h}}{\mathbf{h}^T\mathbf{A}_k\mathbf{h}}, \end{aligned} \tag{4.16}$$

where $\tilde{\mathbf{c}}(\omega)$ and $\tilde{\mathbf{s}}(\omega)$ are defined as:

$$\tilde{\mathbf{c}}(\omega_k) = [0, -\sin\omega_k, .., -(L-1)\sin(L-1)\omega_k]^T, \tag{4.17a}$$

$$\tilde{\mathbf{s}}(\omega_k) = [0, -\cos\omega_k, \ldots, -(L-1)\cos(L-1)\omega_k]^T, \tag{4.17b}$$

which leads to the following form:

$$G(\omega_k) = \frac{\mathrm{Tr}(\mathbf{D}_k\mathbf{H})}{\mathrm{Tr}(\mathbf{A}_k\mathbf{H})}, \tag{4.18}$$

where $\mathbf{D}_k = \mathbf{s}_k\tilde{\mathbf{c}}_k^T - \mathbf{c}_k\tilde{\mathbf{s}}_k^T$ and $\mathbf{H} = \mathbf{h}\mathbf{h}^T$. Using this form, group delay constraints in (4.11) can be expressed as:

$$\mathrm{Tr}(\mathbf{A}_k\mathbf{H})G_l(\omega_k) \leq \mathrm{Tr}(\mathbf{D}_k\mathbf{H}) \leq \mathrm{Tr}(\mathbf{A}_k\mathbf{H})G_u(\omega_k), \tag{4.19}$$

for $0 \leq k \leq K_g$. Finally (4.19) can be separated into two sets of group delay constraints as:

$$\mathrm{Tr}(\mathbf{L}_k\mathbf{H}) \leq 0,\ 0 \leq k \leq K_g, \tag{4.20a}$$

$$\mathrm{Tr}(\mathbf{U}_k\mathbf{H}) \geq 0,\ 0 \leq k \leq K_g, \tag{4.20b}$$

where $\mathbf{L}_k = G_l(\omega_k)\mathbf{A}_k - \mathbf{D}_k$ and $\mathbf{U}_k = G_u(\omega_k)\mathbf{A}_k - \mathbf{D}_k$. Using (4.20a) and (4.20b) leads to the following optimization based FIR filter design formulation with group delay constraints:

$$
\begin{aligned}
\min_{\mathbf{H}\in\mathbb{R}^{L\times L}} \quad & \mathrm{Tr}(\mathbf{A}_s\mathbf{H}) && (4.21a)\\
\text{subject to} \quad & \mathrm{Tr}(\mathbf{A}_k\mathbf{H}) \leq a_k,\ 0 \leq k \leq K_u, && (4.21b)\\
& \mathrm{Tr}(\mathbf{A}_k\mathbf{H}) \geq b_k\ 0 \leq k \leq K_l, && (4.21c)\\
& \mathrm{Tr}(\mathbf{L}_k\mathbf{H}) \leq 0,\ 0 \leq k \leq K_g, && (4.21d)\\
& \mathrm{Tr}(\mathbf{U}_k\mathbf{H}) \geq 0,\ 0 \leq k \leq K_g, && (4.21e)\\
& \mathbf{H} \succeq 0. && (4.21f)
\end{aligned}
$$

Though (4.21) is a relaxed convex SDP, it does not guarantee rank-1 solution matrix $\mathbf{H}$. By combining formulation (3.18) and (4.21), iterative formulations that can produce low-rank solution matrices for group delay constrained FIR filter design are obtained as:

$$
\begin{aligned}
\min_{\mathbf{H}^{i+1}\in\mathbb{R}^{L\times L}} \quad & \mathrm{Tr}(((1-\xi)\mathbf{A}_s - \xi\mathbf{u}_\ell^i{\mathbf{u}_\ell^i}^T)\mathbf{H}^{i+1}) && (4.22a)\\
\text{subject to} \quad & \mathrm{Tr}(\mathbf{A}_k\mathbf{H}^{i+1}) \leq a_k,\ 0 \leq k \leq K_u, && (4.22b)\\
& \mathrm{Tr}(\mathbf{A}_k\mathbf{H}^{i+1}) \geq b_k\ 0 \leq k \leq K_l, && (4.22c)\\
& \mathrm{Tr}(\mathbf{L}_k\mathbf{H}^{i+1}) \leq 0,\ 0 \leq k \leq K_g, && (4.22d)\\
& \mathrm{Tr}(\mathbf{U}_k\mathbf{H}^{i+1}) \geq 0,\ 0 \leq k \leq K_g, && (4.22e)\\
& \mathbf{H}^{i+1} \succeq 0. && (4.22f)
\end{aligned}
$$

$$
\begin{aligned}
\min_{\mathbf{H}^{i+1}\in\mathbb{R}^{L\times L}} \quad & \mathrm{Tr}(((1-\xi)\mathbf{A}_s - \xi\mathbf{u}_\ell^i{\mathbf{u}_\ell^i}^T)\mathbf{H}^{i+1}) && (4.23a)\\
\text{subject to} \quad & \mathrm{Tr}(\mathbf{A}_k\mathbf{H}^{i+1}) \leq a_k,\ 0 \leq k \leq K_u, && (4.23b)\\
& \mathrm{Tr}(\mathbf{A}_k\mathbf{H}^{i+1}) \geq b_k\ 0 \leq k \leq K_l, && (4.23c)\\
& \mathrm{Tr}(\mathbf{u}_\eta^i{\mathbf{u}_\eta^i}^T\mathbf{H}^{i+1}) \leq \kappa^i,\ \forall\eta \in [1, L] \setminus \ell, && (4.23d)\\
& \mathrm{Tr}(\mathbf{L}_k\mathbf{H}^{i+1}) \leq 0,\ 0 \leq k \leq K_g, && (4.23e)\\
& \mathrm{Tr}(\mathbf{U}_k\mathbf{H}^{i+1}) \geq 0,\ 0 \leq k \leq K_g, && (4.23f)\\
& \mathbf{H}^{i+1} \succeq 0. && (4.23g)
\end{aligned}
$$

n	$h_n^\star$	n	$h_n^\star$	n	$h_n^\star$	n	$h_n^\star$
1	-0.0049	11	-0.0418	21	0.1235	31	-0.0057
2	-0.0114	12	0.0908	22	0.1273	32	-0.0128
3	-0.0099	13	0.1904	23	0.1316	33	-0.0282
4	0.0094	14	0.1811	24	0.1593	34	-0.0441
5	0.0418	15	0.0628	25	0.1922	35	-0.0482
6	0.0616	16	-0.0841	26	0.1948	36	-0.0373
7	0.0388	17	-0.1610	27	0.1524	37	-0.0197
8	-0.0298	18	-0.1268	28	0.0858	38	-0.0059
9	-0.1033	19	-0.0215	29	0.0296		
10	-0.1184	20	0.0777	30	0.0020		

Table 4.2: Group delay constrained FIR filter coefficients for *Design 4.2* are given in 4 significant digits.

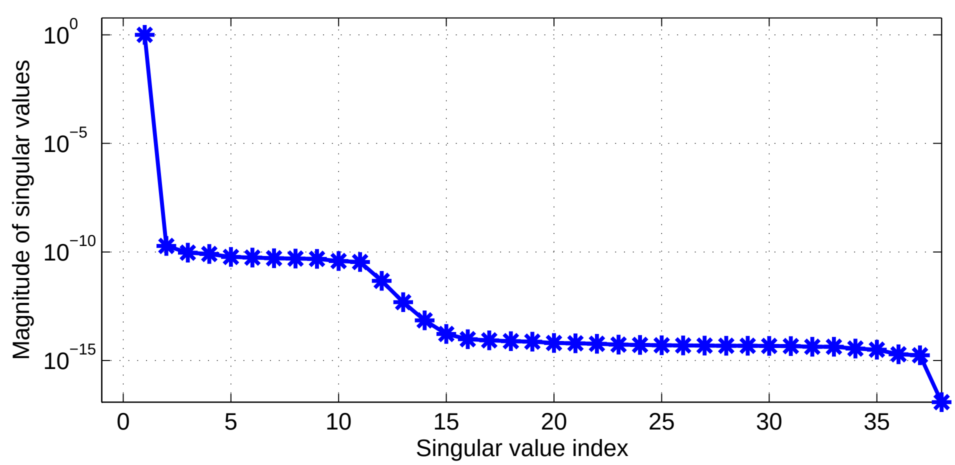

Figure 4.6: Singular values of $\mathbf{H}^i$ at iteration $i = 4$ that are obtained by solving *Design 4.2* using DIRR.

Proposed iterative technique is capable of replacing a non-convex QCQP problem with a convex SDP problem as in the example of phase constrained FIR filter design. Similarly, (4.22) is the iterative convex representation of original non-convex QCQP formulation of group delay constrained filter design problem. Hence, unlike existing least squares based techniques, which obtain approximations to desired group delay response, proposed technique is capable of designing FIR filters with group delay mask constraints. Next, group delay constrained FIR filter design examples by using (4.22) and (4.23) are demonstrated.

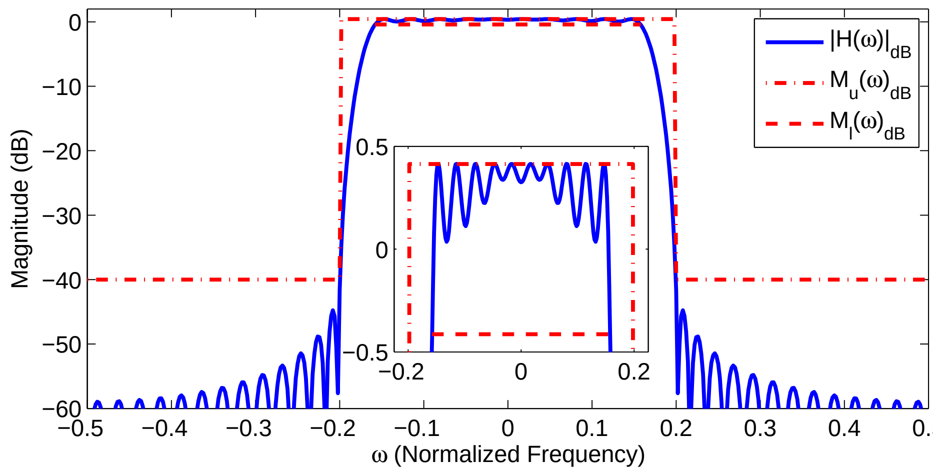

Figure 4.7: Magnitude response of $L^{\star} = 38$ length FIR filter coefficients obtained by DIRR. Magnitude response satisfies the constraints of *Design 4.2*. Stop band energy level is $-56dB$.

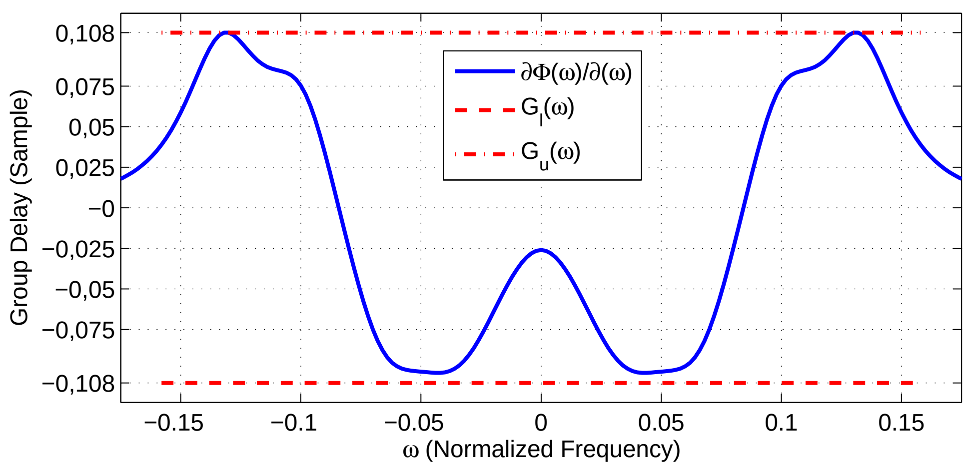

Figure 4.8: Group delay of $L^{\star} = 38$ length anticausal FIR filter coefficients obtained by DIRR. Group delay satisfies the constraints of *Design 4.2*. Constraint values $(G_u(\omega_k) = -G_l(\omega_k) = 0.108)$ are determined according to differentiation of Φ relative to frequency samples.

Design 4.2 *Given the magnitude and group delay mask constraints,* $M_l(\omega)$*,* $M_u(\omega)$ *shown in* Figure 2.1 *and* $G_l(\omega_k)$*,* $G_u(\omega_k)$ *shown in* Figure 4.5*, respectively, design the lowest order filter with minimum stop band energy.*

n	$h_n^\star$	n	$h_n^\star$	n	$h_n^\star$	n	$h_n^\star$
1	-0.0048	11	-0.0827	21	0.1126	31	0.0126
2	-0.0131	12	-0.0185	22	0.0867	32	0.0381
3	-0.0164	13	0.0208	23	0.0348	33	0.0363
4	-0.0030	14	-0.0262	24	0.0051	34	0.0147
5	0.0281	15	-0.1553	25	0.0029	35	-0.0072
6	0.0576	16	-0.2886	26	0.0025	36	-0.0159
7	0.0554	17	-0.3308	27	-0.0153	37	-0.0120
8	0.0076	18	-0.2456	28	-0.0407	38	-0.0045
9	-0.0622	19	-0.0841	29	-0.0480		
10	-0.1038	20	0.0574	30	-0.0253		

Table 4.3: Group delay constrained FIR filter coefficients for *Design 4.3* are given in 4 significant digits.

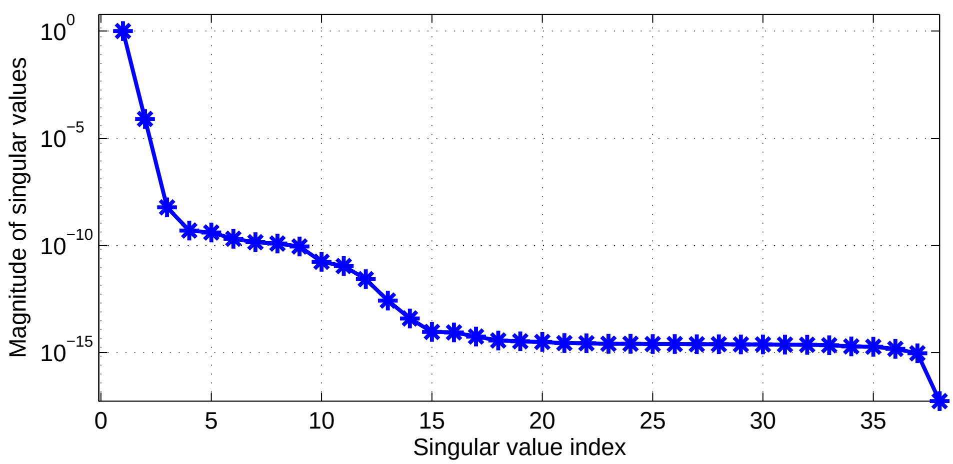

Figure 4.9: Singular values of $\mathbf{H}^i$ at iteration $i = 16$ that are obtained by solving *Design 4.3* using DIRR.

To obtain filter coefficients for this problem, the optimization problem in (4.22) is solved using DIRR algorithm in *Algorithm 5* with $\lambda = 1 - (R^i)^\alpha$ for $\alpha = 1$. Proposed DIRR based design technique has converged to a solution in 4 iterations on the direction of the 6^{th} left singular vector with singular value ratio of $R^i = 1$ for $i = 4$. Obtained $L^\star = 38$ length filter coefficients are given in *Table 4.2*. The magnitude response and the group delay of the obtained coefficients are given in *Figure 4.7* and *Figure 4.8*, respectively. The stop band energy of magnitude

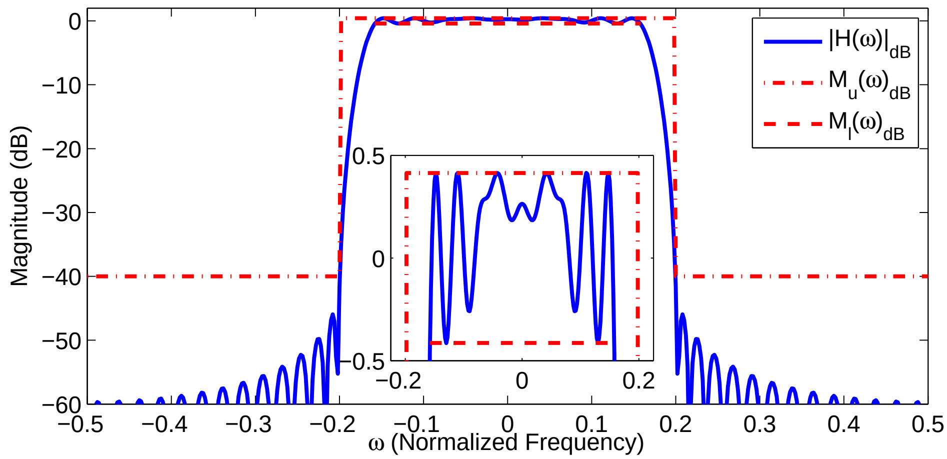

Figure 4.10: Magnitude response of $L^{\star} = 38$ length FIR filter coefficients obtained by DIRR. Magnitude response satisfies the constraints of *Design 4.3*. Stop band energy level is $-57dB$.

response in *Figure 4.7* is found to be $-56dB$. As observed all the constraint on the magnitude response and group delay of the filter are well satisfied. Resulting singular values of obtained solution matrix are shown in *Figure 4.6*. As it can be observed, first singular value is dominant compared to other singular values, whose energy percentage are below 10^{-10}.

Design 4.3 *Given the magnitude and group delay mask constraints,* $M_l(\omega)$, $M_u(\omega)$ *shown in* Figure 2.1 *and* $G_l(\omega_k)$, $G_u(\omega_k)$ *shown in* Figure 4.11*, respectively, design the lowest order filter with minimum stop band energy.*

To obtain filter coefficients for this problem, the optimization problem in (4.23) is solved using DIRR algorithm in *Algorithm 6* with $\lambda = 1 - (R^i)^\alpha$ for $\alpha = 1$. Proposed DIRR based design technique has converged to a solution in 16 iterations on the direction of the 5^{th} left singular vector with singular value ratio of $R^i = 0.99992$ for $i = 16$. Obtained $L^{\star} = 38$ length filter coefficients are given in *Table 4.3*. The magnitude response and the group delay of the obtained coefficients are given in *Figure 4.10* and *Figure 4.11*, respectively. The stop band energy of magnitude response in *Figure 4.10* is found to be $-57dB$. As observed

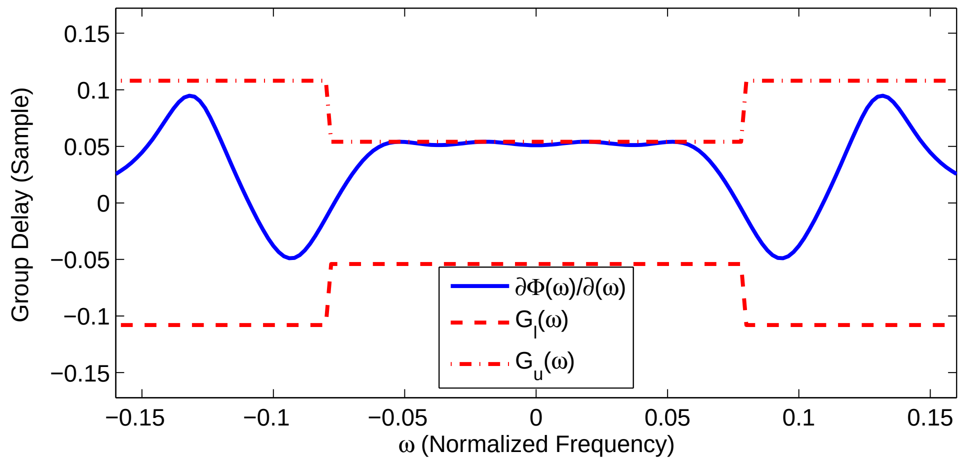

Figure 4.11: Group delay of $L^{\star} = 38$ length anticausal FIR filter coefficients obtained by DIRR. Group delay satisfies the constraints of *Design 4.3*. Constraint values ($G_u(\omega_k) = -G_l(\omega_k) = 0.054$ for $|\omega_k| \leq 0.08$ and $G_u(\omega_k) = -G_l(\omega_k) = 0.108$ for $0.08 \leq |\omega_k| \leq 0.16$) are determined according to differentiation of Φ relative to frequency samples.

all the constraints on the magnitude response and group delay of the filter are well satisfied. Resulting singular values of obtained solution matrix are shown in *Figure 4.9*. As it can be observed, first singular value is dominant compared to other singular values. Note that rank-1 solution matrix could not be obtained by (4.22) since constraints in this design are tight.

Chapter 5

Conclusions and Future Work

In this thesis, a new flexible design technique for FIR filter design is proposed. First, FIR filter design problem is cast as a non-convex SDP. Then, by relaxing the rank-1 constraint of the constructed optimization problem, a convex SDP is obtained. By using the proposed directed rank refinement algorithm, an approximately rank-1 solution to the convex SDP is found. Hence, filter coefficients obtained by factorizing the solution matrix well satisfy the constraints of the original problem. Performed numerical examples show that proposed technique is capable of obtaining practically rank-1 solution matrices even under tight phase and group delay mask constraints. Numerical results obtained by DIRR are also comparable to designs that are obtained by optimal FIR filter design techniques. Though DIRR has increased complexity compared to optimal filter design techniques, it provides control over performance tradeoff between magnitude, phase and group delay responses. The main contribution of this paper is a general convex SDP formulation for the design of FIR filters with spectral mask constraints such as phase, group delay and magnitude response constraints. Hence, proposed technique serves as a general and flexible FIR filter design formulation that is capable of handling a large set of constraints without requiring any sort of approximations. Obtained results show that proposed technique can be used in designing FIR filters with desired magnitude response, phase response and group delay characteristics.

Proposed FIR filter design technique can also be used in various other research areas since semidefinite programming is used in many other applications [59]. Since the main challenge in semidefinite programming is to obtain a solution vector from a solution matrix, proposed iterative rank refinement technique can serve as a solution to this problem. Hence, the application of proposed DIRR on various other problems that make use of SDP, i.e., multiple-input multiple-output (MIMO) problems, magnetic resonance imaging problems and power grid problems [59, 66], is considered as future work.

Bibliography

[1] T. Davidson, "Enriching the art of FIR filter design via convex optimization," *IEEE Signal Process. Mag.*, vol. 27, pp. 89–101, May 2010.

[2] B. Shenoi, *Introduction to Digital Signal Processing and Filter Design.* Wiley, 2005.

[3] L. Jackson, *Digital Filters and Signal Processing.* Springer, 1996.

[4] K. Steiglitz, T. Parks, and J. Kaiser, "Meteor: a constraint-based FIR filter design program," *IEEE Trans. Signal Process.*, vol. 40, pp. 1901–1909, Aug 1992.

[5] I. Selesnick, M. Lang, and C. Burrus, "Constrained least square design of FIR filters without specified transition bands," *IEEE Trans. Signal Process.*, vol. 44, pp. 1879–1892, Aug 1996.

[6] A. E. Cetin, O. Gerek, and Y. Yardimci, "Equiripple FIR filter design by the fft algorithm," *IEEE Signal Process. Mag.*, vol. 14, pp. 60–64, Mar 1997.

[7] J. McClellan and T. Parks, "A unified approach to the design of optimum FIR linear-phase digital filters," *IEEE Trans. Circuit Theory*, vol. 20, pp. 697–701, November 1973.

[8] J. Adams and J. Sullivan, "Peak-constrained least-squares optimization," *IEEE Trans. Signal Process.*, vol. 46, pp. 306–321, Feb 1998.

[9] E. Y. Remez, *General computational methods of Chebyshev approximation: the problems with linear real parameters.* Washington, DC: ERDA Div. Phys. Res., 1962.

[10] T. Stathaki and I. Fotinopoulos, "Equiripple minimum phase FIR filter design from linear phase systems using root moments," *IEEE Trans. Circuits Syst. II*, vol. 48, no. 6, pp. 580–587, 2001.

[11] L. Rabiner, J. McClellan, and T. Parks, "FIR digital filter design techniques using weighted chebyshev approximation," *Proc. IEEE*, vol. 63, no. 4, pp. 595–610, 1975.

[12] A. Dutra, L. Lovisolo, E. da Silva, and P. S. R. Diniz, "Successive approximation FIR filter design," in *IEEE Int. Symp. on Circuits and Systems (ISCAS)*, pp. 149–152, 2011.

[13] T. Parks and J. McClellan, "Chebyshev approximation for nonrecursive digital filters with linear phase," *IEEE Trans. Circuit Theory*, vol. 19, no. 2, pp. 189–194, 1972.

[14] L. Rabiner, B. Gold, and C. McGonegal, "An approach to the approximation problem for nonrecursive digital filters," *IEEE Trans. Audio Electroacoust.*, vol. 18, no. 2, pp. 83–106, 1970.

[15] K. Kose and A. E. Cetin, "Low-pass filtering of irregularly sampled signals using a set theoretic framework [lecture notes]," *IEEE Signal Process. Mag.*, vol. 28, pp. 117–121, July 2011.

[16] T. Saramaki, "Finite impulse response filter design," *Handbook for digital signal processing*, pp. 155–277, 1993.

[17] J. Mattingley and S. Boyd, "Real-time convex optimization in signal processing," *IEEE Signal Process. Mag.*, vol. 27, pp. 50–61, May 2010.

[18] M. H. Er and C. K. Siew, "Design of FIR filters using quadratic programming approach," *IEEE Trans. Circuits Syst. II*, vol. 42, pp. 217–220, Mar 1995.

[19] S.-P. Wu, S. Boyd, and L. Vandenberghe, "FIR filter design via semidefinite programming and spectral factorization," in *Proc. of the 35th IEEE Conf. on Decision and Control*, vol. 1, pp. 271–276 vol.1, 1996.

[20] M. S. Lobo, L. Vandenberghe, S. Boyd, and H. Lebret, "Applications of second-order cone programming," *Linear Algebra Appl.*, vol. 284, no. 13, pp. 193–228, Nov. 1998.

[21] W. S. Lu, "Design of nonlinear-phase FIR digital filters: a semidefinite programming approach," in *Proc. of the 1999 IEEE Int. Symp. on Circuits and Systems (ISCAS '99)*, vol. 3, pp. 263–266 vol.3, 1999.

[22] J. Coleman and D. Scholnik, "Design of nonlinear-phase FIR filters with second-order cone programming," in *42nd Midwest Symp. on Circuits and Systems*, vol. 1, pp. 409–412 vol. 1, 1999.

[23] H. Q. Ta and T. Le-Nhat, "Design of FIR filter with discrete coefficients based on mixed integer linear programming," in *9th Int. Conf. on Signal Process. (ICSP 2008)*, pp. 9–12, 2008.

[24] S. Boyd and L. Vandenberghe, *Convex Optimization*. Cambridge, U.K.: Cambridge University Press, 2004.

[25] Y. Nesterov and A. Nemirovski, *Interior-Point Polynomial Algorithms in Convex Programming*. Society for Industrial and Applied Mathematics, 1994.

[26] Y. Ye, *Interior point algorithms: theory and analysis*, vol. 44. John Wiley & Sons, 2011.

[27] J. F. Sturm, "Using sedumi 1.02, a MATLAB toolbox for optimization over symmetric cones," *Optimization Methods and Software*, vol. 11-12, pp. 625–653, 1999.

[28] M. Grant and S. Boyd, "CVX: Matlab software for disciplined convex programming, version 2.0 beta." `http://cvxr.com/cvx`, Sept. 2012.

[29] M. Grant and S. Boyd, "Graph implementations for nonsmooth convex programs," in *Recent Advances in Learning and Control* (V. Blondel, S. Boyd, and H. Kimura, eds.), Lecture Notes in Control and Information Sciences, pp. 95–110, Springer-Verlag Limited, 2008. `http://stanford.edu/~boyd/graph_dcp.html`.

[30] O. Herrmann, "Design of nonrecursive digital filters with linear phase," *Electronics Letters*, vol. 6, no. 11, pp. 328–329, 1970.

[31] T. I. Laakso, V. Valimaki, M. Karjalainen, and U. K. Laine, "Splitting the unit delay [fir/all pass filters design]," *IEEE Signal Process. Mag.*, vol. 13, pp. 30–60, Jan 1996.

[32] V. Madisetti, *Digital Signal Processing Fundamentals*. Boca Raton, FL, USA: CRC Press, Inc., 2nd ed., 2009.

[33] Z. Lin and Y. Liu, "FIR filter design with group delay constraint using semidefinite programming," in *IEEE Int. Symp. on Circuits and Systems (ISCAS 2006)*, pp. 2505–2508, May 2006.

[34] F. Cruz-Roldan, P. Martin-Martin, J. Saez-Landete, M. Blanco-Velasco, and T. Saramaki, "A fast windowing-based technique exploiting spline functions for designing modulated filter banks," *IEEE Trans. Circuits Syst. I*, vol. 56, pp. 168–178, Jan 2009.

[35] H. Bauschke and J. Borwein, "On projection algorithms for solving convex feasibility problems," *SIAM Review*, vol. 38, no. 3, pp. 367–426, 1996.

[36] J. Lofberg, "Yalmip : a toolbox for modeling and optimization in matlab," in *IEEE Int. Symp. on Computer Aided Control Systems Design*, pp. 284–289, Sept 2004.

[37] K. C. Toh, M. Todd, and R. H. Tütüncü, "Sdpt3 – a matlab software package for semidefinite programming," *OPTIMIZATION METHODS AND SOFTWARE*, vol. 11, pp. 545–581, 1999.

[38] S. P. Wu, S. Boyd, and L. Vandenberghe, "FIR filter design via spectral factorization and convex optimization," in *Applied and Computational Control, Signals and Circuits* (B. N. Datta, ed.), pp. 215–242 vol.1, Boston, MA: Birkhauser, 1999.

[39] Y. Ye and S. Zhang, "New results on quadratic minimization," *SIAM Journal on Optimization*, vol. 14, no. 1, pp. 245–267, 2003.

[40] A. Beck and Y. C. Eldar, "Strong duality in nonconvex quadratic optimization with two quadratic constraints," *SIAM Journal on Optimization*, vol. 17, pp. 844–860, Sept. 2006.

[41] Y. Huang and S. Zhang, "Complex matrix decomposition and quadratic programming," *Mathematics of Operations Research*, vol. 32, pp. pp. 758–768, Aug. 2007.

[42] Y. K. Alp, M. Dedeoglu, and O. Arikan, "Ultra-wideband orthogonal pulse shape set design by using hermite-gaussian functions," in *IEEE 20th Signal Process. and Communications Applications Conf. (SIU)*, pp. 1–4, 2012.

[43] Y. K. Alp, O. Arikan, and A. Bayri, "Phase-only beam synthesis by iterative semidefinite relaxations with rank refinement," in *European Signal Process. Conf. (EUSIPCO)*, pp. 1–5, Sept 2013.

[44] J. Dattorro, *Convex Optimization & Euclidean Distance Geometry*, ch. 4. California: Meboo Publishing, J. Dattorro ed., 2005.

[45] T. Nguyen, "Digital filter bank design quadratic-constrained formulation," *IEEE Trans. Signal Process.*, vol. 43, pp. 2103–2108, Sep 1995.

[46] X. Wu, Z. Tian, T. Davidson, and G. Giannakis, "Optimal waveform design for uwb radios," *IEEE Trans. Signal Process.*, vol. 54, pp. 2009–2021, June 2006.

[47] T. Davidson, Z.-Q. Luo, and J. Sturm, "Linear matrix inequality formulation of spectral mask constraints with applications to FIR filter design," *IEEE Trans. Signal Process.*, vol. 50, pp. 2702–2715, Nov 2002.

[48] M. Dedeoglu, Y. K. Alp, and O. Arikan, "FIR filter design by iterative convex relaxations with rank refinement," in *22nd Signal Proc. and Communications Applications Conf. (SIU)*, pp. 654–657, April 2014.

[49] A. E. Cetin, O. N. Gerek, and Y. Yardimci, "Equiripple FIR filter design by the fft algorithm," *IEEE Signal Process. Mag.*, vol. 14, pp. 60–64, Mar 1997.

[50] X. Lai, "Optimal design of nonlinear-phase fir filters with prescribed phase error," *IEEE Trans. Signal Process.*, vol. 57, pp. 3399–3410, Sept 2009.

[51] Z. Lin and Y. Liu, "Design of arbitrary complex coefficient wls fir filters with group delay constraints," *IEEE Trans. Signal Process.*, vol. 57, pp. 3274–3279, Aug 2009.

[52] J. Adams, "Fir digital filters with least-squares stopbands subject to peak-gain constraints," *IEEE Trans. Circuits Syst.*, vol. 38, pp. 376–388, Apr 1991.

[53] J. Yen, "On nonuniform sampling of bandwidth-limited signals," *IRE Trans. Circuit Theory*, vol. 3, pp. 251–257, Dec 1956.

[54] A. Aldroubi and K. Gröchenig, "Nonuniform sampling and reconstruction in shift-invariant spaces," *SIAM Review*, vol. 43, pp. 585–620, Apr. 2001.

[55] R. Vaughan, N. Scott, and D. White, "The theory of bandpass sampling," *IEEE Trans. Signal Process.*, vol. 39, pp. 1973–1984, Sep 1991.

[56] K. M. Anstreicher, "Semidefinite programming versus the reformulation-linearization technique for nonconvex quadratically constrained quadratic programming," *J. Glob. Optim.*, vol. 43, pp. 471–484, 2009.

[57] L. Vandenberghe and S. Boyd, "Semidefinite programming," *SIAM Review*, vol. 38, pp. 49–95, 1994.

[58] B. Gärtner and J. Matouvsek, *Approximation Algorithms and Semidefinite Programming*. Draft, May 2011.

[59] Z.-Q. Luo, W.-K. Ma, A.-C. So, Y. Ye, and S. Zhang, "Semidefinite relaxation of quadratic optimization problems," *IEEE Signal Process. Mag.*, vol. 27, pp. 20–34, May 2010.

[60] G. Pataki, "On the rank of extreme matrices in semidefinite programs and the multiplicity of optimal eigenvalues," *Mathematics of Operations Research*, vol. 23, pp. pp. 339–358, May 1998.

[61] M. Fazel, *Matrix Rank Minimization with Applications*. PhD thesis, Stanford University, Department of Electrical Engineering, 2002.

[62] M. Fazel, H. Hindi, and S. P. Boyd, "A rank minimization heuristic with application to minimum order system approximation," in *IEEE Proc. of the 2001 American Control Conf.*, vol. 6, pp. 4734–4739, IEEE, 2001.

[63] A. M.-C. So, J. Zhang, and Y. Ye, "On approximating complex quadratic optimization problems via semidefinite programming relaxations," *Math. Program.*, vol. 110, pp. 93–110, Mar. 2007.

[64] B. Parlett and W. Poole, Jr., "A geometric theory for the \$qr\$, \$lu\$ and power iterations," *SIAM Journal on Numerical Analysis*, vol. 10, no. 2, pp. 389–412, 1973.

[65] W. S. Lu, "Design of nonlinear-phase FIR digital filters: a semidefinite programming approach," in *Proc. of the 1999 IEEE Int. Symp. on Circuits and Systems (ISCAS '99)*, vol. 3, pp. 263–266 vol.3, Jul 1999.

[66] H. Zhu and G. Giannakis, "Estimating the state of ac power systems using semidefinite programming," in *North American Power Symp. (NAPS), 2011*, pp. 1–7, Aug 2011.

[67] A. Papoulis, *Signal Analysis.* New York, San Francisco, Paris: McGraw-Hill, pp. 232-233, 1977.

Appendix A

Algorithms

A.1 Section 2.2: Linear Programming Based FIR Filter Design

Algorithm 1 An implementation for designing non-linear phase FIR filters using LP based model given in (2.11) .

Definitions:

$\overrightarrow{\mathbf{r}}$: Last L samples of $\mathbf{r}$; i.e. $\overrightarrow{\mathbf{r}}_1 = \mathbf{r}_L, ..., \overrightarrow{\mathbf{r}}_L = \mathbf{r}_{2L-1}$.

$\overleftarrow{\mathbf{r}}$: First $L-1$ samples of $\mathbf{r}$. Since $\mathbf{r}$ is symmetric, $\overleftarrow{\mathbf{r}}$ is equivalent to last $L-1$ samples of $\overrightarrow{\mathbf{r}}$ in reverse ordering; i.e. $\overleftarrow{\mathbf{r}}_1 = \mathbf{r}_1, ..., \overleftarrow{\mathbf{r}}_{L-1} = \mathbf{r}_{L-1}$.

$\tilde{\mathbf{v}}(\omega_k)$: Since Fourier Transform (FT) of symmetric $\mathbf{r}$ is equivalent to Discrete Cosine Transform (DCT) of $\overrightarrow{\mathbf{r}}$, $\tilde{\mathbf{v}}(\omega_k)$ are defined as DCT vectors for $\overrightarrow{\mathbf{r}}$ as: $\tilde{\mathbf{v}}(\omega_k)=[1, 2\cos(\omega_k), ..., 2\cos((L\text{–}1)\omega_k)]^T$, for $0 \leq k \leq K_u = 500$.

Algorithm:

1: Construct (2.11) or (2.12) by putting $\mathbf{r} = \overrightarrow{\mathbf{r}}$, $\mathbf{v}(\omega_k) = \tilde{\mathbf{v}}(\omega_k)$ and removing (2.11e) or (2.12f), respectively. Then, solve for $\overrightarrow{\mathbf{r}}$.

2: Obtain $\overleftarrow{\mathbf{r}}$ from $\overrightarrow{\mathbf{r}}$.

3: Obtain $\mathbf{r}$ using $\mathbf{r} = [\overleftarrow{\mathbf{r}}^T, \overrightarrow{\mathbf{r}}^T]^T$.

4: Apply a spectral factorization algorithm on $\mathbf{r}$ to obtain filter coefficients $\mathbf{h}$. A spectral factorization algorithm that obtains $\mathbf{h}$ with minimum phase response, is provided in *Algorithm 3* [67].

Algorithm 2 An implementation for designing linear phase FIR filters using LP based model given in (2.13).

Definitions:

$\overrightarrow{\mathbf{h}}$: Last $(L+1)/2$ samples of $\mathbf{h}$, i.e. $\overrightarrow{\mathbf{h}}_1 = \mathbf{h}_{(L+1)/2}, ..., \overrightarrow{\mathbf{h}}_{(L+1)/2} = \mathbf{h}_L$, if $\mathbf{h}$ is odd length, and last $L/2$ samples of $\mathbf{h}$, i.e. $\overrightarrow{\mathbf{h}}_1 = \mathbf{h}_{(L/2)+1}, ..., \overrightarrow{\mathbf{h}}_{L/2} = \mathbf{h}_L$, if $\mathbf{h}$ is even length.

$\overleftarrow{\mathbf{h}}$: First $(L-1)/2$ samples of $\mathbf{h}$ if $\mathbf{h}$ is odd length, and first $L/2$ samples of $\mathbf{h}$ if $\mathbf{h}$ is even length. Since $\mathbf{h}$ is symmetric, $\overleftarrow{\mathbf{h}}$ is equivalent to last $(L-1)/2$ samples of $\overrightarrow{\mathbf{h}}$ in reverse ordering, i.e. $\overleftarrow{\mathbf{h}}_1 = \mathbf{h}_1, ..., \overleftarrow{\mathbf{h}}_{(L-1)/2} = \mathbf{h}_{(L-1)/2}$, if $\mathbf{h}$ is odd length, and $\overleftarrow{\mathbf{h}}$ is equivalent to last $L/2$ samples of $\overrightarrow{\mathbf{h}}$ in reverse ordering, i.e. $\overleftarrow{\mathbf{h}}_1 = \mathbf{h}_1, ..., \overleftarrow{\mathbf{h}}_{L/2} = \mathbf{h}_{L/2}$, if $\mathbf{h}$ is even length.

$\tilde{\mathbf{v}}(\omega_k)$: Since Fourier Transform (FT) of symmetric $\mathbf{h}$ is equivalent to Discrete Cosine Transform (DCT) of $\overrightarrow{\mathbf{h}}$, $\tilde{\mathbf{v}}(\omega_k)$ are defined as DCT vectors for $\overrightarrow{\mathbf{h}}$ as; $\tilde{\mathbf{v}}(\omega_k)$=$[1, 2\cos(\omega_k), ..., 2\cos((L–2)\omega_k/2)]^T$, for $0 \leq k \leq K_u$ if $\mathbf{h}$ is odd, and $\tilde{\mathbf{v}}(\omega_k)$=$[2\cos(\omega_k/2), 2\cos(3\omega_k/2), ..., 2\cos((L-1)\omega_k/2)]^T$, for $0 \leq k \leq K_u$ if $\mathbf{h}$ is even ($K_u = 500$).

Algorithm:

1: Construct (2.13) or (2.14) by putting $\mathbf{h} = \overrightarrow{\mathbf{h}}$, $\mathbf{v}(\omega_k) = \tilde{\mathbf{v}}(\omega_k)$ and removing (2.13d) or (2.14f), respectively. Then, solve for $\overrightarrow{\mathbf{h}}$.

2: Obtain $\overleftarrow{\mathbf{h}}$ from $\overrightarrow{\mathbf{h}}$.

3: Obtain $\mathbf{h}$ using $\mathbf{h} = [\overleftarrow{\mathbf{h}}^T, \overrightarrow{\mathbf{h}}^T]^T$. Hence, $\mathbf{h}$ is symmetric and possesses a linear phase response.

Algorithm 3 A spectral factorization algorithm that is using Kolmogorov 1939 approach [67]. Resulting filter coefficients $\mathbf{h}$ provide minimum phase response.

Definitions:

$\overrightarrow{\mathbf{r}}$: Last L samples of $\mathbf{r}$; i.e. $\overrightarrow{\mathbf{r}}_1 = \mathbf{r}_L, ..., \overrightarrow{\mathbf{r}}_L = \mathbf{r}_{2L-1}$.

$\tilde{\mathbf{v}}(\omega_k)$: Since Fourier Transform (FT) of symmetric $\mathbf{r}$ is equivalent to Discrete Cosine Transform (DCT) of $\overrightarrow{\mathbf{r}}$, $\tilde{\mathbf{v}}(\omega_k)$ are defined as DCT vectors for $\overrightarrow{\mathbf{r}}$ as: $\tilde{\mathbf{v}}(\omega_k)$=$[1, 2\cos(\omega_k), ..., 2\cos((L–1)\omega_k)]^T$, for $1 \leq k \leq K$, where $K = 100L$ chosen.

Algorithm:

1: Compute FT of $\mathbf{r}$ by computing DCT of $\overrightarrow{\mathbf{r}}$; i.e. $R(\omega_k) = \overrightarrow{\mathbf{r}}^T \tilde{\mathbf{v}}(\omega_k)$.

2: Compute $\Gamma(\omega_k) = \frac{1}{2}\ln(R(\omega_k))$.

3: Obtain $\Pi(\omega_k) = \mathcal{H}(\Gamma(\omega_k))$ by computing Hilbert Transform (HT) of $\Gamma(\omega_k)$.

4: Compute filter coefficients, which provide minimum phase response, by computing the following inverse discrete FT: $h_n = \mathcal{F}^{-1}(e^{\Gamma(\omega_k)+j\Pi(\omega_k)}) = \frac{1}{K}\sum_{k=1}^{K}(e^{\Gamma(\omega_k)+j\Pi(\omega_k)})e^{j2\pi kn/K}$, for $1 \leq n \leq L$.

A.2 Section 2.3: Semidefinite Programming Formulation

Algorithm 4 An implementation for designing non-linear phase FIR filters using SDP based model given in (2.41).

Definitions:

$\mathbf{H}$: $L \times L$ positive semidefinite symmetric matrix.

$\mathbf{A}_s$: Definition is given in (2.7).

$\mathbf{A}_k$: Definition is given just after (2.5).

$\mathbf{v}(\omega_k)$: Fourier Transform (FT) vectors for each frequency are defined as: $\mathbf{v}(\omega_k)$=$[1, e^{(j\omega_k)}, ..., e^{(j(L-1)\omega_k)}]^T$, for $0 \leq k \leq K_u = 500$.

Algorithm:

Solve (2.41) for $\mathbf{H}$.

Obtain $\tilde{\mathbf{h}}$ from $\mathbf{H}$ using (2.44).

A.3 Section 3.1: Directed Iterative Rank Refinement

Algorithm 5 Proposed directed iterative rank refinement algorithm.

Definitions:

$\mathbf{H}^i$: $L \times L$ positive semidefinite symmetric matrix at iteration i.

$\mathbf{A}_k$: Definition is given just after (2.5).

$\mathbf{u}_\ell^i$: ℓ^{th} singular vector of solution matrix $\mathbf{H}^i$ at iteration i.

$\mathbf{v}(\omega_k)$: Fourier Transform (FT) vectors for each frequency are defined as: $\mathbf{v}(\omega_k)=[1, e^{(j\omega_k)}, ..., e^{(j(L-1)\omega_k)}]^T$, for $0 \leq k \leq K_u = 500$.

N_{iter}: Maximum number of iterations for direction ℓ.

Algorithm:

$\mathbf{u}_\ell^{i=0} \leftarrow \mathbf{0}$.
Depending on the design, solve one of (3.3), (3.19), (4.9), (4.22) for $\mathbf{H}^{i=1}$.
if Optimization problem is feasible **then**
    Apply SVD to $\mathbf{H}^{i=1}$
    if $R^1_{j=0} \geq \rho$ in (3.17) **then**
        Optimization is successful: $\mathbf{H}^I \leftarrow \mathbf{H}^{i=1}$.
    else
        $j \leftarrow 1$.
        while $j \leq L$ and $R^i_{j-1} \leq \rho$ **do**
            $i \leftarrow 1, R^{i=1} \leftarrow R^i_{j-1}$.
            while $R^i \leq \rho$ and $i \leq N_{iter}$ **do**
                $i \leftarrow i + 1$.
                Depending on the design problem, solve one of (3.3), (3.19), (4.9), (4.22) for $\mathbf{H}^i$ with $\ell = j$.
                Apply SVD to $\mathbf{H}^i$.
                Find R^i using (3.17) and update $\lambda(R^i)$.
            end while
            $R^i_j \leftarrow R^i$, $\mathbf{H}^I \leftarrow \mathbf{H}^i$.
            $j \leftarrow j + 1$.
        end while
    end if
    Apply SVD to $\mathbf{H}^I$, and find its singular values.
    $\mathbf{h} = \mathbf{u}_1^I \sqrt{\sigma_1^I}$.
end if

A.4 Section 3.3: Directed Iterative Rank Refinement with Cost Functions and Rank Constraints

Algorithm 6 Proposed directed iterative rank refinement algorithm for rank constrained SDP formulations with cost functions.

Definitions: Definitions are the same with *Algorithm 5.*

Algorithm:

$\mathbf{u}_\ell^{i=0} \leftarrow \mathbf{0}$ and $\kappa^0 = 0.2$.
Solve (3.20) or (4.23) for $\mathbf{H}^{i=1}$.
if Optimization problem is feasible **then**
    Apply SVD to $\mathbf{H}^{i=1}$
    if $R^1_{j=0} \geq \rho$ in (3.17) **then**
        Optimization is successful: $\mathbf{H}^I \leftarrow \mathbf{H}^{i=1}$.
    else
        $j \leftarrow 1$.
        while $j \leq L$ and $R^i_{j-1} \leq \rho$ **do**
            $i \leftarrow 1, R^{i=1} \leftarrow R^i_{j-1}$ and $\kappa^1 \leftarrow \kappa^0/2$.
            while $R^i \leq \rho$ and $i \leq N_{iter}$ **do**
                $i \leftarrow i + 1$.
                Solve (3.20) or (4.23) for $\mathbf{H}^i$.
                if (3.20) is feasible **then**
                    Apply SVD to $\mathbf{H}^i$.
                    Find R^i using (3.17) and update $\lambda(R^i)$.
                    $\kappa^i \leftarrow \kappa^{i-1}/2$.
                else
                    $i \leftarrow i - 1$.
                    $\kappa^i \leftarrow (\kappa^i + \kappa^{i^\star})/2$.
                end if
            end while
            $R^i_j \leftarrow R^i$, $\mathbf{H}^I \leftarrow \mathbf{H}^i$.
            $j \leftarrow j + 1$.
        end while
    end if
    Apply SVD to $\mathbf{H}^I$, and find its singular values.
    $\mathbf{h} = \mathbf{u}_1^I \sqrt{\sigma_1^I}$.
end if